April 2011

Design of a Servo Driven Adjustable Pick and Place Mechanism

Arvind Srinivasan
Worcester Polytechnic Institute

Buddhi M. Paranamana
Worcester Polytechnic Institute

Owen B. Butler
Worcester Polytechnic Institute

William Andrew Powers
Worcester Polytechnic Institute

Design of a Servo Driven, Adjustable Pick and Place Mechanism

As a Major Qualifying Project

Submitted to the faculty

Of the

Worcester Polytechnic Institute

Worcester, MA

In partial fulfillment of the requirements for the

Degree of Bachelor of Science

On

29 April 2011

By

Owen Butler (ME ’11)

Buddhi Paranamana (ME ’11)

William Powers (ME ’11)

Arvind Srinivasan (ME ’11)

Project Advisor: Professor Robert L Norton

Department of Mechanical Engineering

Abstract

The goal of this project was to design a tooling station consisting of three of the same linkage mechanisms providing motion along three different axes. Each of the linkages needed to be driven by a servo motor to achieve variable output stroke between zero and fifty six millimeters and to reduce the replacement cost of cams in the sponsor's production-line machinery. Each mechanism is a six-bar linkage consisting of a slider, which is constrained within a slot in the main rocker whose motion is guided by a crank. The rocker turns about a ground pivot and is pivoted to a connecting rod which then drives a linear motion rail. The mechanism was designed to handle the torque and friction forces that will be applied. A right-angle gearbox and servo motor were chosen to drive the linkage. Three linkages were efficiently packaged within the 250 mm x 250 mm x 1000 mm work envelope specified by the sponsor to deliver motion along three different axes.

Table of Contents

Table of Figures

Table of Tables

Introduction

The sponsoring company for this project has high-speed production lines equipped with assembly machines that contain many accurate cam driven linkages. The machine consists of one or two camshafts that drive every tooling station along an indexing conveyor belt. The follower train of each cam is connected to a linkage mechanism whose output is the end-of-arm-tooling (EOAT). There is very accurate timing between the conveyor and the camshaft that runs at constant speed. The multiple cams have different profiles based on the required output motion of the linkage.

There are however, some disadvantages pertaining to the use of cam driven machinery throughout the sponsor's factory. One particular concern is with the problem of cam and follower wear on many machines. The replacement of cams is expensive due to down time of the machine and the cost of manufacturing the cam. One of the other major disadvantages is the lack of flexibility of cam motion outputs. Once a cam profile has been generated for a specified output motion, it cannot be used to carry out any other production operation.

One of the methods to improve flexibility is to operate each tooling station motion with its own servo motor. There will be no longer a need to run the mechanism input at constant speed and theoretically, numerous ranges of stroke for different segments of input rotation could be obtained. Servo motors offer accurate control of the mechanism's output position, velocity and acceleration controlled with feedback loops.

The goal of this project is to design a flexible tooling station consisting of three servo driven linkage mechanisms with different stroke outputs. Many linkage models with adjustability factors have been researched and the optimal linkage that suits the project sponsor's criteria was chosen for further analysis and design optimization.

Two mechanisms were designed and kinematic, dynamic, and stress analyses were conducted. A variation of the design shown in **Figure 1** was used as the basic model for the mechanism and was obtained from the "Mechanisms and Mechanical Devices Sourcebook" (Sclater & Chironis, 2001). The linkage has an input crank attached to a slotted link via a slider (point A). This link turns about a pivot at the opposite end, and it is connected to an output slider (point C) near the middle of its length. The output slider is attached to the slotted link by a

sliding joint and thus produces a straight line motion. The longest link of the linkage shown as the "Slotted link" in **Figure 1** can also be adjusted by moving its pivot point vertically by turning a crank at the bottom labeled as the "Adjustment".

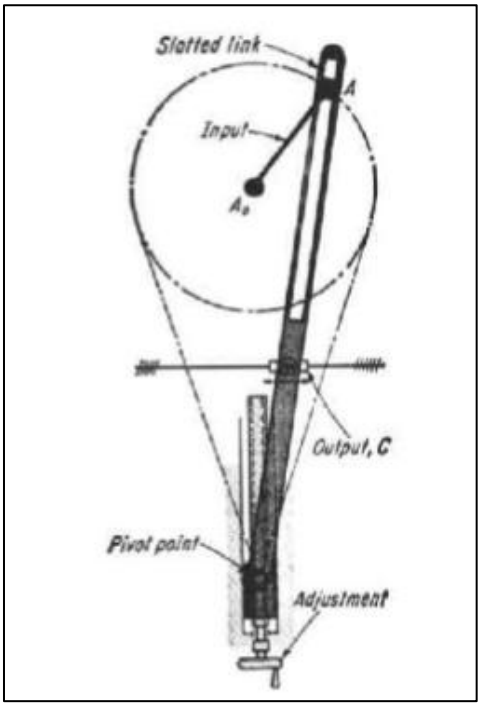

Figure 1: Adjustable pivot mechanism to change output stroke by Slater and Chironis

The software Pro/Engineer Wildfire 4.0™ was extensively used for the design and analysis of the linkage. The geometric constraints and packaging requirements were provided by the sponsor and guided the design of the linkage. An accurate model of the linkage was used for the Pro/Mechanisms application to conduct kinematic and dynamic studies.

The servo motor's input parameters were derived using data from program Dynacam™ and MathCad. The slider served as the output of the linkage and its position, velocity, acceleration and jerk equations were mathematically derived and tested. Dynamic analysis was further conducted using Pro/Mechanism in order to show that the mechanism operated under the safety factors provided by the sponsor. The design description and the results of the design along with the iterative steps taken will be further described in the report.

Goal Statement

Design a tooling station with servo-driven linkages for variable stroke output and output motions along three different axes

Task Specifications

1) A linkage mechanism for the desired output will be designed.
2) The linkage will be driven by a servo motor
3) One tooling station needs to fit within in an envelope of 250 mm by 250 mm by 1000 mm.
4) At least 3 mechanisms need to fit within the above envelope.
5) At least 2 mechanisms need to work on the product along one axis.
6) The output stroke of the end-of-arm-tooling (EOAT) needs to be adjustable, up to a maximum of 56mm.
7) The absolute position adjustability of ± 30 mm relative to a reference fixed point is needed
8) Static and fatigue failure safety factors of 2.0 will be used.
9) A minimum of 10-year life on all failure calculations of the mechanisms will be used.
10) All manufacturers' engineering recommendations such as de-rating factors and service factors will be considered.

Background

When creating a linkage there are many methods available to design the optimum linkage for an application. The same holds true for designing an adjustable linkage. This section explores several of these methods, both of an analytical and a physical nature. One can use analytical methods and equations or graphical methods to design a linkage. Once designed, the linkage still must be made, so a good design will incorporate both the best equations for the path to be followed, and a reasonable method of production and construction.

There has been much work in the field of adjustable linkages, ranging from those that are only adjustable when stopped to linkages that adjust link lengths while in motion. More commonly occurring, are linkages that are set to one position, run, then stopped and reset before moving again. These can be used to calibrate a machine, or to provide more variability to a machine's capabilities.

Some linkages can adjust their own lengths during movement to provide more accurate or more flexible coupler curves. One type (Rastegar & Yuan, 2001) uses smart materials to adjust the coupler link. Such materials, like piezoelectric ceramics, actively adjust size or shape in order to keep the coupler point in a more accurate position. This and similar methods can reduce vibration in the output motion and improve overall performance. A similar method is to allow the link or pivots to flex, and their exact positions are then determined by external loads similar to a spring in compression or tension.

A third type of linkage that can adjust during motion provides actuators on one or more links. These can be used to shorten or lengthen a link and change the coupler curve. One likely application of this would be in an assembly line or conveyor system where there are two possible destinations for one object. A pick-and-place arm could pick up the item and deliver it to either place simply by extending the length of one link during its motion.

Additionally, there are linkages not specifically designed for continuous automatic adjustment. Although it is possible to attach an actuator to many of these, they are designed to be discretely or manually adjusted. Beyond adjusting the link lengths, three methods for doing this include adjusting the output pivot point, adjusting the crank pivot point (or another ground pivot

should the linkage contain more than four links), and creating a fifth link that locks with another link at a variety of possible angles.

It is also possible to adjust the location of a fixed pivot. This is most readily seen on a simple four bar slider crank. As can be seen in **Figure 2** (Mechanism, 2007), the crank controls the stroke of the slider and changing the distance between the crank and the slider can change the top dead center position of the slider. Moving the ground pivot of the crank will result in a one to one shift in the slider's position. This is especially useful when a slight adjustment of location along a single axis is needed; although, in more complicated systems, changing a ground pivot (if there are more than 4 links it does not necessarily have to be the crank pivot) can change the output motion in addition to its phase.

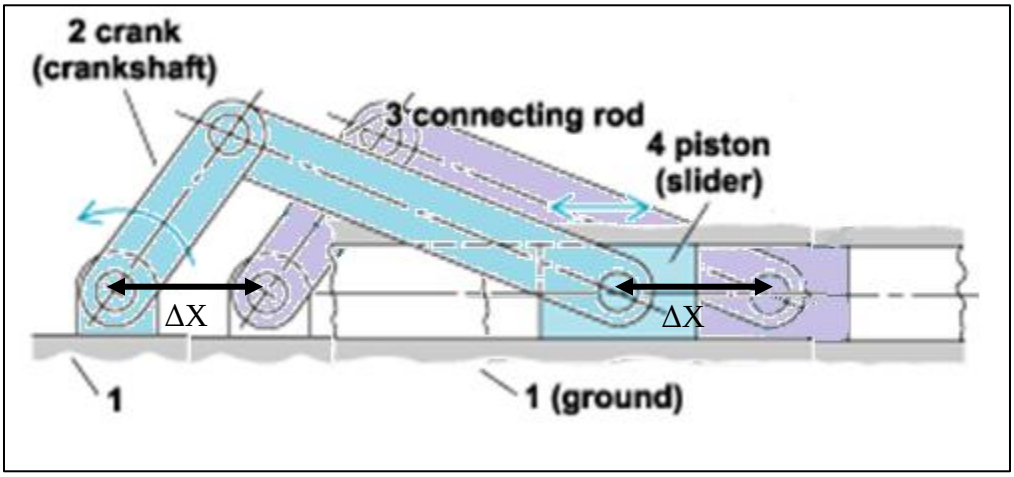

Figure 2: Four bar Slider Crank

By moving the pivot between the ground (link 1) and the crank (link 2) a distance ΔX along the horizontal axis, the slider will change location an exactly equal amount. In this manner a small adjustment can be made to the output location by only changing the location of the ground (link 1). Many methods are available for accomplishing this including, but not limited to, an open slot with a locking mechanism (such as a nut and bolt), a ratcheting or geared mechanism, and preset holes or slots in the ground link to accept the end of link 2.

It is also possible to have an adjustable linkage by adding more links. Creating a five bar linkage will provide significantly more flexibility in terms of possible outputs. Naik and Amarnath have developed a method by which five links are originally made, then one is locked

into place with another, creating a four bar linkage (Naik & Amarnath, 1989). This can be used mathematically, with the equations they have laid out, but it works equally well physically where one pivot can be locked into place to reduce a five bar linkage to four bars. When placed in an assembly machine, for example, it can be adjusted to get the most efficient and accurate output. Should the output need to be changed, it can be adjusted again at a future date.

For example, the five bar linkage in **Figure 3** (Naik & Amarnath, 1989) can be reduced to a four bar by locking joint *C* to make links *b* and *c* a single link. Alternatively, joint *D* can be locked to make links *c* and *d* a single link. This would change the length of link *BD* and *CE*, respectively, represented by the dashed lines in **Figure 3**. In a manufacturing setting, the most likely use would be to adjust the output motion minutely when first setting up a machine. It could also be used to readjust a machine if it developed a small error.

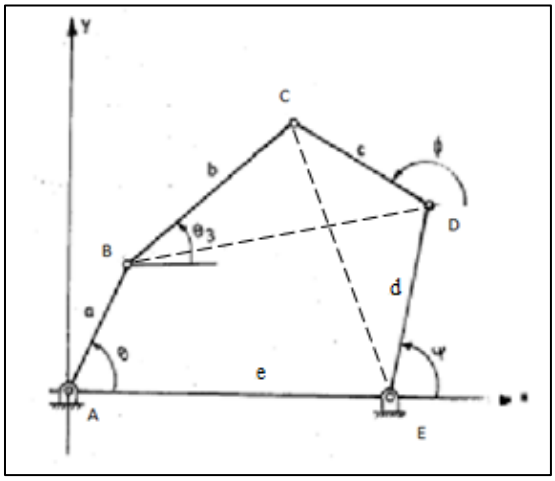

Figure 3: Naik and Amarnath's Reduced Five Bar

To solve this numerically, the five bar closed loop equations would be written with the appropriate angle made a constant, instead of variable. The reason behind using five bar equations is that when one angle becomes fixed, the five bar equation reduces to a solvable state, but does not contain sums of squares. If four bar equations were used the two locked links would be treated as one, but this would require the sum of the squares of the links and significantly complicate the solution to the closed loop vector equations.

The "Mechanisms and Mechanical Devices Sourcebook" (Sclater & Chironis, 2001), mentions a few adjustable-stroke mechanisms. Since the required type of motion for this project

is a straight line, the adjustable-slider drive proved to be most relevant. The adjustable-slider drive (Sclater & Chironis, 2001) (left) with a kinematic diagram (right) is shown in **Figure 4**.

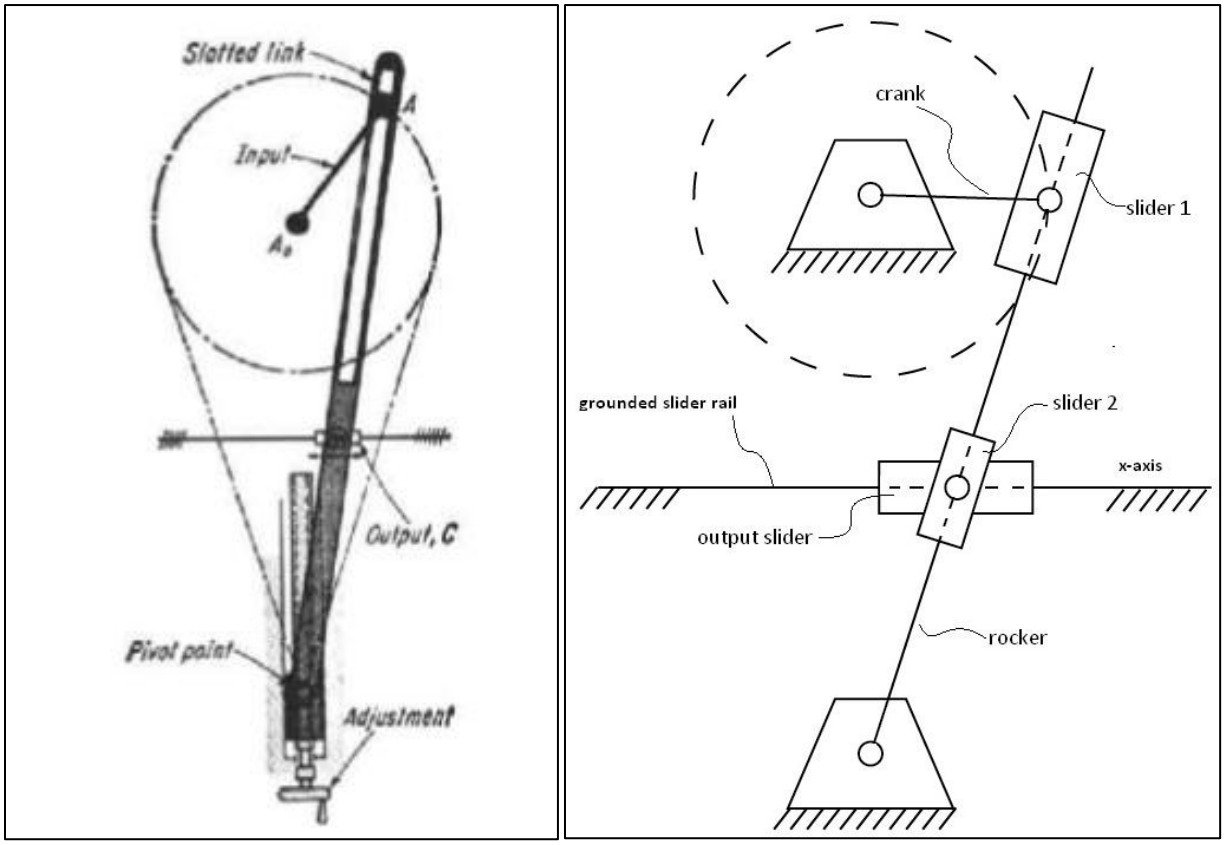

Figure 4: Adjustable-slider drive

The output will always be a straight line along the x-axis. The crank and rocker pivots are both pin joints; however, the joint between the crank and the rocker is a two degree of freedom (DOF) joint – it can translate along the long axis of the rocker and rotate in the X-Y plane. Similarly, the output slider is attached to the rocker with a two DOF joint. The output slider is then connected to the grounded slider rail by a one DOF translating joint. Using the Kutzbach equation shown below the degrees of freedom for the mechanism was calculated.

$$m = 3(n - j - 1) + \sum_{n=1}^{j} f_i$$

$$m = 3(5 - 7 - 1) + 10 = 1$$

where n = 5 links, j = 7 joints, and the sum of degree of freedoms of the joints = 10.

In addition, this mechanism provides the user with the ability to adjust the rocker pivot along the vertical axis in order to generate different output levels. The closer the rocker pivot is moved to the crank pivot, the larger the range of the output slider will become.

A major shortcoming of this linkage is that the output range can never be greater than the length of the crank. A simple way to overcome this difficulty is to switch the positions of the output slider and the rocker pivot, as shown in **Figure 5** and **Figure 6**. By placing the rocker pivot between the output and the crank, the output range can be theoretically increased from the length of the crank to infinity (although link lengths and vibrations would restrict it in practical uses).

Design Process

Design Iterations

Looking at the three linkages that were previously analyzed, the adjustable slider drive linkage shown in **Figure 4** was chosen. This design was chosen because the size of the parts was much smaller than the other designs while still getting the desired stroke length. The size of the linkage is the most important aspect of our design considerations because it needs to be able to fit three of the linkages in the same envelope on different axes.

Before running any analysis on the linkage, the link lengths that will be used in the assembly needed to be initialized. A preliminary design as used for the kinematic and dynamic analyses of the linkage. Design iterations were performed to alter the kinematics and dynamics.

The kinematic design of **Figure 4** was modified initially and established the preliminary design of the linkage. The kinematic diagram can be seen in **Figure 5**. As before the output slider's motion is constrained on the x-axis. The crank and rocker pivots are both pin joints; and the joint between the crank and the rocker is a two degree of freedom (DOF) joint as before. The main difference is that the grounded slider rail and the pivot of the rocker switched locations. The previous design in the background research limited the output stroke of the slider to be less than the length of the crank. With the modified design shown in **Figure 5**, greater stroke is achieved for the same amount of crank rotation as before. The degrees of freedom for the linkage in **Figure 5** were calculated as follows:

$$m = 3(5 - 7 - 1) + 10 = 1$$

where n = 5 links, j = 7 joints, and the sum of degree of freedoms of the joints = 10.

The degree of freedom is the same as that of the linkage in **Figure 4**. This is because the only difference is that the location of the grounded slider rail and the rocker's pivot were switched. The equations defining the kinematics of the output slider will be later discussed in the report.

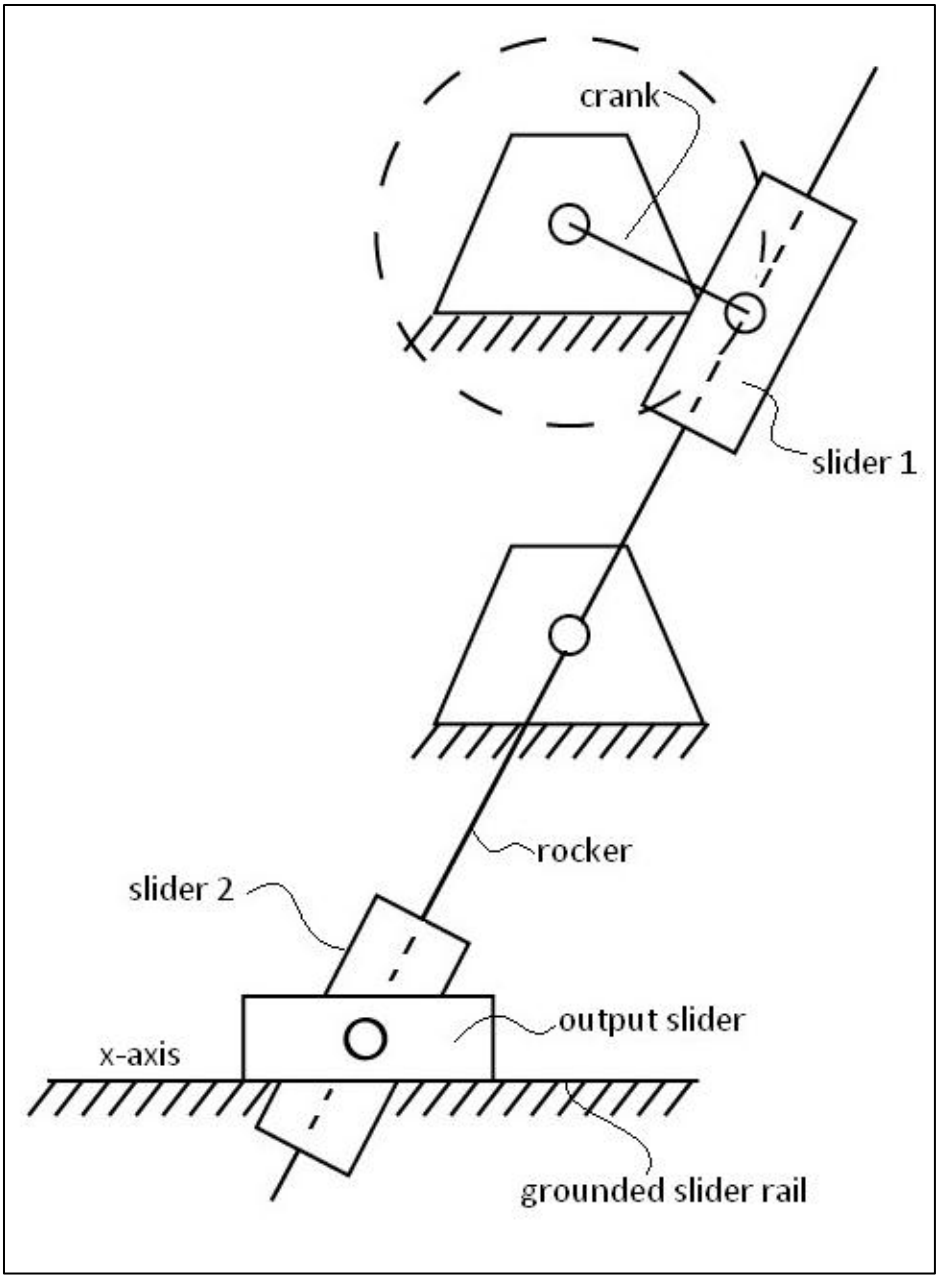

Figure 5: Kinematic Diagram of the preliminary design

The first iteration's Pro/Engineer model is shown in **Figure 6**. There are two slider slots that allow the crank to rotate and the slider to translate while the rocker is pinned to ground. The link lengths for this model were chosen based on the drawing of the linkage found in the background section.

After finalizing the dimensions of the parts, the linkage was placed in its pre-determined work space. Also, all the off-the-shelf parts were added into the model. The off-the-shelf parts consist of the THK rail and slider, the thrust bearings, washers, bolts and the servo motor. The THK rail was introduced as requested by the sponsor, as it is a common part used in their assembly line machines. The THK slider is mounted to the ground as the rail is used to obtain the desired output. This is the reverse specifications of its common use. The reason for this reverse setup is because the sponsor uses the THK rail and slider as seen in the preliminary design. The end-of-arm-of- tooling could also be mounted on any location along the rail giving the sponsor additional flexibility to place the linkage away from the end effect.

The preliminary design in **Figure 6** is a variation of the linkage from the background research that in **Figure 4**. The differences between the two linkages are the position of the ground pivot and the slider mechanism. In **Figure 4**, the ground pivot is at the bottom of the rocker and the slider is located at the middle of the rocker, which moves up and down within the rocker. The slider mechanism runs within the rocker similarly to the original linkage. This change was made because the output stroke could never be greater than the crank length; however, in the preliminary design iteration, the output stroke is longer the crank length.

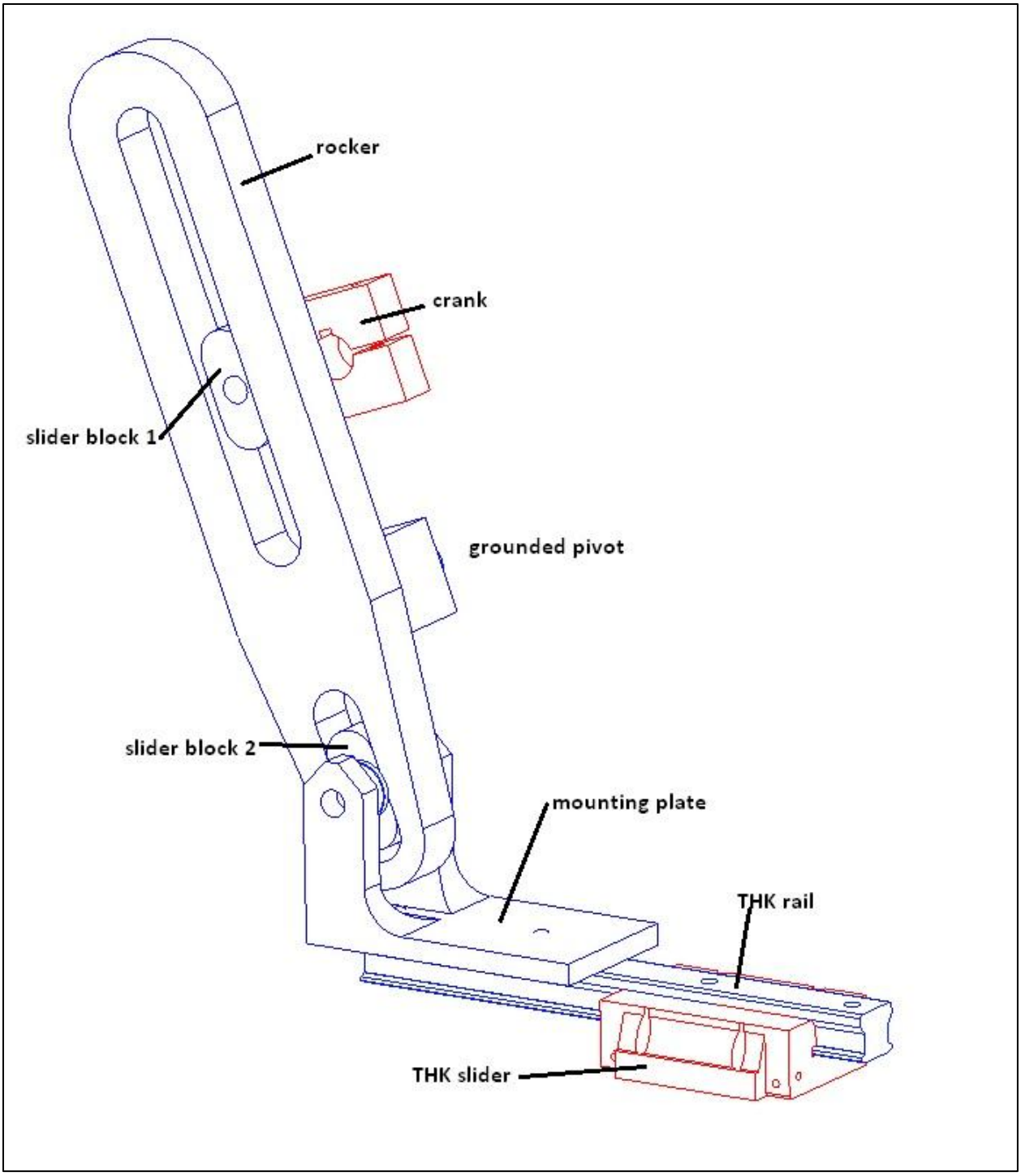

Figure 6: Preliminary Design of the mechanism

Once this design was complete, Pro/Engineer was used to run dynamic tests on the model. After running dynamic tests on the design, it was observed that the slot at the bottom of the rocker was prone to wear and fail often because a great deal of stress will be acting within

this slot. This was an issue considering the fact that this mechanism would be used in a production line machine with extremely high number of cycles per day.

An alternate design was desired to avoid the problem of wear inside another slot on the rocker. In addition, a better dynamic performance was also necessary. The second design iteration's kinematic diagram can be seen in **Figure 7**. According to the Kutzbach equation, the degrees of freedom for the linkage were calculated as shown below.

$$m = 3(5 - 9 - 1) + 16 = 1$$

where n = 5 links, j = 9 joints, and the sum of degree of freedoms of the joints = 16

The derivation of the kinematic equation defining the motion of the output slider will be discussed later in the report. The main change in this design is that the slider joint between the output slider and the rocker was replaced with a connecting rod. The output slider's motion was still constrained on the x-axis (grounded slider rail). This design reduced the wear in the slot of the rocker.

An alternate design was proposed by the team to ensure less ware. This second design shown in **Figure 8** would replace the bottom slider with another crank which is connected to the LM THK rail.

Similar to the initial design, the mechanism was also placed in its work space with all the necessary parts. In this case the off the shelf parts consist of the THK rail and slider, the thrust bearings, cranks to connect to the bottom of the rocker, washers, bolts and the servo motor. The design also includes a plate that connects to the THK rail. This plate was designed to house the unique rocker and double-crank system that is at the bottom of the linkage. The final version of the linkage can be seen in **Figure 8**.

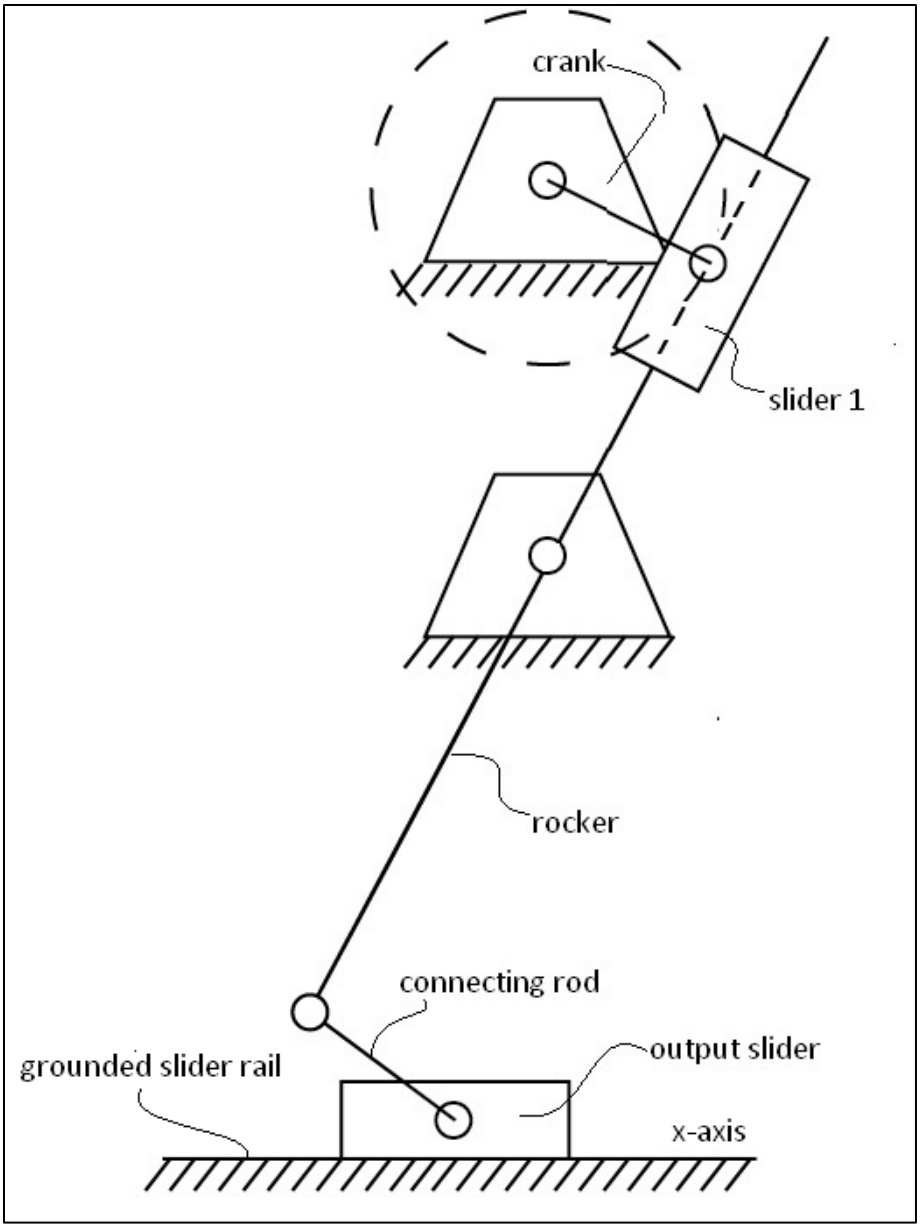

Figure 7: Kinematic diagram for the second iteration and the finalized linkage

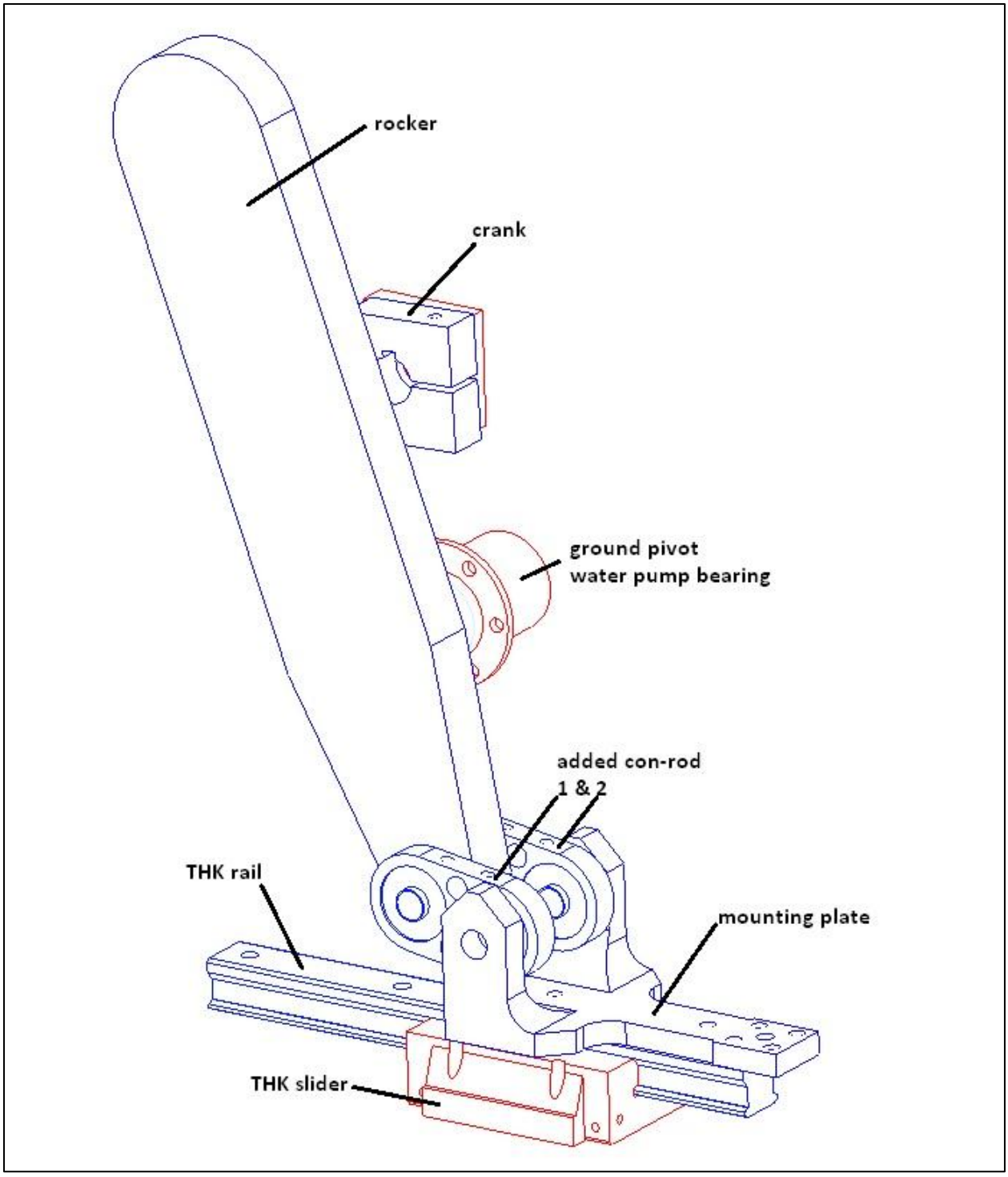

Figure 8: Final design of the linkage mechanism

Kinematic analysis of the preliminary design

The preliminary design was first analyzed and its kinematic equations for the slider's position, velocity, acceleration and jerk are as follows:

Position: $x(\Theta) = -h\frac{l_2\cos(\Theta)}{l_1 + l_2\sin(\Theta)}$

Velocity: $\dot{x}(\Theta) = \omega(\Theta) = h\frac{{l_2}^2\cos(\Theta)^2}{(l_1+l_2\sin(\Theta))^2} + h\frac{l_2\sin(\Theta)}{l_1 + l_2\sin(\Theta)}$

Acceleration: $\ddot{x}(\Theta) = \alpha(\Theta) = h\frac{l_2\cos(\Theta)}{l_1 + l_2\sin(\Theta)} - 2h\frac{{l_2}^3\cos(\Theta)^3}{(l_1+l_2\sin(\Theta))^3} - 3h\frac{{l_2}^2\cos(\Theta)\sin(\Theta)}{(l_1+l_2\sin(\Theta))^2}$

Jerk: $\dddot{x}(\Theta) = j(\Theta) = 6h\frac{{l_2}^4\cos(\Theta)^4}{(l_1+l_2\sin(\Theta))^4} - 4h\frac{{l_2}^2\cos(\Theta)^2}{(l_1+l_2\sin(\Theta))^2} + 3h\frac{{l_2}^2\sin(\Theta)^2}{(l_1+l_2\sin(\Theta))^2} - h\frac{l_2\sin(\Theta)}{l_1+l_2\sin(\Theta)} + 12h\frac{{l_2}^3\cos(\Theta)^2\sin(\Theta)}{(l_1+l_2\sin(\Theta))^3}$

Where

Θ – angular position of the crank

l_2 – length of the crank

l_1 – distance between the two fixed pivots of the crank and the rocker

h – distance between the fixed pivot of the rocker and the fixed slider axis

These dimensions have been labeled in **Figure 9**. All the equations above are with respect to the angular position of the crank, Θ and were derived with the help of the kinematic diagram (**Figure 5**). The zero axis for angular rotation is the vertical line. The crank angle, Θ is with respect to the vertical line between the pivots of the crank and the rocker. The adjustment parameter in the above quantities is l_1 because the fixed pivot of the rocker is the point that can be adjusted to achieve different stroke lengths. However, this change creates different profiles

for position, velocity and acceleration. An optimum ratio between l_1 and l_2 that resulted in steady velocity and accelerations was found in the following analysis. In MathCad, the kinematic equations were evaluated for small incremental values of angular positions, Θ from 0 to 360 degrees and for different l_1 values. The data was then exported to Microsoft Excel to clearly show the position, velocity and acceleration trends. The lengths used for the other parameters are as follows: l_2 = 15 mm and h = 25 mm. The l_1 values were incremented by 1.5 mm to obtain different slider displacements, velocities and accelerations.

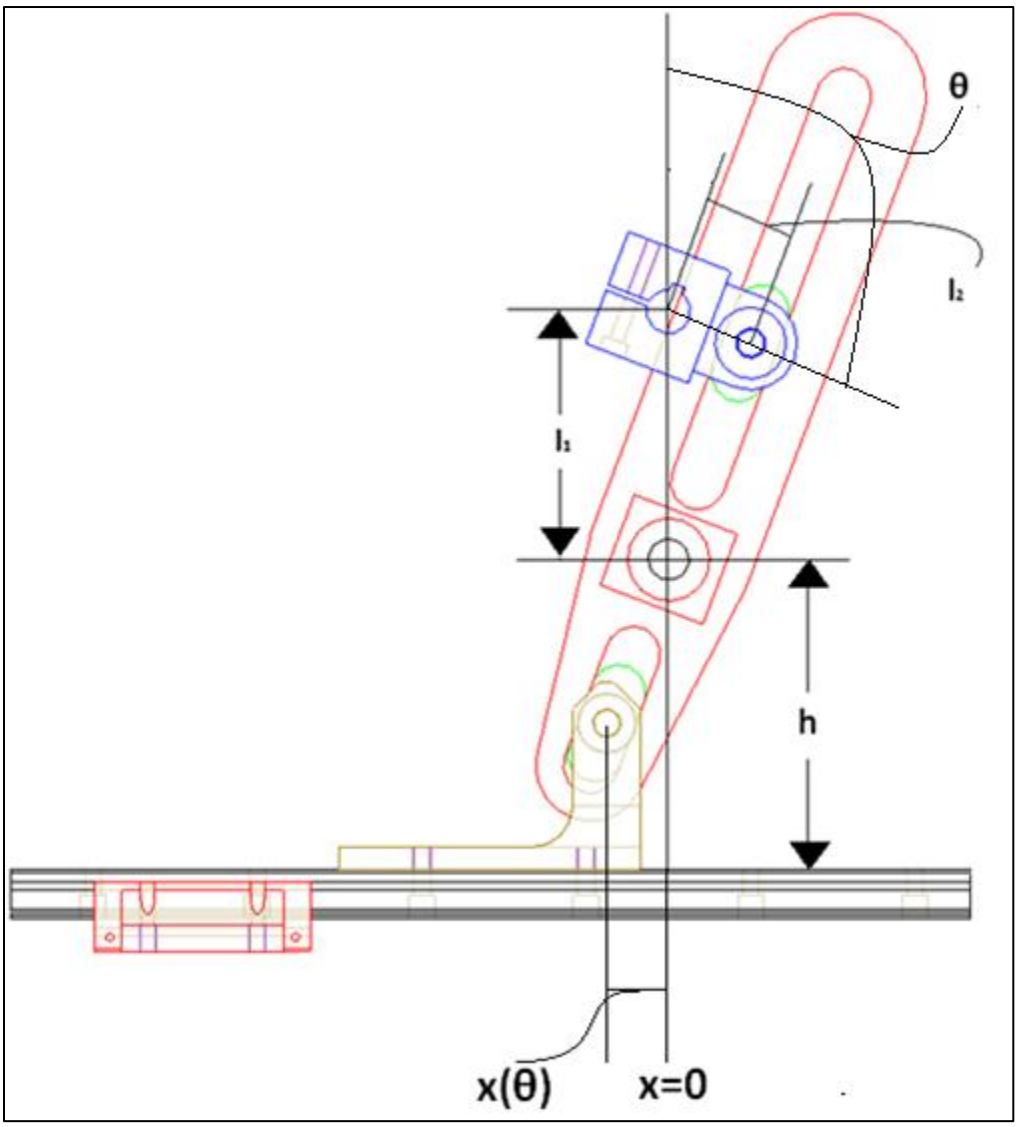

Figure 9: Preliminary design dimension labels

The functions for the position, velocity, and acceleration of the slider were plotted in MathCad by applying the crank angle from zero to 360 degrees. The family of curves can also be seen in

Appendix A – MathCad worksheets for kinematic analysis of the linkages and stress analysis of the along with the calculations performed. These graphs were imported to Microsoft Excel and were plotted for 8 different link length ratios between l_1 and l_2. These graphs for the position, velocity and acceleration of the slider can be seen in **Figure 10** through **Figure 12** respectively. As can be seen from the figures, there are 8 different curves for each kinematic quantity representing 8 different link ratios.

The curves were plotted for one complete crank revolution. The curves helped identify the dynamically unsteady ranges of operation of the slider. As can be seen by **Figure 11**and **Figure 12**, there are huge sudden jumps in the velocity and acceleration. These spikes show unsteady and dynamically unfavorable areas of operation. Lines A and B in all the graphs show the smoothest range of operation where there are no sudden jumps in velocities and accelerations. The middle red line shows the zero position of crank angle and slider position. The slider does not see jumps in velocity and acceleration between -120 degrees and +120 degrees (lines A and B). Any region outside of this range of crank angle would be unfavorable in terms of jumps in forces and vibrations throughout the linkage.

As can be seen from the graphs, the "30" curve was the smoothest curve. The corresponding l_1 value of 30 mm is shown in the "30" curve. After selecting this curve, all the link lengths (labeled in **Figure 9**) were multiplied by a factor of 3 such that the desired maximum stroke of 56 mm was achievable. For the CAD model, the link lengths that were chosen were as follows: l_2 = 30 mm, l_1 = 90 mm and h = 75 mm (see **Figure 9** for labels). These link length values and the range of crank angles were applied to the linkage in Pro/Engineer for further kinematic and force analyses.

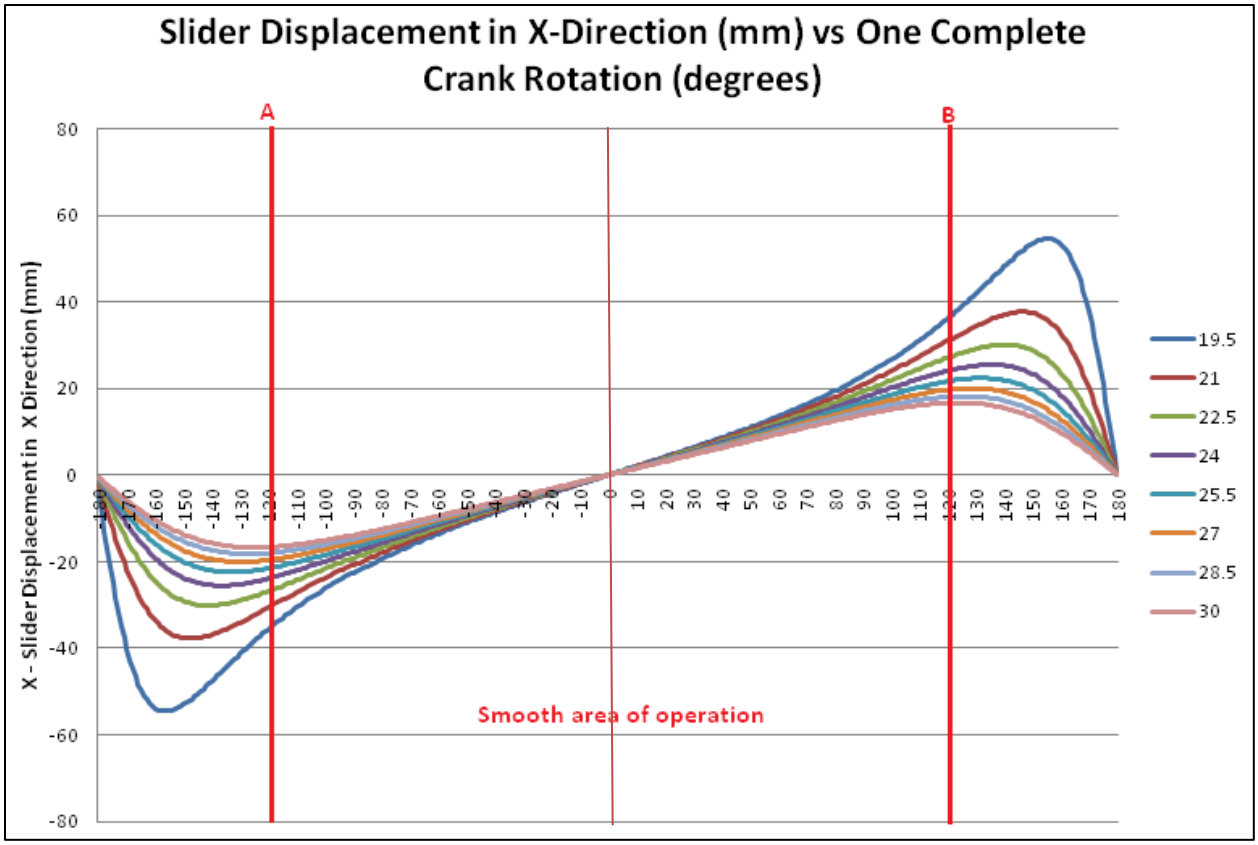

Figure 10: Slider displacement curves for different link length ratios with respect to crank angular position

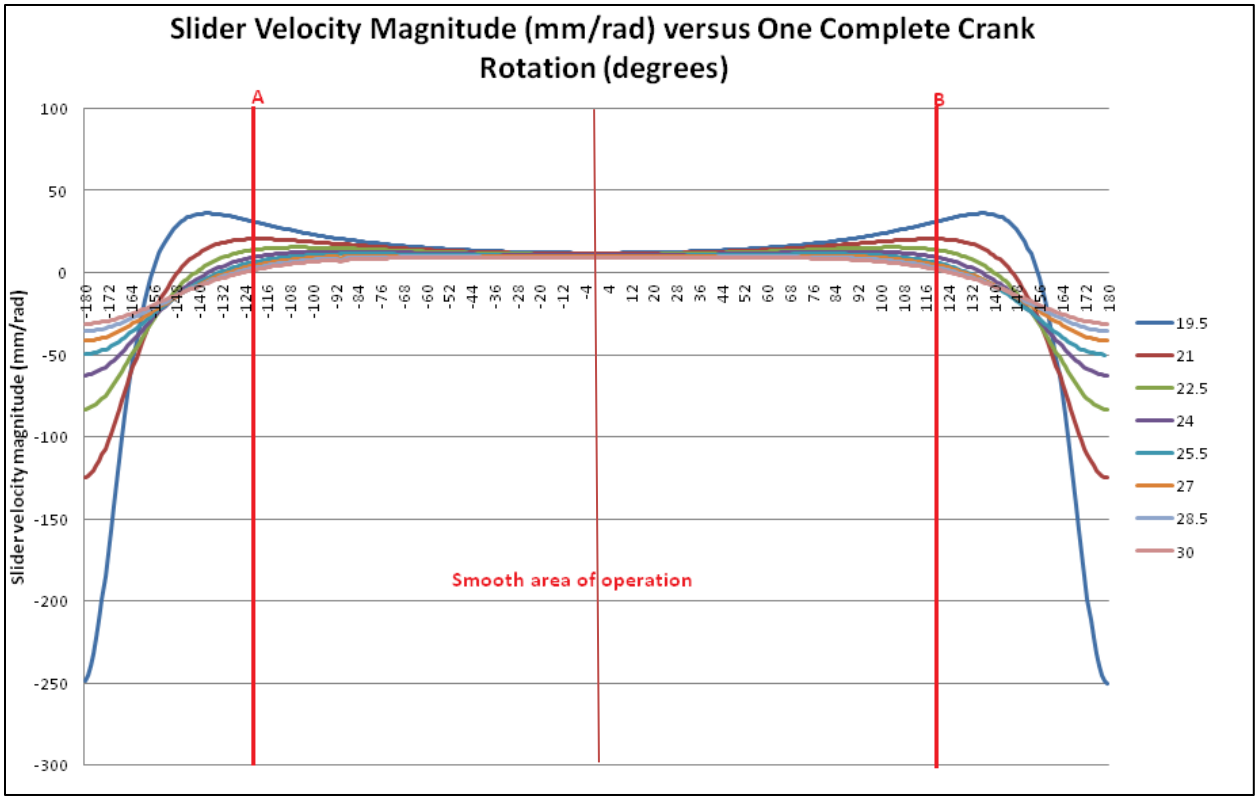

Figure 11: Slider velocity curves for different link length ratios with respect to crank angular position

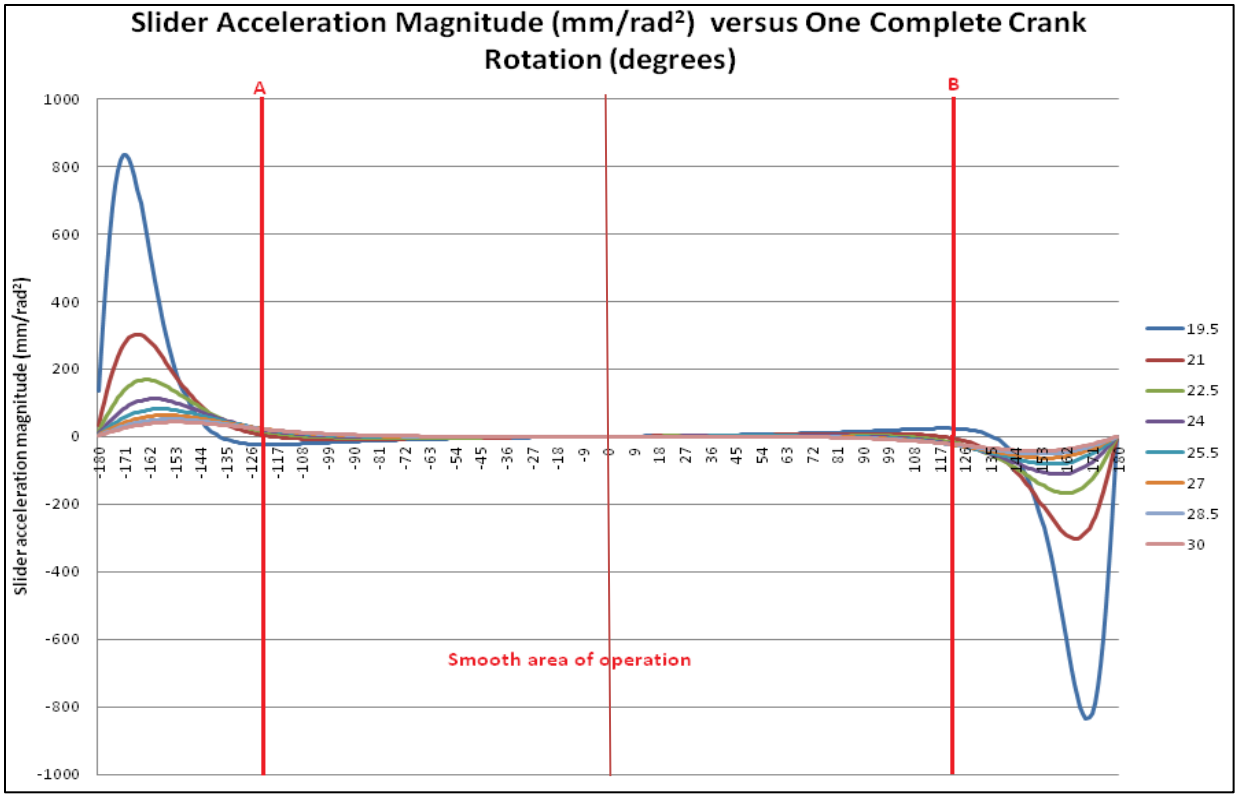

Figure 12: Slider acceleration curves for different link length ratios with respect to crank angular position

The crank's rotation follows a total path of 240 degrees or ±120 degrees from the zero (vertical) axis. As shown in **Figure 13**, the top portion of the crank's rotation was categorized as the smooth area of operation. For the 240 degrees of crank rotation, the link lengths were modified to yield a stroke of 56 mm. At point x=0, the crank is vertically upwards at a crank angle of zero degrees. The crank angular position can be controlled by a servo motor to avoid rotation along the downward portion of the dashed circle shown in **Figure 13**. As mentioned earlier, this area results in the spikes in slider's velocity and acceleration, which will cause unsteady vibrations throughout the linkage. Note that **Figure 13** is not to scale and has just been used to demonstrate a path for the crank's rotation and the resulting position of the slider.

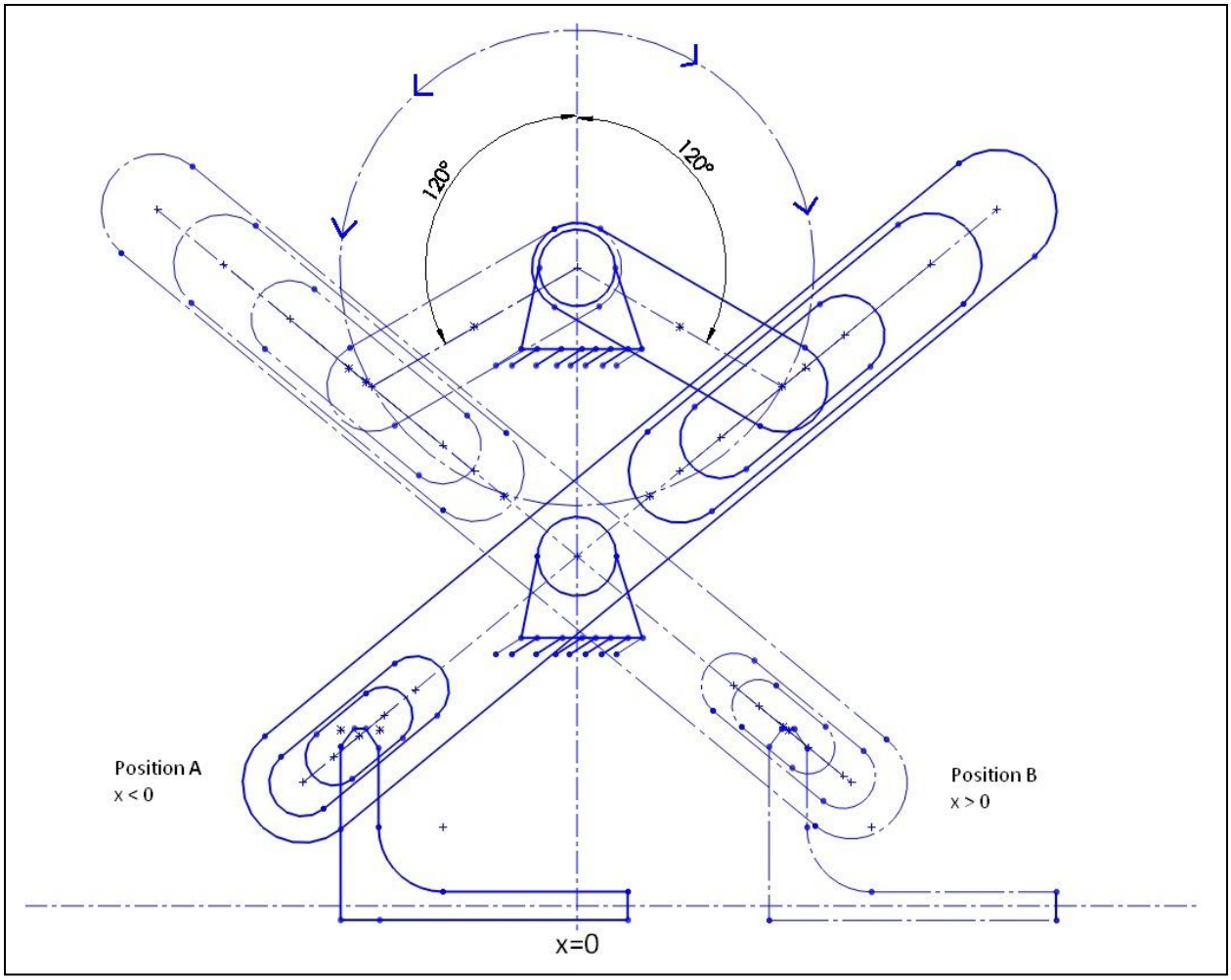

Figure 13: Slider position with respect to angular position range of the crank

Modeling of the crank's angular position inputs with respect to time

A servo motor was the desired motor type to be used to run the crank of the linkage. In order to conduct a detailed kinematic, force and torque analysis on Pro/Engineer, a table of servo angular position versus time (in seconds) was necessary. A convenient way to derive this input function for the servo motor was to use program Dynacam™. The angular positions for the linkage's motion from the previous analysis were taken to be 240 degrees. The desired cycle time for the linkage was 0.25 seconds. In order to achieve a complete cycle of the linkage, a total of 480 degrees of crank rotation was necessary. The following calculation was used to determine the input rpm speed for program Dynacam™.

$$\frac{480\ degrees}{0.25\ seconds} = 1920\frac{deg}{sec} * \frac{60\ sec}{1\ min} * \frac{1\ rev}{360\ deg} = 320\ \frac{rev}{min} = 320\ rpm$$

The calculated speed of 320 rpm was used for the input rpm for program Dynacam™.

The software simulates the follower motion based on desired user inputs for different segments of cam rotation. These segments are based on different ranges of one full cam revolution. One needs to specify the start and end conditions for the follower motion with respect to segments of cam rotation. In order to simulate, the two segments of crank rotation for the linkage mechanism, two segments were used in Dynacam™. This mechanism must rotate through 240 degrees of crank rotation from position A to position B of the linkage as shown in **Figure 13**.

In Dynacam™, a complete cam revolution of 360 degrees was needed, and two equal cam rotation segments were used. Polynomial functions were used for each of the segments in order to set the boundary conditions such that a continuous acceleration function without infinite jerk can be obtained. These boundary conditions represent the motion of a follower in the software. To simulate crank rotation, these boundary conditions represented the rotation of the crank. The start and end for the first segment was 0 and 240 degrees of crank rotation respectively. For the second segment, the start and end positions were switched to 240 and 0 degrees of crank rotation respectively.

Figure 14 shows the boundary condition values for the first segment of motion. The position values at start and finish are 0 and 240 degrees respectively. The velocity and jerk were set as zero for start and finish. The acceleration was set to zero at start but was not specified for the end condition. In Dynacam™, the required crank degrees were input as millimeters. As seen in the right portion of **Figure 15**, the resulting polynomial function for this segment is a sixth degree polynomial.

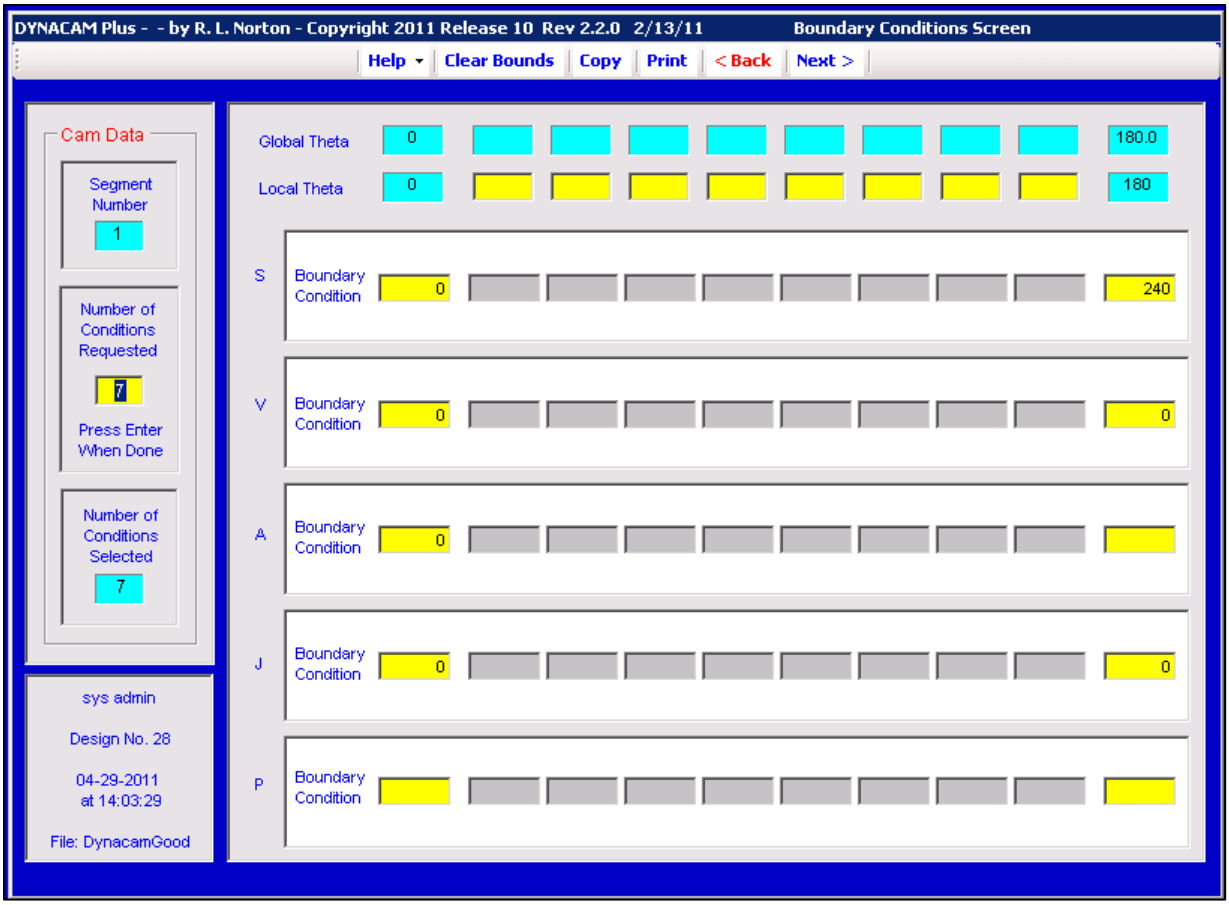

Figure 14: Definition of boundary conditions for the first segment

Boundary Conditions Selected and Resulting Displacement Equation Coefficients

Boundary Conditions Selected

Coefficients for S Equation with Theta/Beta as Variable

Boundary Conditions Imposed

Function	Theta	% Beta	Boundary Cond.
Disp	0	0	0
Veloc	0	0	0
Accel	0	0	0
Jerk	0	0	0
Disp	180	1	240
Veloc	180	1	0
Jerk	180	1	0

Equation Resulting

Exponent	Coefficient
0	0.000 000
1	0.000 000
2	0.000 000
3	0.000 000
4	2,400.000 000
5	-3,360.000
6	1,200.000 000

Figure 15: Boundary conditions and resulting polynomial for the first segment

For the second segment whose boundary conditions are shown in **Figure 16**, the start and end positions were 240 and 0; the velocity was zero at start and end; the acceleration

was not specified at start and was zero at end; the jerk was again zero at both ends. The resulting polynomial function for the second segment was a sixth degree polynomial as seen in **Figure 17**.

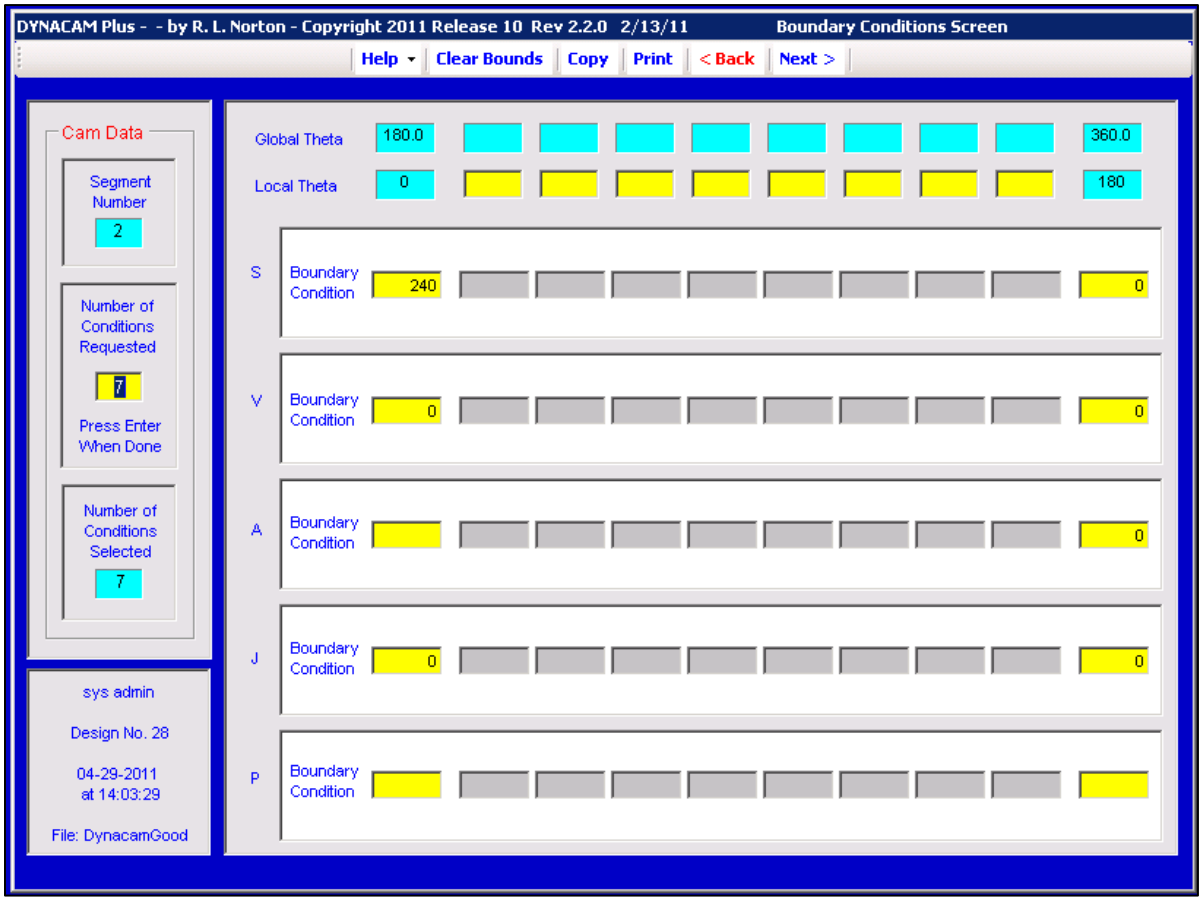

Figure 16: Definition of boundary conditions for the second segment

Boundary Conditions Selected and Resulting Displacement Equation Coefficients

Boundary Conditions Selected

Coefficients for S Equation with Theta/Beta as Variable

Boundary Conditions Imposed

Function	Theta	% Beta	Boundary Cond.
Disp	0	0	240
Veloc	0	0	0
Jerk	0	0	0
Disp	180	1	0
Veloc	180	1	0
Accel	180	1	0
Jerk	180	1	0

Equation Resulting

Exponent	Coefficient
0	240.000 000
1	0.000 000
2	-1,200.000
3	0.000 000
4	3,600.000 000
5	-3,840.000
6	1,200.000 000

Figure 17: Boundary conditions and resulting polynomial for the second segment

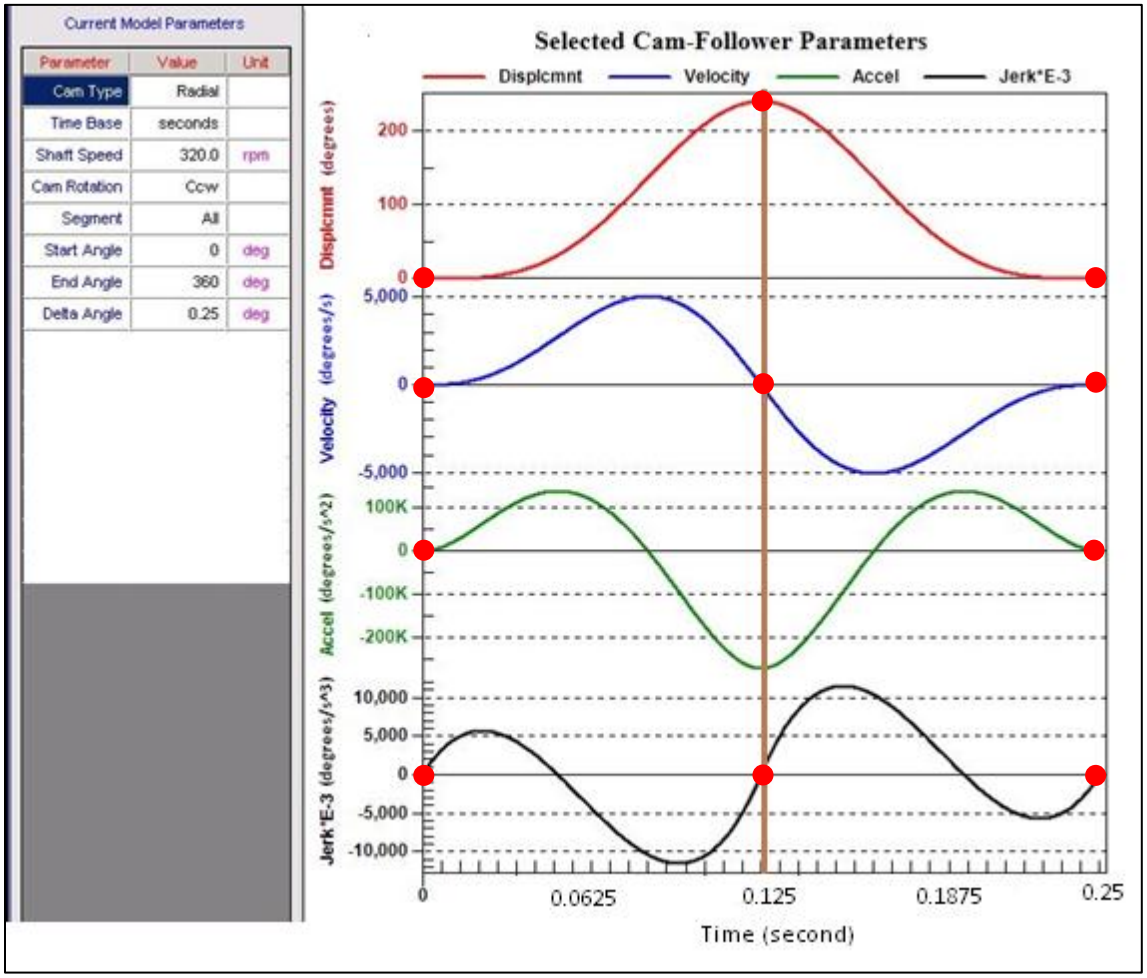

Figure 18: SVAJ plot for both the segments

The plotting tool in the program plots the position (S), velocity (V), acceleration (A) and jerk (J) functions for all the segments. The SVAJ functions are represented by the plots in **Figure 18**. The brown line in the middle of the curves indicates two equal segments of motion. Due to the specified boundary conditions, the acceleration is a continuous polynomial function and the jerk has a value of zero at the start and finish. The SVAJ plots have also been modified for the reader so that the vertical axis shows the units in terms of degrees. For instance, the position curve is in degrees and the velocity is in degrees per second. The horizontal axis shows the units of time starting from zero to 0.25 seconds. These curves show the rotation of the crank in the linkage mechanism as the crank rotates from zero to 240 degrees in 0.125 seconds and returning to zero in 0.125 seconds.

A dataset extracted from the Dynacam™ analysis in order to be used a set of angular position inputs versus time. The modeling of the crank's rotation over its necessary range with respect to time allowed for a table of values that could be used for the servo motor in Pro/Engineer.

This data table was imported into Pro/Engineer as a text format and was fed in as the profile for the built-in servo motor. The quarter degree increments of crank angle were chosen in program Dynacam™ due to the fact that the built-in servo motor application in Pro/Engineer applies its own formula between position and time points. With quarter degree angle increments, this error or noise was minimized. However, it can be seen later in the report how the curves for the higher derivatives of displacement along with the torque and forces have noise. The analysis for kinematics and dynamics was first conducted on the preliminary design. For the finalized design, the same table was used but with different conversion factors. This will be discussed in the following section.

Kinematic analysis of the finalized design

Similar to first design approach, a geometric method was taken to derive an equation for the slider's position with respect to one variable – crank angular position. The linkage model in **Figure 19** (along with the kinematic diagram shown in **Figure 7**) was used to derive an equation for the motion of the slider. This equation is as follows:

$$x(\Theta) = \sqrt{{l_4}^2 - [h - d(\cos(\tan^{-1}\frac{l_2\cos(\Theta)}{l_1 + l_2\sin(\Theta)}))]^2} + d(sin(\tan^{-1}\frac{l_2\cos(\Theta)}{l_1 + l_2\sin(\Theta)}))$$

Where:

Θ – angular position of the crank

l_2 – length of the crank

l_1 – distance between the two fixed pivots of the crank and the rocker

h – distance between the fixed pivot of the rocker and the fixed slider axis

l_4 – length of the small connecting rod

d – distance between the rocker's fixed pivot and con-rod pivot

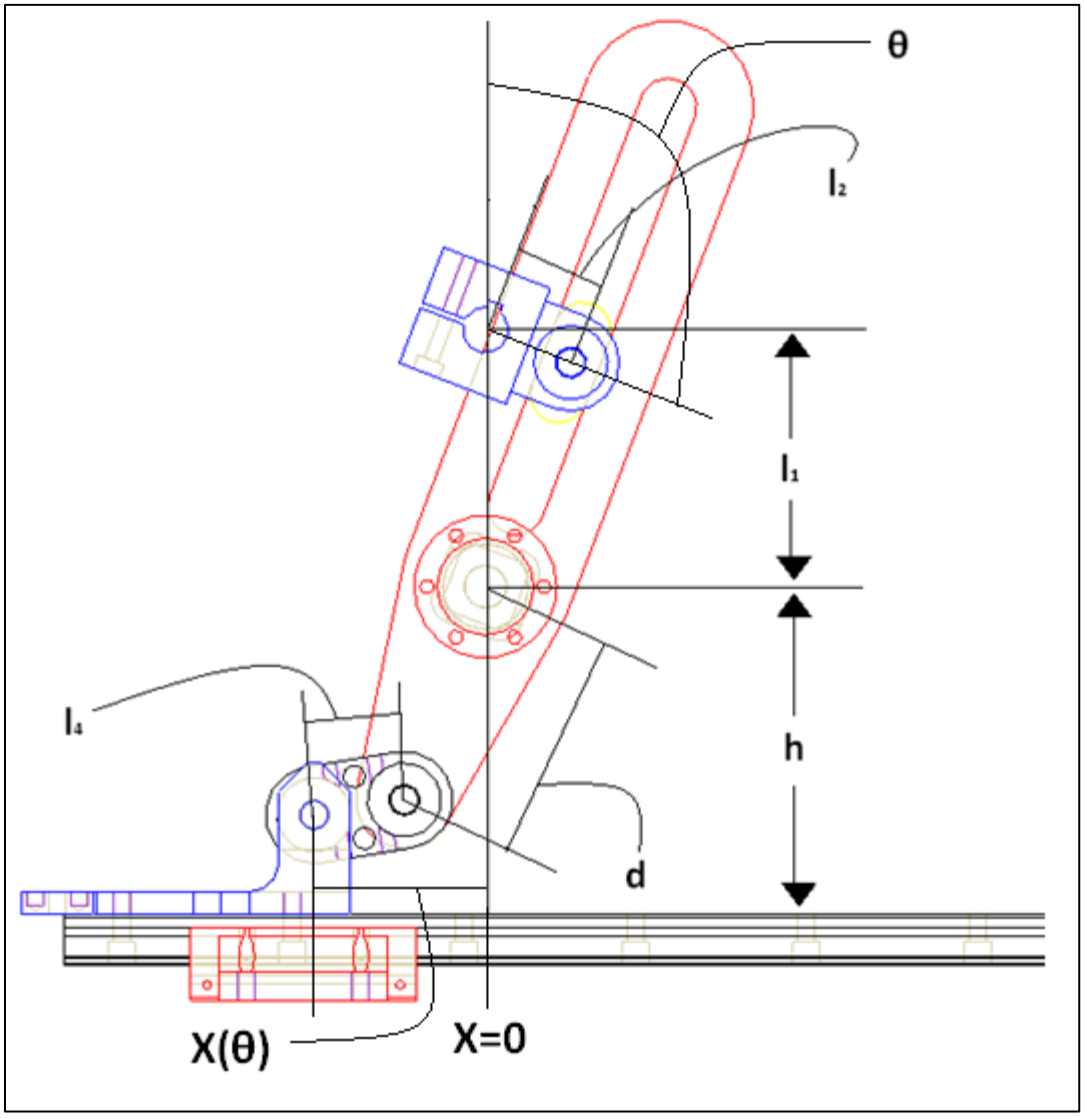

Figure 19: Final linkage dimension labels

MathCad could only symbolically display the velocity function and was able to numerically calculate both the acceleration and jerk, as shown in

Appendix A – MathCad worksheets for kinematic analysis of the linkages and stress analysis of the

Since the final design was created after and based on the preliminary design, much of the work could be used for both. The link lengths were already set, with only a small adjustment

necessary to achieve the desired output length. The same methods were used in MathCad and Microsoft Excel to produce a set of data points for the angular position of the crank. The original link lengths for the crank, rocker and the distances between the pivots were used again with the added connecting rod. This link caused a slight change in the locations of maximum and minimum stroke. The shortened stroke only required the crank to move a total of 222 degrees, instead of 240; however, the output stroke was not changed, and the crank angle has a one to one relationship with the output position over this range. Therefore, the same time and position results from Dynacam^{TM} could be used, once the crank angle was reduced by a ratio of 222/240. This was done in both Excel and Dynacam^{TM} to confirm the results.

The mathematical results found from the previous equations are shown in the successive tables and graphs.

Table 1 shows the link lengths used and resulting stroke. **Figure 20** shows the crank angle versus time with 0 degrees being the central vertical axis of the linkage. **Figure 21** shows the slider position over the same time, normalized about its own center (which is 31.89 mm from the central, vertical axis of the linkage). It can be seen that the two functions are directly related. Both functions reach their maximum, minimum, and zero values at the same time. The two functions are not linearly related; however, the slider's position has a "pseudo-dwell" at its max and min, while the crank angle does not.

Table 1: Links and Stroke from mathematical analysis of the final linkage

Dimension description	Length (mm)
Link 4 (added Con-rod)	32
Link 2 (Crank)	32
d (Rocker from pivot to Link 4)	80
Link 1 (Ground link between Crank and Rocker pivots)	90
h (Rocker pivot to horizontal sliding axis of output)	77.39
Max Slider Position (from central, vertical axis)	60.34
Min Slider Position (from central, vertical axis)	3.45
Slider Range	56.89

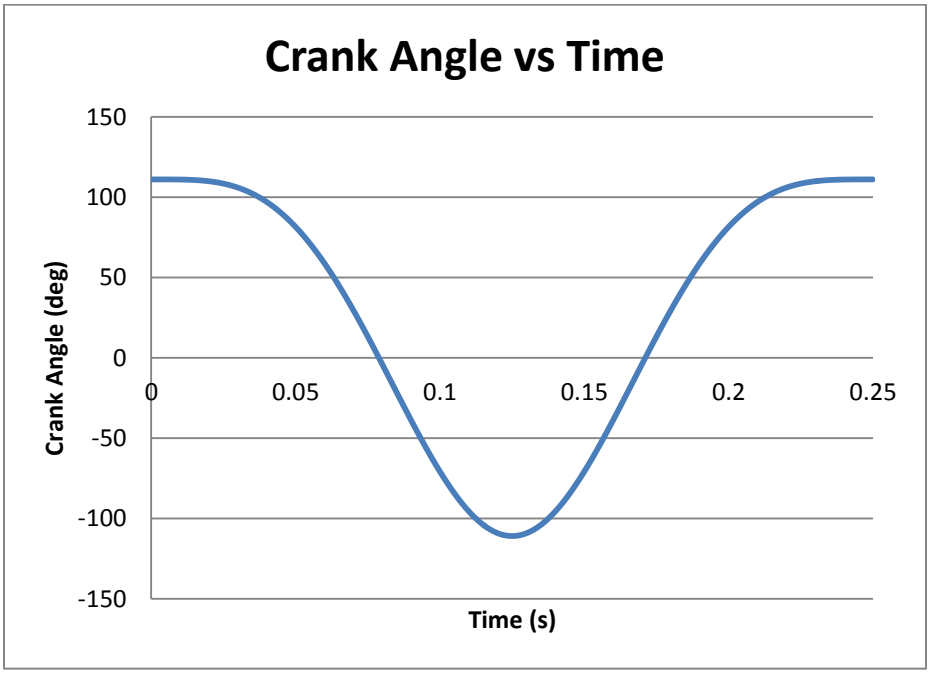

Figure 20: Mathematical Crank Angle vs. Time

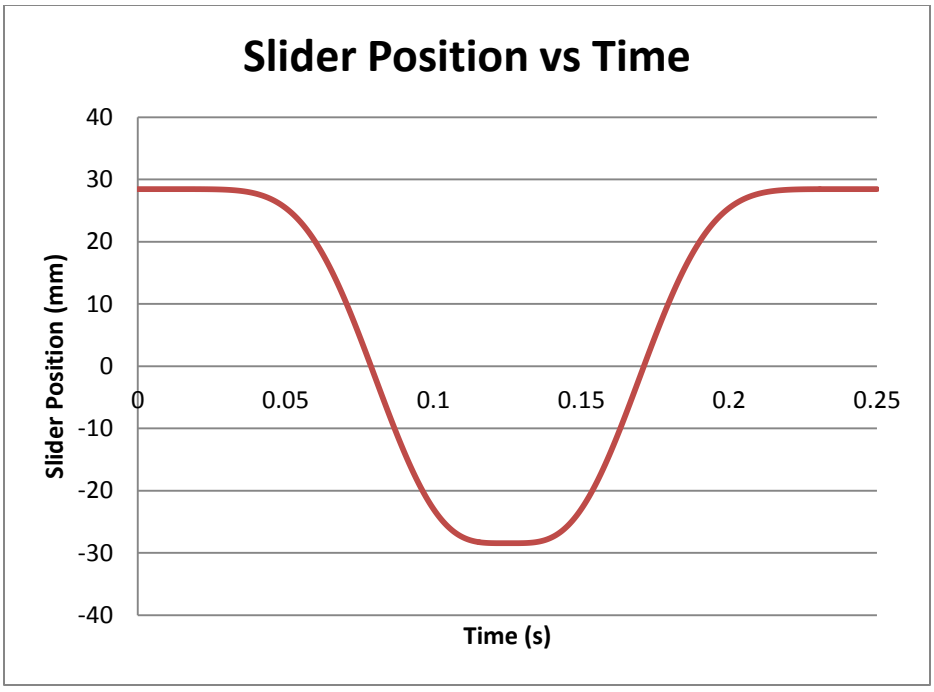

Figure 21: Mathematical Slider position vs. Time

Inverse Kinematic Equations

The inverse kinematic equations are useful to allow the sponsor to select an output function, and receive an input function. To do so, the output of the slider is defined and the input crank angles necessary are found. A similar method to solving the regular kinematic equations was used. In this case, the vector loop equations were solved for θ_2 (the crank angle) with respect to X (the slider output). In order to do so, the linkage was broken into two separate crank-slider mechanisms, as shown in **Figure 22** and **Figure 23**. The linkage was split at the rocker's ground pivot and two mechanisms were evaluated.

In the bottom linkage, seen in **Figure 22**, X is the input and φ_2 was the output. In the top linkage, seen in **Figure 23**, φ_7 was the input and was directly related to φ_2 from the bottom linkage. φ_6 was the output of the top linkage and was related to θ_2 of the entire mechanism (the crank angle). The equations were quite complicated, but took the form of a quadratic equation, as shown below. In each case, the A, B, and C values correspond to known values, while the φ values were the outputs, solved using the quadratic formula. These calculations can be seen in **Appendix A** – MathCad worksheets for kinematic analysis of the linkages and stress analysis of the rocker. The

procedure for the entire inverse kinematics work can be found in *Design of Machinery* (Norton, 2008).

$$A \cdot \tan^2\left(\frac{\phi_2}{2}\right) + B \cdot \tan\left(\frac{\phi_2}{2}\right) + C = 0$$

$$A := d - K_1$$

$$B := 2 \cdot c$$

$$C := -d - K_1$$

$$K_1 := \frac{a^2 - b^2 + c^2 + d^2}{2a}$$

$$A_2 \cdot \tan^2\left(\frac{\phi_6}{2}\right) + B_2 \cdot \tan\left(\frac{\phi_6}{2}\right) + C_2 = 0$$

$$A_2 := -(e + g)$$

$$B_2 := -2 \cdot K_2$$

$$C_2 := e - g$$

$$K_2 := \frac{-e \cdot \cos(\phi_7)}{\sin(\phi_7)}$$

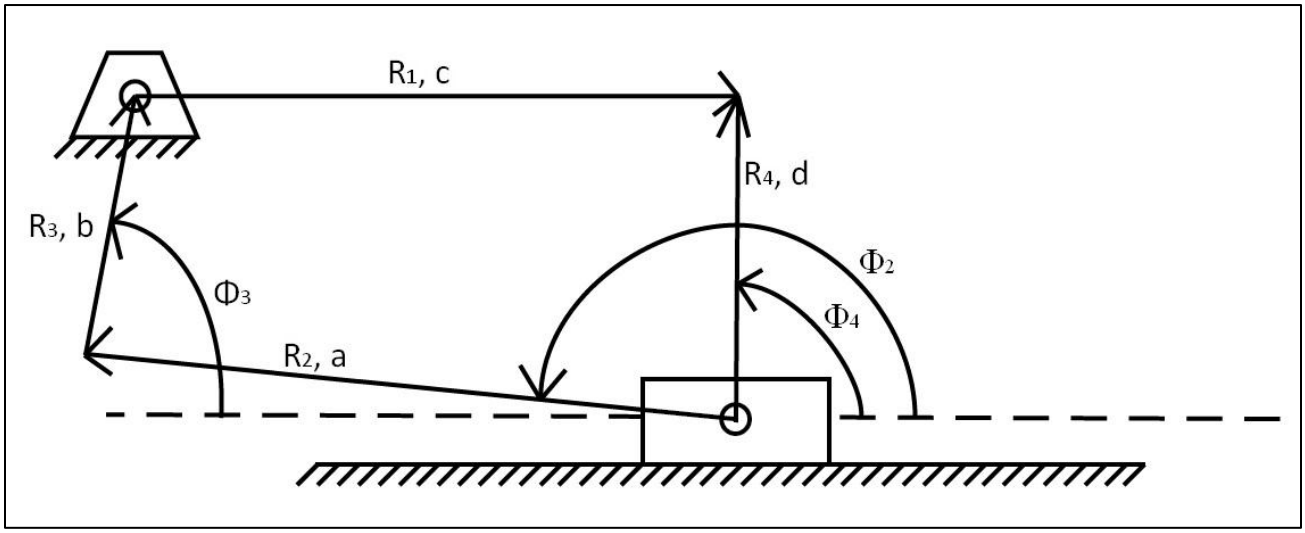

Figure 22: Vector loop diagram for bottom slider

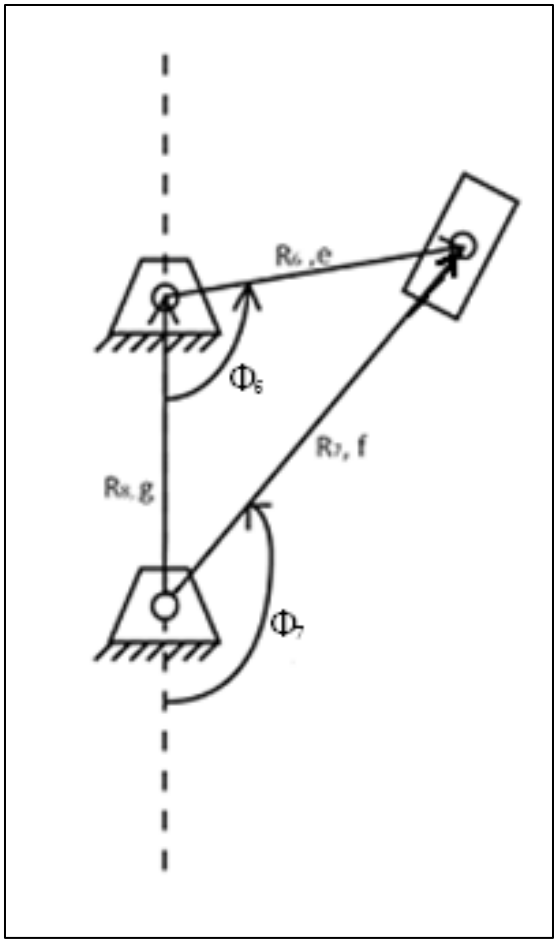

Figure 23: Vector loop diagram for top slider

Results

Creating the Geometry for the Parts in Pro/Engineer

The geometry for the parts must be defined before an analysis can be conducted in Pro/Mechanism. Pro/Engineer will be used to model the individual components. Once the all of the parts have been modeled, they will be statically assembled within the assembly package of Pro/Engineer. The static assembly will then be imported into Pro/Mechanism where dynamic conditions will be defined so an analysis can be conducted of the moving system. The material properties for each of the components will be defined in the units of millimeters, grams, s, and N.

To create an Assembly in Pro/Engineer each solid part must be properly constrained when it is placed. This requires reducing the degrees of freedom (DOF) of each part to the appropriate level. For example, any ground part will have 0 DOF while a simple crank will have 1 DOF (rotation). The reduction of degrees of freedom is done by selecting assembly operations such as mate, insert, align, offset, orient, coordinate system, and tangent from the assembly menu. Multiple operations may be applied until all of the degrees of freedom are accounted for.

In addition to reducing DOF, redundancies must be eliminated. A redundancy occurs when two constraints prevent the same motion from occurring, when either one of the constraints would suffice. While Pro/Engineer can assemble and run a kinematic analysis on assemblies with redundancies, Pro/Mechanism cannot run any dynamic analyses if a single redundancy exists.

Using Kutzbach's Equation, the correct number of degrees of freedom was found to be 1, and redundancies were eliminated. The Kutzbach Equation is:

$$m = 3(n - j - 1) + \sum_{n=1}^{j} f_i$$

Where *m* is the DOF for the entire system, *n* is the number of links in the system, *j* is the total number of joints in the system, and f_i is the DOF for each joint, which are summed together. This applies to any closed loop linkage, but by using the f_i values from each joint added in Pro/Engineer, the redundancies can be caught and eliminated. The linkage in Pro/Engineer contains 5 links and 9 joints with a total of 16 DOF, making Kutzbach's Equation equal:

$$m = 3(5 - 9 - 1) + 16 = 1$$

Since the linkage should have 1 DOF (or one output for each input), there are no redundancies. If *m* had been 0, the mechanism would not have moved in Pro/Engineer. Had *m* been greater than 1, there would have been more than one possible output for any given input. Pro/Mechanism was able calculate the forces that are acting on the rocker so the singularity functions can be solved and stress analysis carried out on the rocker.

Material Selection for the parts

The material selection was based on criteria such as wear conditions and the standard materials used in the sponsor's production line. The material selected for the crank, the slider on the rail mount and the rocker is A2 tool steel. This metal shows good machining characteristics and offers higher strength than typical machining materials such as Aluminum 6061 and MIC 6. A2 tool steel offers greater strength and wear resistance as well in a high speed environment.

The slider on the rail mount is attached to the end of arm tooling and might encounter wear in terms of contact with other parts while the mechanism is in motion. Wear resistance is important for such a part.

The rocker has a slider block translating inside its slot and hence, wear resistance is very important in this high friction application. An alternate consideration would be to machine the rocker out of Aluminum MIC 6 and fasten a steel insert inside the slot. This however, would be a more expensive approach. A lower grade steel such as Carbon Steel 1040 could be used and tempered and hardened. Post processes to increase hardness again add cost to the part. A2 tool steel hence was the most suitable for this application.

Final Linkage Descriptions

The final design of the linkage has specific link widths and lengths that are required to get the desired stroke output. There are also many standard parts that can be easily bought from a number of manufacturers. **Figure 24** shows the final design in wireframe using Pro/Engineer.

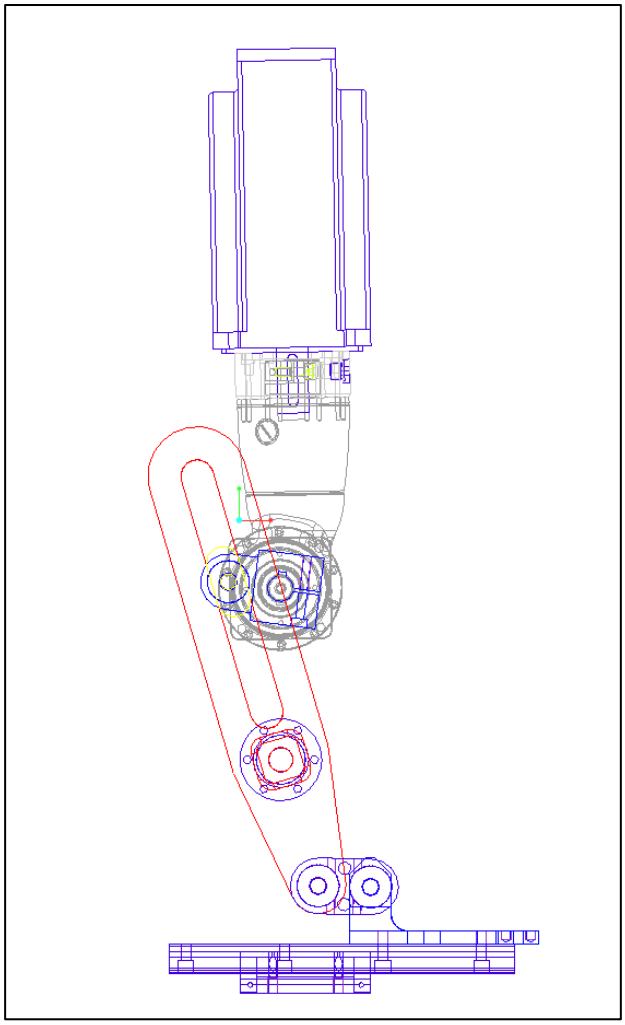

Figure 24: Final Linkage Design

Custom manufactured Parts

Throughout the design process, ease of machining and fabrication of a part was kept in mind. Some parts that the linkage uses are standard parts that the sponsor uses and the other custom parts are variations of those designs. The custom parts are discussed in detail in this section and there detailed dimensioning drawings can be found in **Appendix B** – Custom Parts Drawings.

The width of the rocker, shown in

Figure 25, is 20 mm, or about 0.787 inches, because it will have the most force acting upon it throughout the motion. There is also an extension added to the back of the rocker, which allows for the bearing to attach the rocker to the mounting plate without interfering with the slider.

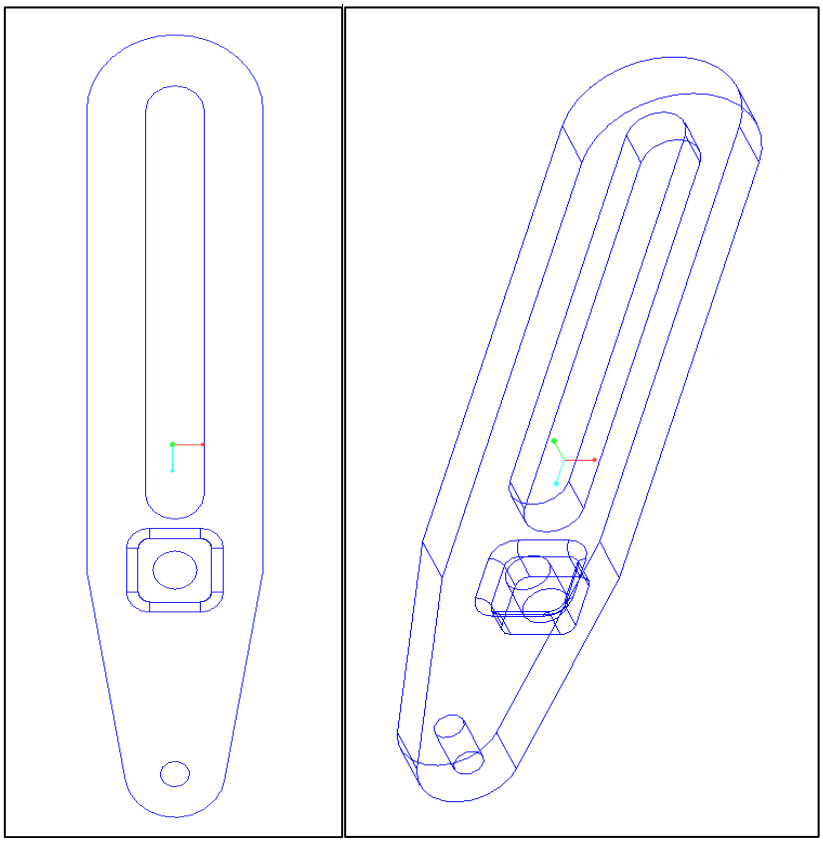

Figure 25: Finalized Rocker

The slider, shown in **Figure 26**, in the rocker is a 15 mm wide block with rounded edges. This block will slide within the rocker along a 5 mm thick wall that is left on the front of the rocker for additional torsion prevention.

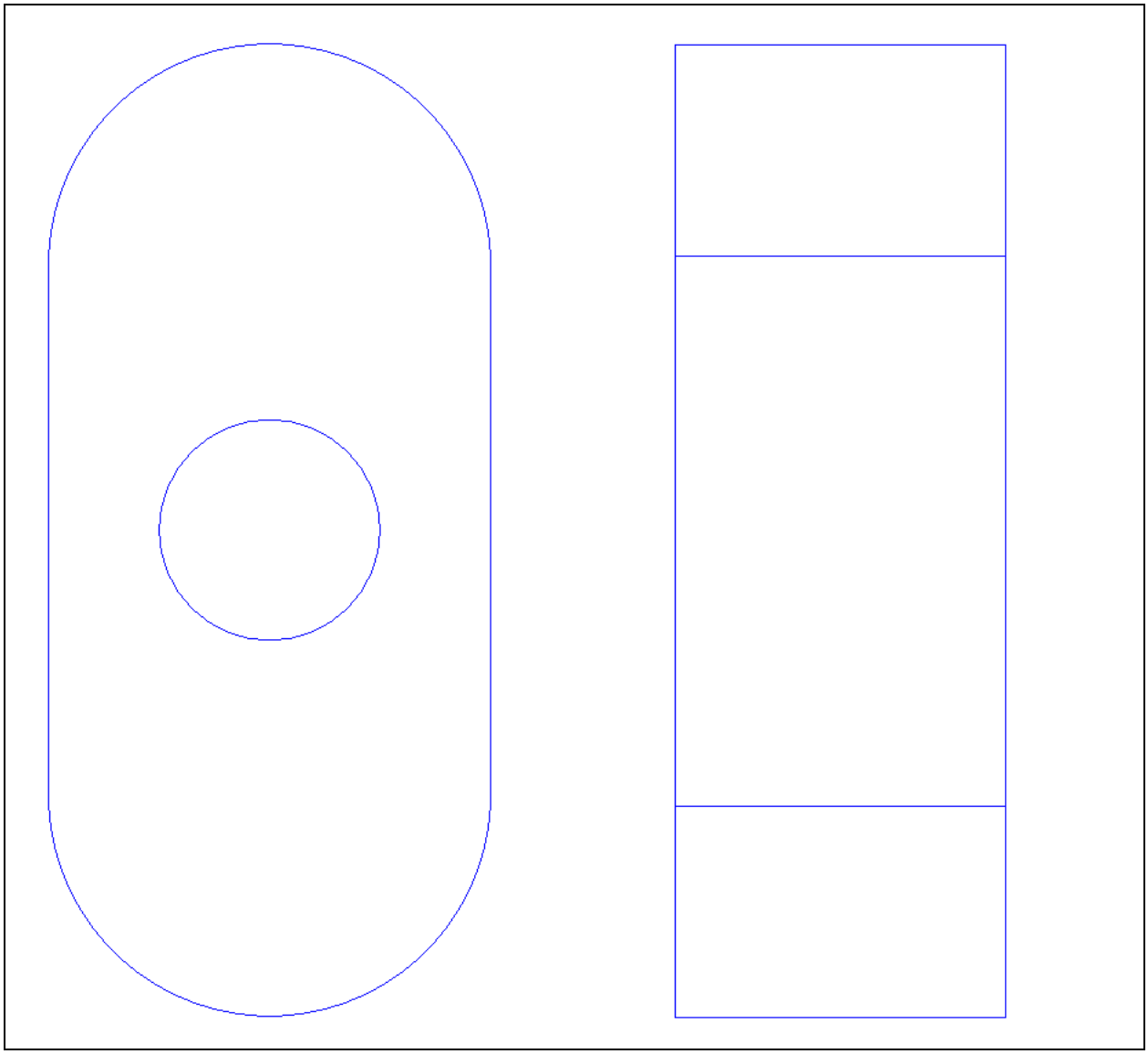

Figure 26: Slider block in the rocker

The crank shown in **Figure 27** is connected to the servo motor is 32 mm long from center axis to center axis. It has two different widths, one being the same as the standard crank that is used at the bottom of the assembly and one being 15 mm thick. There is a key way that attaches to the servo motor shaft that is built in. This key way locks into place by a screw that is screwed through the top of the crank above the hole. This screw pulls the slit, which is cut out of the top of the crank, together as it is tightened. This locks the key hole into position and allows for a secure grip on the servo motor shaft.

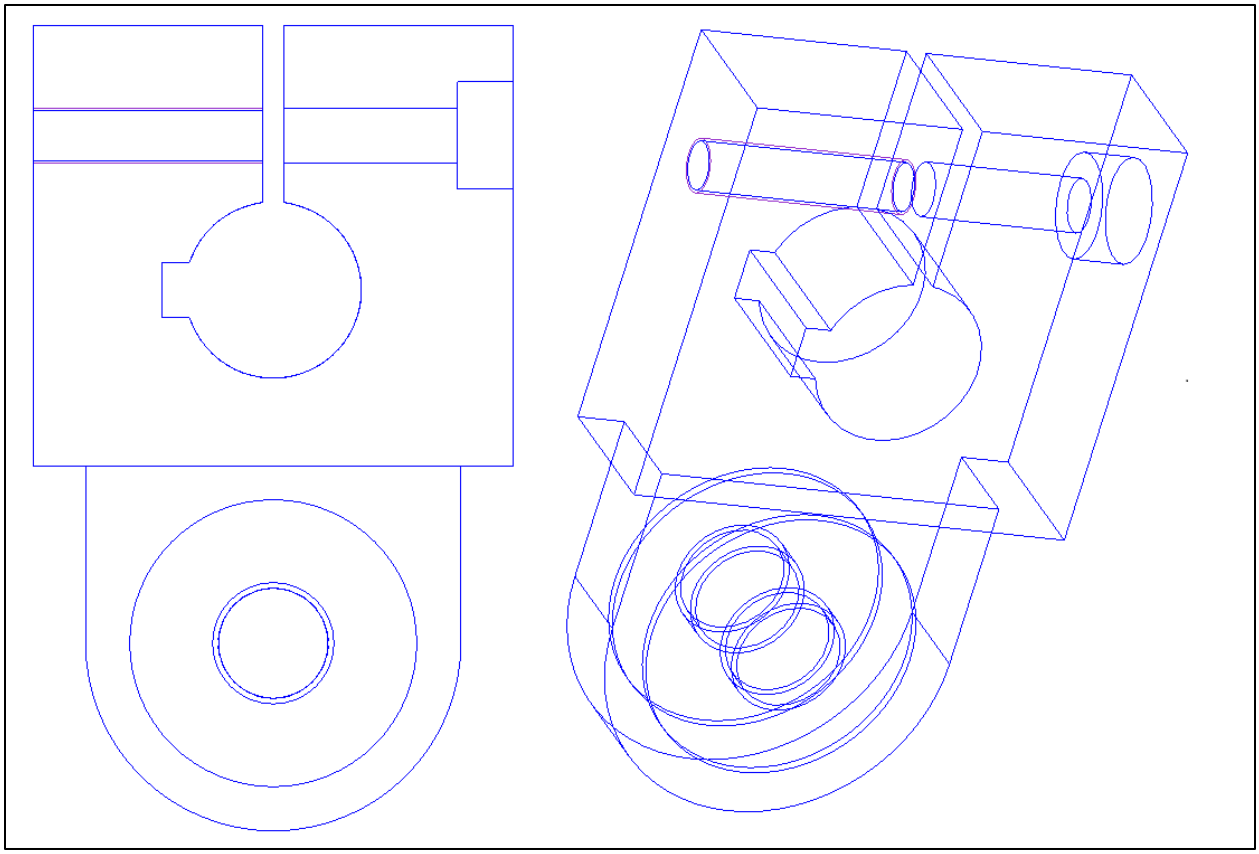

Figure 27: Finalized Crank on Servo Motor

The mounting plate shown in **Figure 28** is made out of steel and has two tapped holes on the top that follow the same sizes as the clearance holes on the THK rail. It has the proper amount of width for it to have five threads of the screw attached to it. The beams that are extruded from the base are 10 mm thick and have large fillets and chamfers to handle the forces that will be acting on them.

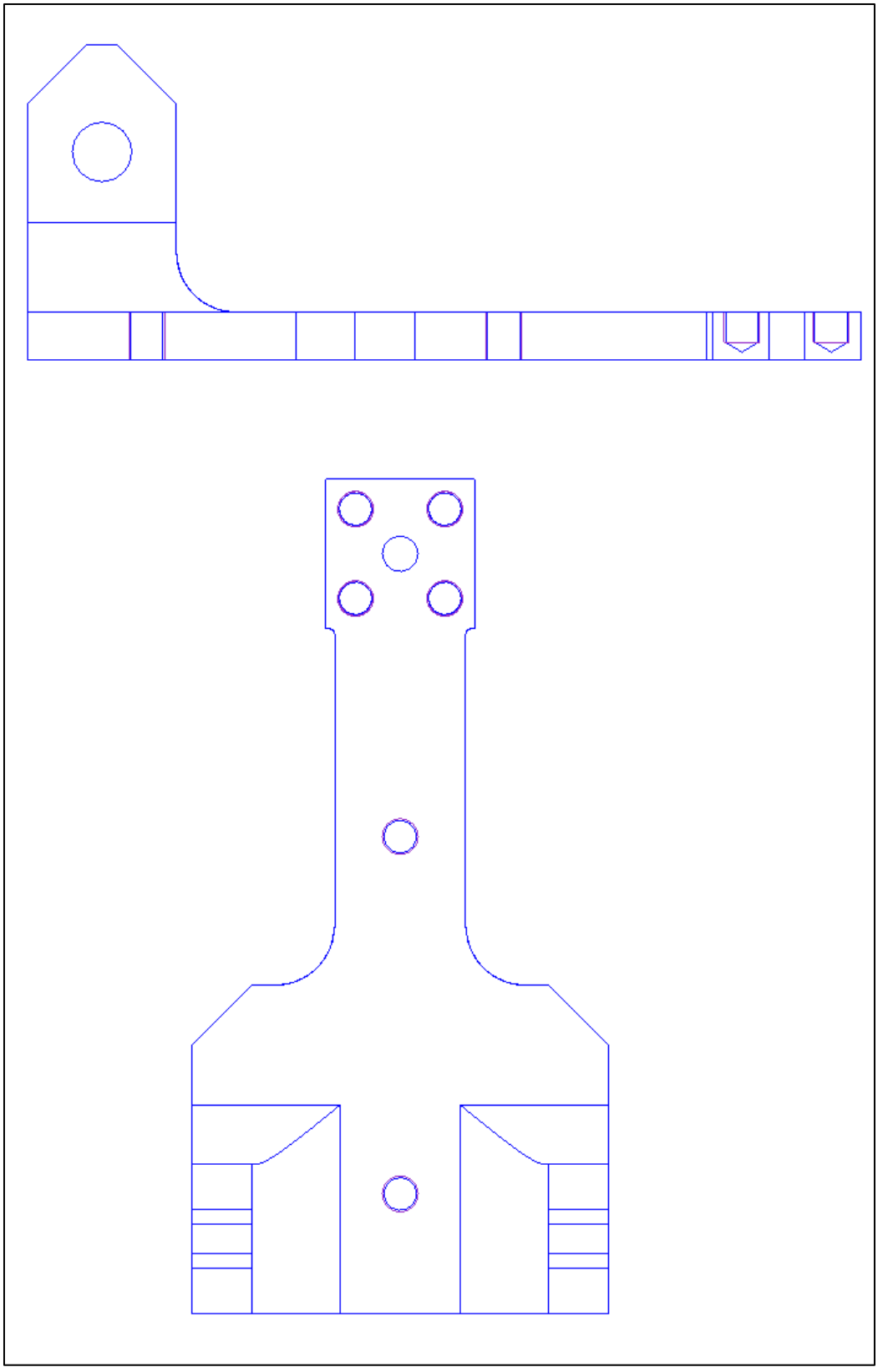

Figure 28: Finalized Mounting Plate

Standard Parts

The off the shelf parts consist of the THK rail and slider, the cranks connected at the bottom of the rocker, bolts and the servo motor. The THK rail and slider that are being used consist of a SHS-20C rail from the company THK. The cranks that are being used are the typical cranks that Gillette uses and have the proper bearings inside of each hole. The bolts and pins are from McMaster-Carr, which supplies products used to maintain manufacturing plants and large commercial facilities worldwide, so they are very easy to get large quantities of them for a small price. The product number of the screw that will connect the mounting plate to the THK rail is 92196A137 and has a 6-40 thread size per inch and a length of 0.5 inches or 12.7 mm. The product number of the screw that will connect the servo crank to the servo motor shaft is 91292A410 and has a thread size of M6 with a 1 mm pitch and a length of 55 mm.

Creating the Assembly within Pro/Engineer

After a suitable linkage with the proper gearbox and servo motor was completed, three such mechanisms needed to be placed in the workspace. The workspace is dimensioned to be 250X250X1000 mm and should contain all parts of the linkage. The servo motor and gearbox were not required to fit within the designated workspace; however they will be attached to a mounting plate in the future that will extrude from the machine. The final assembly with all the linkages fit within the workspace is shown in **Figure 29**. Additional isometric views and a left side vide can be seen in **Figure 30** and **Figure 31**.

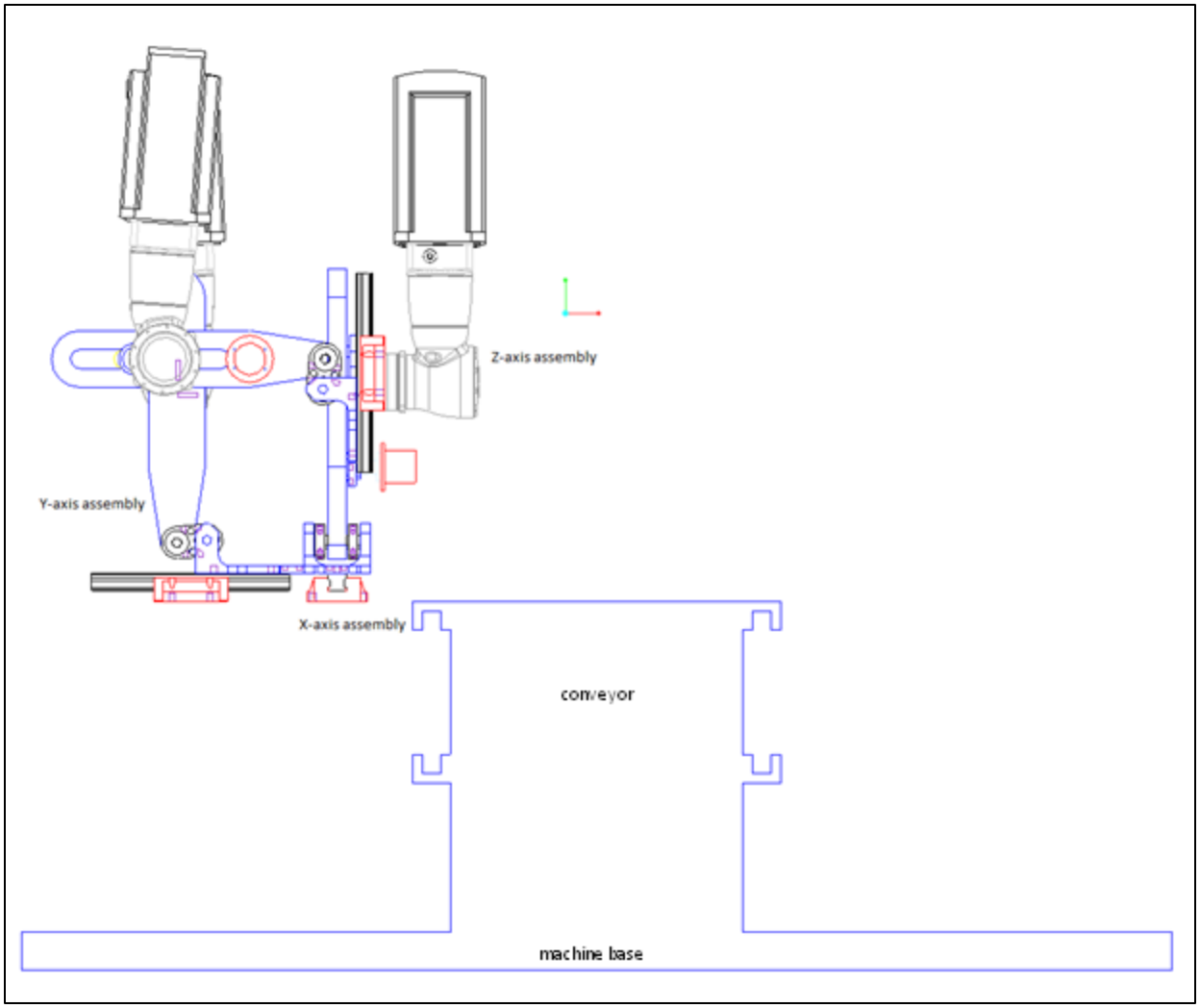

Figure 29: Assemblies within the workspace (Front View)

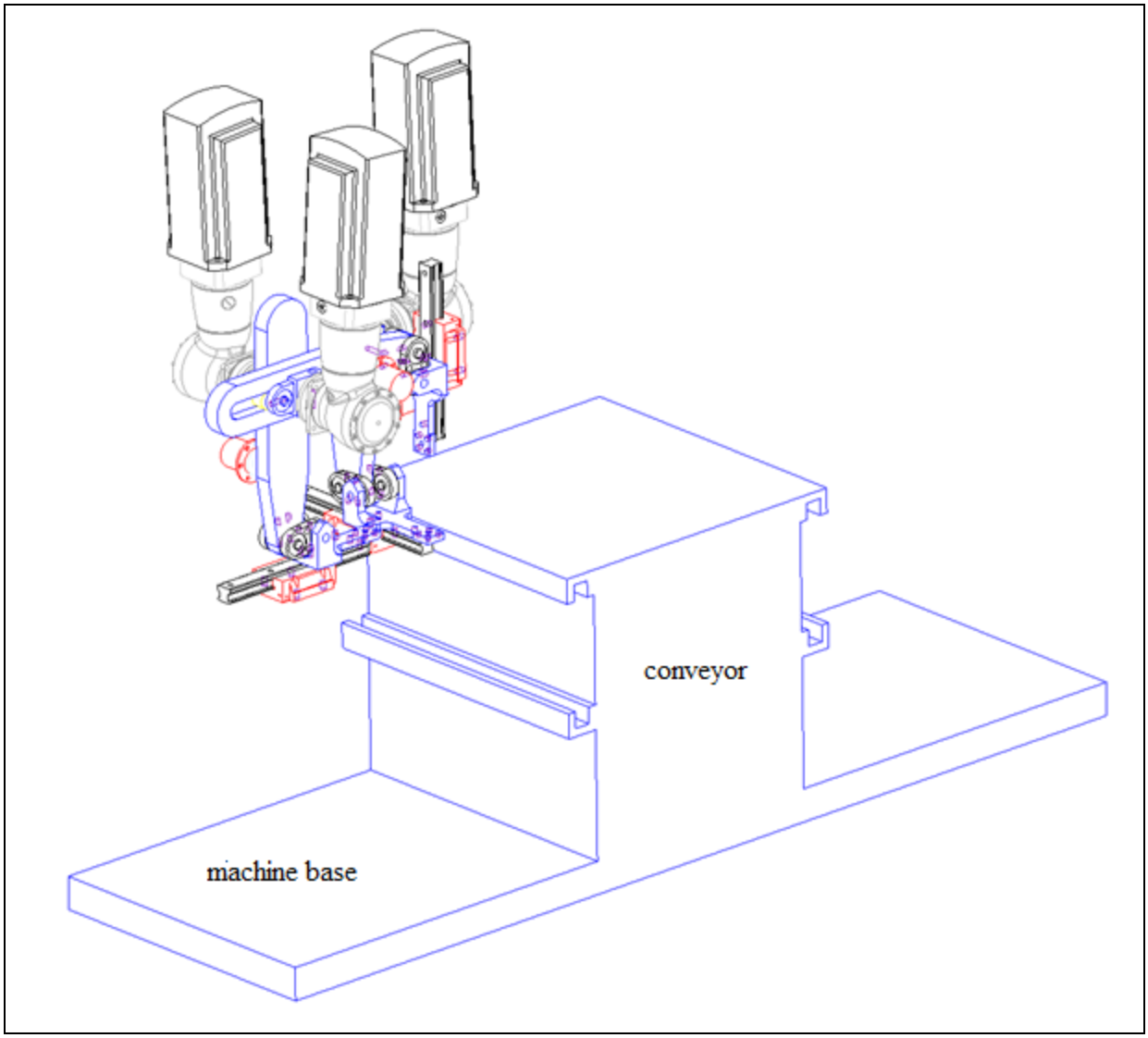

Figure 30: Assemblies within the workspace (Isometric View)

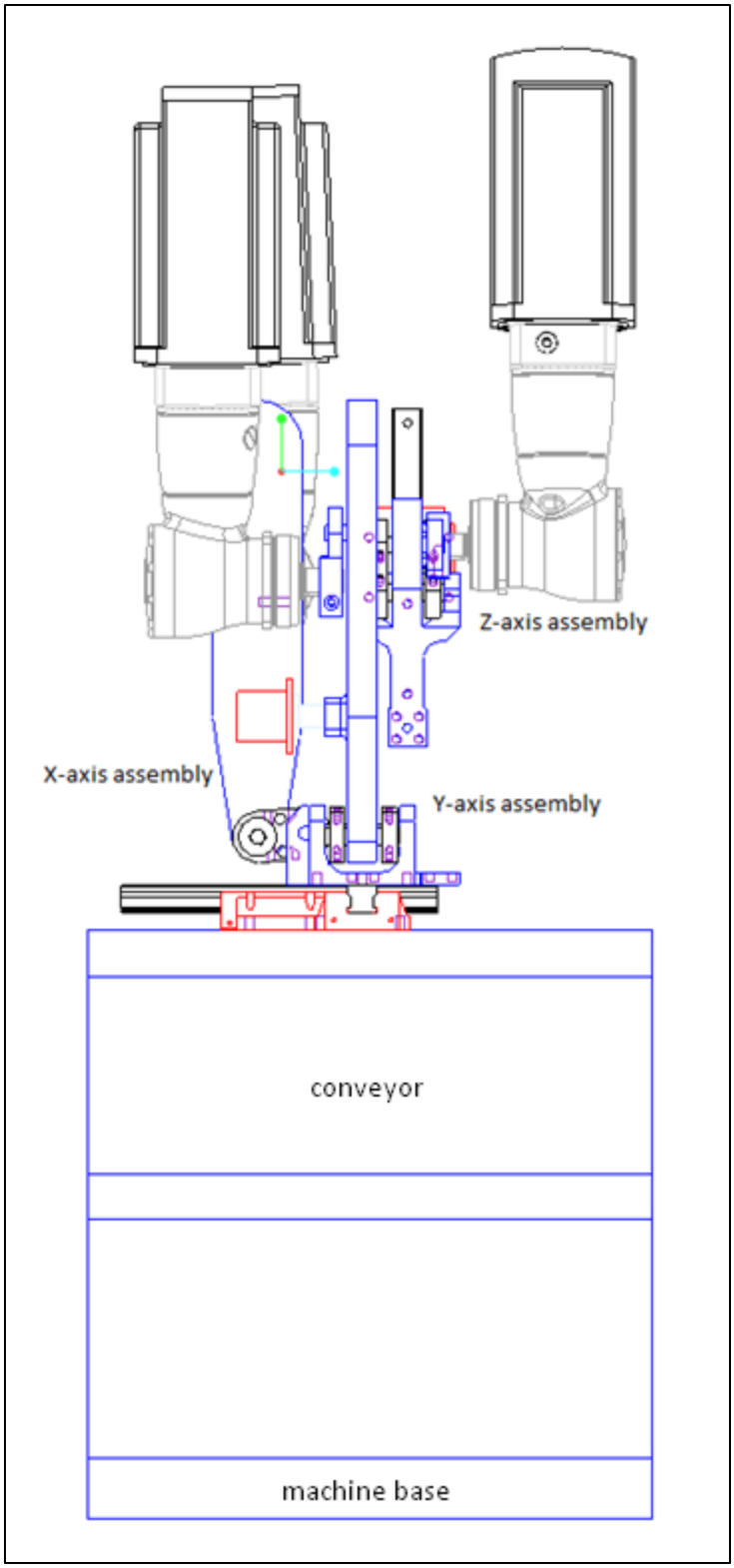

Figure 31: Assemblies within the workspace (Left View)

The placements of these linkages were taken from the drawings sent from our sponsor. The three linkages are placed within the workspace, one on each axis, and their motions are phased so that the end effectors do not collide with one another.

Though our linkage is compact, there is still room for improvement in terms of size. There is only one axis that needs the full 56 mm stroke, which is the y-axis. The z-axis only requires 28 mm and the x-axis only requires 10 mm. This allows us to shrink down the size of the crank or the length of the rocker, which makes our assembly even more compact.

Kinematic Results

The desired range of crank angular positions was determined to be 111^{o} to 222^{o} and the servo profile was established using the data obtained from Dynacam^{TM}. This data was phase shifted to make the crank rotate from 111^{o} to 222^{o} and backward in a total of 0.25 seconds. A set of angular positions with respect to time were the inputs for the servo motor on Pro/Engineer. The software with its in-built servo motor application provided the displacement, velocity and acceleration curves for the THK rail.

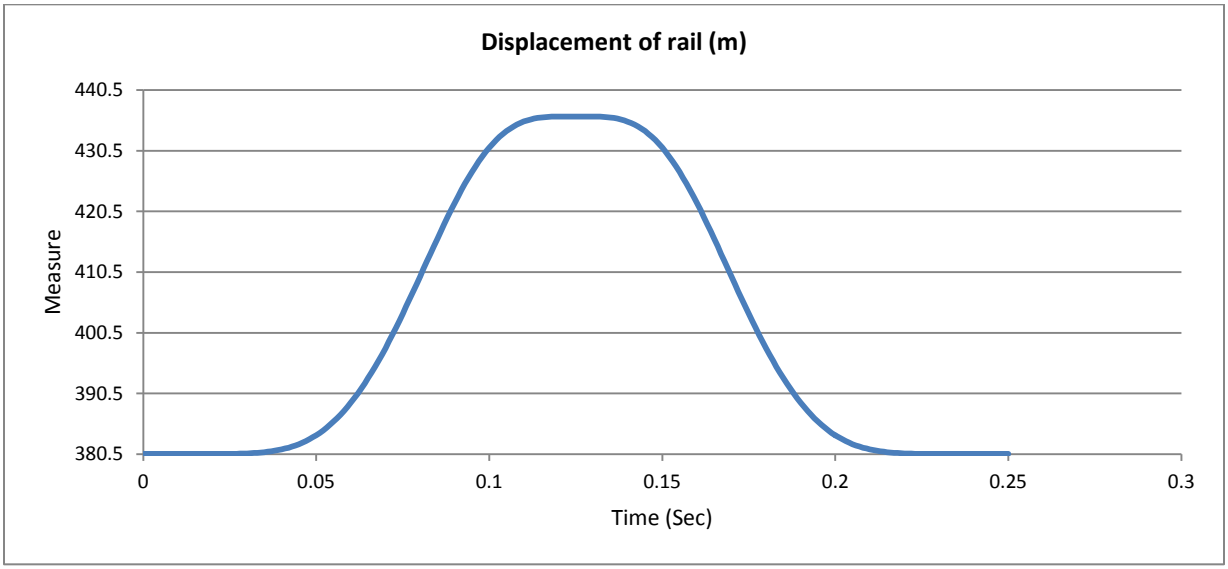

Figure 32: Displacement curve for one cycle

Figure 32 shows the displacement curve of the THK rail moving along a horizontal axis. For the specified range of angular position inputs, approximately 56 mm of stroke from top dead center to bottom dead center is achieved. This was the predicted results from the analysis done

previously. As seen by the mathematical model, there are pseudo-dwells present in the Pro/Engineer simulation as well.

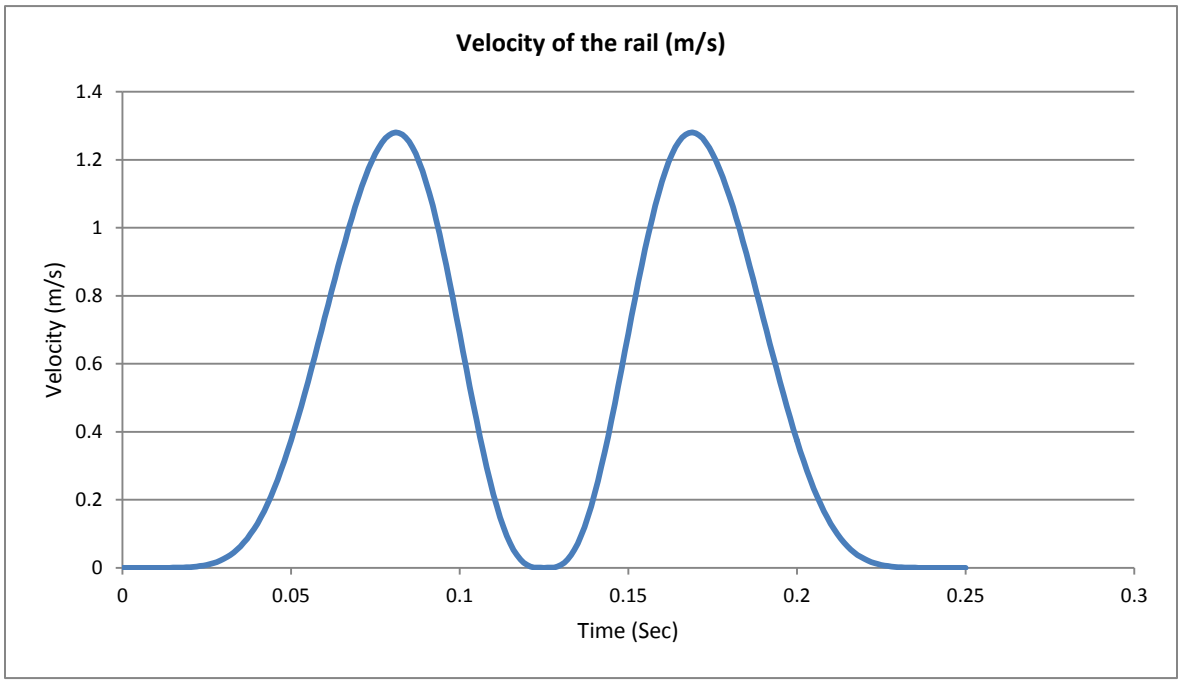

Figure 33: Velocity curve for one cycle

Figure 33 shows the plot of velocity of the THK rail versus time. The peak velocities for the THK rail are approximately 13 m/s and occur right before the highest range is reached. The velocity function has been calculated as the derivate obtained from the slider's position function. The velocities are zero at the top dead center and bottom dead center as the linkage dwells at these points and switches direction.

The acceleration plot of the THK rail versus time can be seen in **Figure 34** with many peaks. The peak acceleration of the linkage is about 55 m/s^2, which is close to 5.5 G's. The acceleration is a continuous function and will also result in continuous jerks. The noise in the acceleration graph is caused due to the internal formulas that Pro/Engineer servo motor application applies to run the simulation (between quarter degree angular position increments as explained earlier) and to calculate the higher order derivatives.

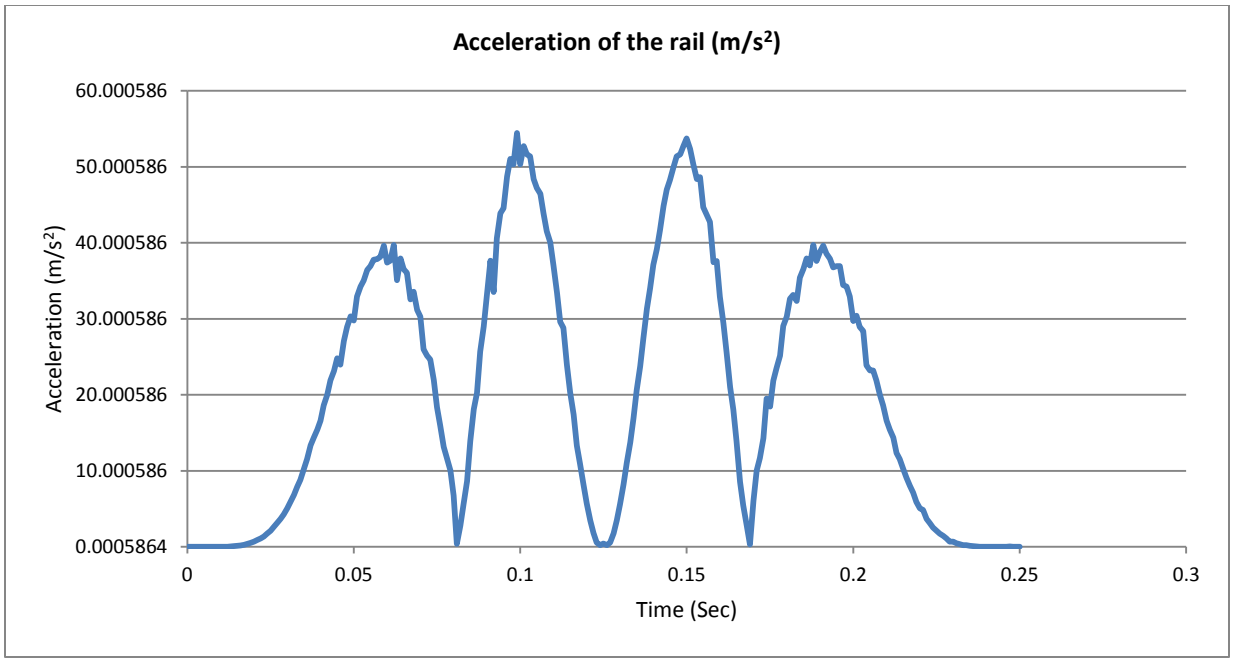

Figure 34: Acceleration curve for one cycle

Pivot/Pin Forces

To complete a dynamic analysis on both versions of the linkage Pro/Mechanism was used. In order for the software to produce accurate results of the joint forces, the overall degree of freedom of the linkage in the model had to be computed to one. This meant that in the assembly, two coincident joint types could not be of the same joint type. For instance, the axis of the water pump bearing and the pin hole in the rocker could not be both pin joints. Instead one had to be a cylindrical joint and the other a pin joint. This analysis was conducted using the Gruebler's equation for a degree-of-freedom analysis. Once the linkage was not over constrained, dynamic analysis was possible.

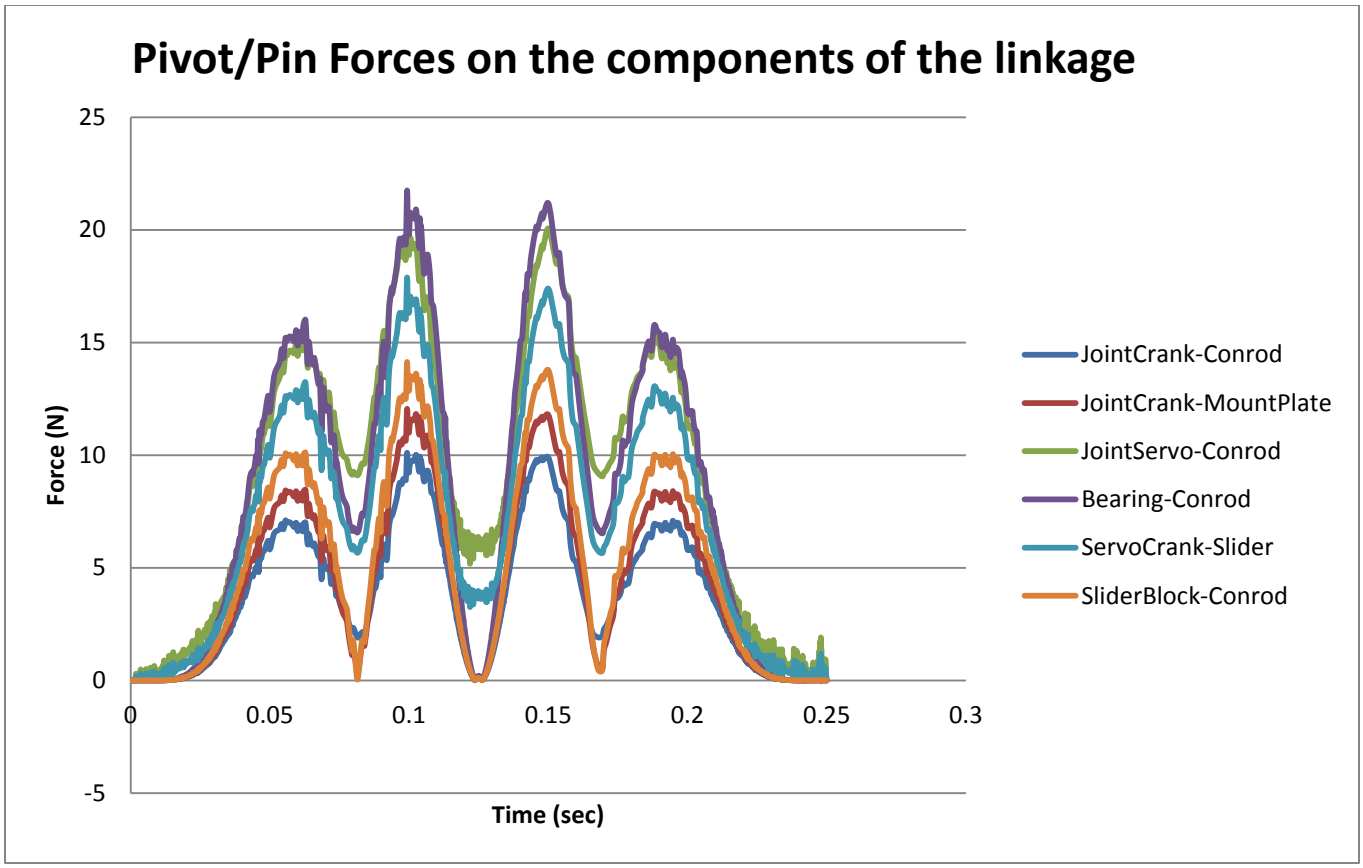

Figure 35: Pivot/Pin Forces on the different components of the final linkage

Figure 35 shows the internal forces (components on components) of the finalized linkage. The force magnitudes are significantly smaller for this linkage, but the force trends throughout the linkage's motion remains similar. Again, the peak forces occur at the point of turning for the linkage i.e. when the slider block reverses direction. This time is approximately t = 0.1 second.

Table 2: Maximum Force magnitudes and their locations

Force Type	Max Force Magnitude (N)
Water Pump Bearing on rocker	21.8
Rail Mount on the bottom crank	10.1
Crank on the top slider	17.9
Servo's shaft on crank	20.7
Bottom crank on rocker	10.1
Top slider block on rocker	14.1

In

Table 2, the maximum forces in can be seen. These numbers are smaller than those of version B. The added crank at the end of the rocker, not only reduces wear on the inside of the rocker's slot, but also improves the linkage dynamically.

These pin forces enable stress analysis to be done on any of the parts in the linkage. Since the rocker is the largest part and also sees the most amounts of forces, stress analysis will be done on the part in the following section. The singularity functions will be developed to find the critical cross-sectional area where the bending moments are the maximum and stress concentration factors based on the geometry will be used to come up with the safety factors needed to pass the design of both the linkages.

Torque Calculations

The axis of the servo motor and the crank was picked for the torque analysis. The peak torque was 0.5 N-m and this would be the required torque to run the linkage. However, this number did not include friction which was accounted for looking at forces at each of the joints. The friction torque analysis is as follows:

Bearing on Rocker

Max Force = 22 N

Torque = 22N * 0.15 * 5mm = 0.0165 N-m

Crank on slider (inside the lever)

Max Force = 18 N

Torque = 18N * 0.15 * 5mm = 0.0135 N-m

Mounting Plate on Second Crank

Max Force = 13 N

Torque = 13N * 0.15 * 5mm = 0.00975 N-m

Second Crank on Rocker

Max Force = 11 N

Torque = 11N * 0.15 * 5mm = 0.00825 N-m

Slider on Rocker

Max Force = 15 N at 0.10 sec

Torque = 15N * 0.2 * 32.38mm = 0.0974 N-m

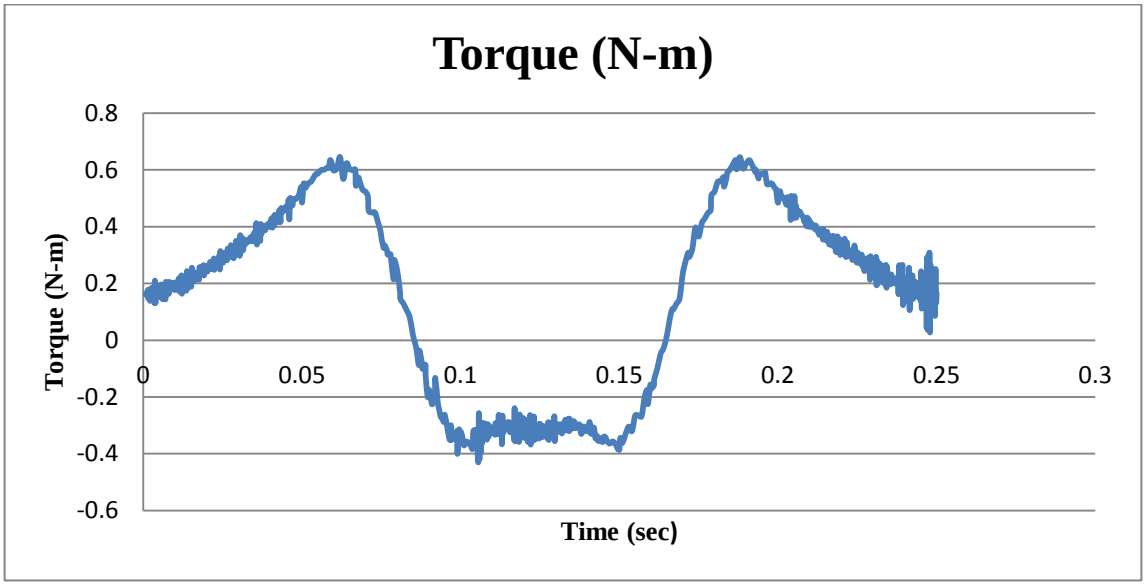

Figure 36: Required torque versus time curve (includes torque added by friction)

These torques were added to the torque at each time step which was obtained from Pro/Engineer. The superimposed torque curve plotted in Microsoft Excel is shown in **Figure 36** resulted in the peak input torque value of 0.645 N-m. The force analysis was used to find the forces at each of these joints. These forces were then multiplied by friction coefficient of 0.15 for the bearings and the radius of the bearing. For the force of the slider block on the rocker, the friction coefficient of 0.12 was used. The distance used was the normal distance between the slider and the crank pivot. This torque then helped with the selection of an appropriate gearbox and servo motor.

Motor and Gearbox Selection

The motor and gearbox selection process required the study of the input torques needed to drive the entire linkage for its range of output motions. The torque analysis was conducted using Pro/Engineer and its results are shown in the succeeding sections of the report. The peak

torque that was recorded was 0.645 N-m, which also included the torque required to overcome friction in the slider joints and the bearings.

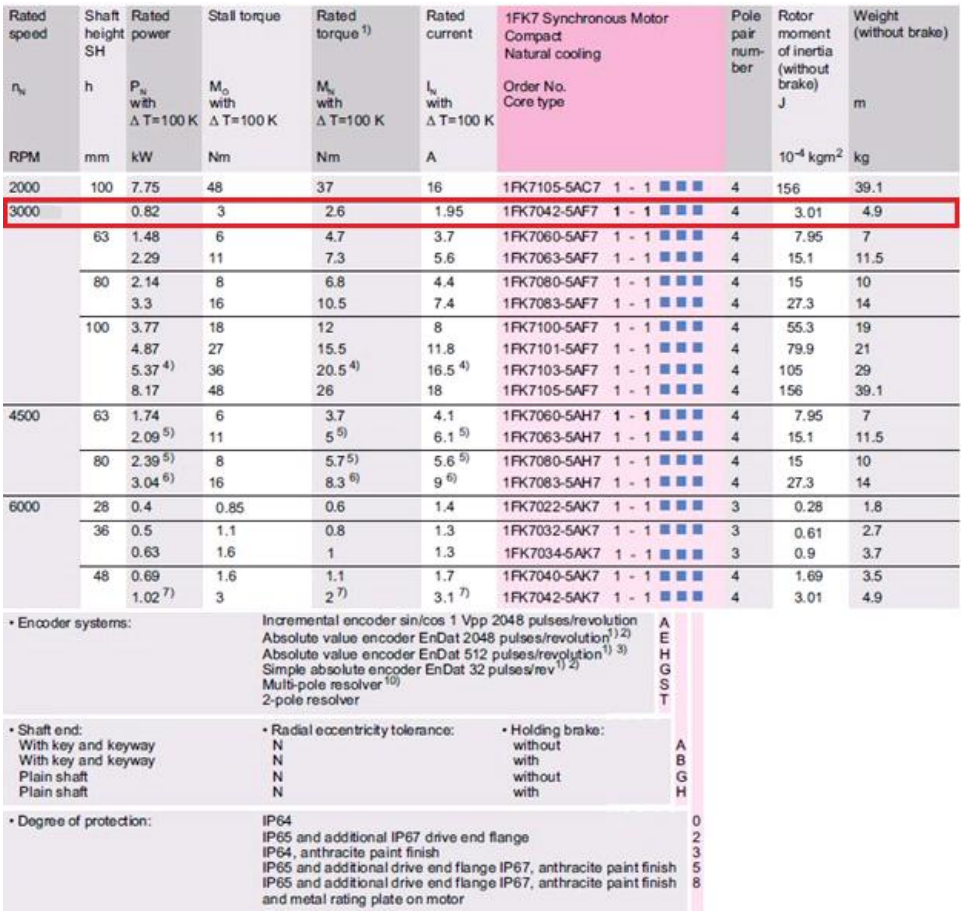

Rated speed n_N RPM	Shaft height SH h mm	Rated power P_N with ΔT=100 K kW	Stall torque M_0 with ΔT=100 K Nm	Rated torque [1] M_N with ΔT=100 K Nm	Rated current I_N with ΔT=100 K A	1FK7 Synchronous Motor Compact Natural cooling Order No. Core type	Pole pair number	Rotor moment of inertia (without brake) J 10^{-4} kgm^2	Weight (without brake) m kg
2000	100	7.75	48	37	16	1FK7105-5AC7 1 - 1 ■■■	4	156	39.1
3000		0.82	3	2.6	1.95	1FK7042-5AF7 1 - 1 ■■■	4	3.01	4.9
	63	1.48	6	4.7	3.7	1FK7060-5AF7 1 - 1 ■■■	4	7.95	7
		2.29	11	7.3	5.6	1FK7063-5AF7 1 - 1 ■■■	4	15.1	11.5
	80	2.14	8	6.8	4.4	1FK7080-5AF7 1 - 1 ■■■	4	15	10
		3.3	16	10.5	7.4	1FK7083-5AF7 1 - 1 ■■■	4	27.3	14
	100	3.77	18	12	8	1FK7100-5AF7 1 - 1 ■■■	4	55.3	19
		4.87	27	15.5	11.8	1FK7101-5AF7 1 - 1 ■■■	4	79.9	21
		5.37 [4]	36	20.5 [4]	16.5 [4]	1FK7103-5AF7 1 - 1 ■■■	4	105	29
		8.17	48	26	18	1FK7105-5AF7 1 - 1 ■■■	4	156	39.1
4500	63	1.74	6	3.7	4.1	1FK7060-5AH7 1 - 1 ■■■	4	7.95	7
		2.09 [5]	11	5 [5]	6.1 [5]	1FK7063-5AH7 1 - 1 ■■■	4	15.1	11.5
	80	2.39 [5]	8	5.7 [5]	5.6 [5]	1FK7080-5AH7 1 - 1 ■■■	4	15	10
		3.04 [6]	16	8.3 [6]	9 [6]	1FK7083-5AH7 1 - 1 ■■■	4	27.3	14
6000	28	0.4	0.85	0.6	1.4	1FK7022-5AK7 1 - 1 ■■■	3	0.28	1.8
	36	0.5	1.1	0.8	1.3	1FK7032-5AK7 1 - 1 ■■■	3	0.61	2.7
		0.63	1.6	1	1.3	1FK7034-5AK7 1 - 1 ■■■	3	0.9	3.7
	48	0.69	1.6	1.1	1.7	1FK7040-5AK7 1 - 1 ■■■	4	1.69	3.5
		1.02 [7]	3	2 [7]	3.1 [7]	1FK7042-5AK7 1 - 1 ■■■	4	3.01	4.9

• Encoder systems:	Incremental encoder sin/cos 1 Vpp 2048 pulses/revolution Absolute value encoder EnDat 2048 pulses/revolution [1) 2)] Absolute value encoder EnDat 512 pulses/revolution [1) 3)] Simple absolute encoder EnDat 32 pulses/rev [1) 2)] Multi-pole resolver [10)] 2-pole resolver	A E H G S T

• Shaft end:	• Radial eccentricity tolerance:	• Holding brake:	
With key and keyway	N	without	A
With key and keyway	N	with	B
Plain shaft	N	without	G
Plain shaft	N	with	H

• Degree of protection:	IP64	0
	IP65 and additional IP67 drive end flange	2
	IP64, anthracite paint finish	3
	IP65 and additional drive end flange IP67, anthracite paint finish	5
	IP65 and additional drive end flange IP67, anthracite paint finish and metal rating plate on motor	8

Figure 37: Siemens 1FK7 series compact motors - core type, natural cooling

In order to fit three linkages in the specified workspace of 250 mm x 250 mm x 1000 mm a right-angle gearbox was chose for better packaging. The sponsor provided the company, Wittenstein as a motor and gearbox vendor. After studying the torque-speed curves of some of their motors, a rated torque and the proper gear reduction required for the linkage was deduced. The selected motor is shown in red ink in **Figure 37**. The servo motor is from Siemens and the product number is 1FK7042-5AF71-1AA0. The rated speed of 3000 rpm and rated torque of 2.6 N-m are favorable for the linkage as the linkage needs to be run at an average input speed of 240 rpm.

Hence, a 10:1 gear reduction was necessary and a Wittenstein right-angle gearbox of the SK060 series was chosen. The gearbox can handle a nominal output torque of 15 N-m,

maximum torque of 20 rpm, nominal input speed of 3000 rpm, and maximum input speed of 5000 rpm. Based on the torque and speed measurements of the linkage and the ratings of the motor, this gearbox seems to be the most suitable for the linkage's operation and packaging requirements. The details of the dimensions and specifications of the motor and gearbox can be seen in **Appendix C** – Motor and Gearbox Specifications.

Stress Analysis

Based on the geometry and the study of forces done on Pro/Engineer, the rocker is the most critical part of the linkage mechanism and is subjected to the maximum loading and bending. Hence, in this sub-section, stress analysis on the rocker will be performed.

The force analysis from Pro/Engineer was used to obtain the forces acting on the rocker which included the slider block on the rocker, the water pump bearing on the rocker, the con-rod on the rocker. The forces were labeled with numeric subscripts for ease of calculations. These force labels and magnitudes are as follows (The stress analysis calculations can be seen in

Appendix A – MathCad worksheets for kinematic analysis of the linkages and stress analysis of the :

F_1 = 15 N → Slider block on rocker

F_2 = 22 N → Water pump bearing on rocker

F_3 = 11 N → second crank on rocker

W = 7.759 N → Weight of the rocker

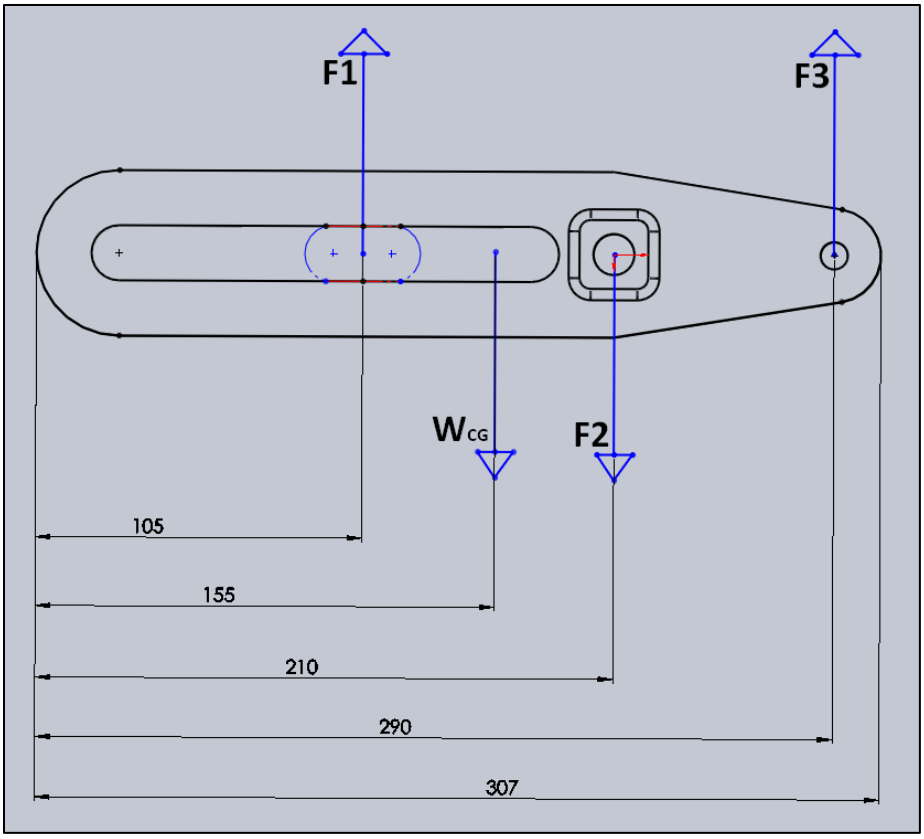

Figure 38: Free Body Diagram of the rocker

Figure 38 shows the free body diagram of the rocker with labeled forces and their locations. For the case of F1 (force of the slider on the rocker), the maximum force magnitude from Pro/Engineer was taken and its location during the motion of the linkage was 105 mm. This number gave us the worst case force that slider block exerts on the rocker.

Based on the loading conditions, the singularity functions for shear, moment, slope and deflection were formulated (These can be seen in

Appendix A – MathCad worksheets for kinematic analysis of the linkages and stress analysis of the). **Figure 39** and **Figure 40** show the shear and moment diagram for the rocker. The maximum bending moment occurs at 0.210 m which is at the exact location of the water pump bearing. The maximum bending moment is of magnitude of 1.15 N and the maximum shear force is of 15 m.

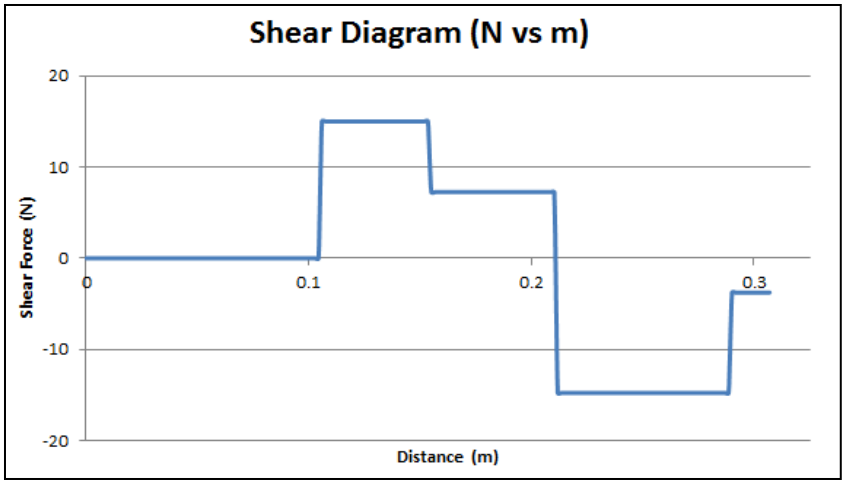

Figure 39: Shear diagram of the rocker

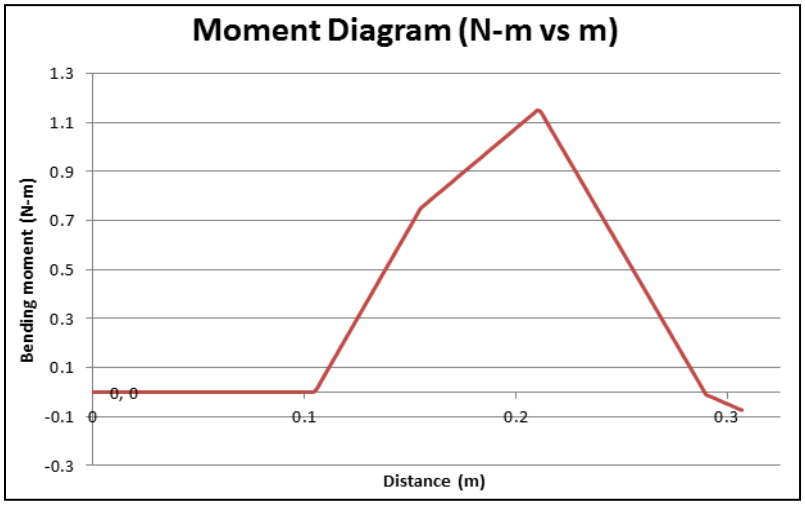

Figure 40: Moment diagram of the rocker

The loading condition for the rocker is also bending, as there is no torsion stresses that would occur along its length. With bending conditions, the stress cubes at the critical points are shown in **Figure 41** and **Figure 42**.

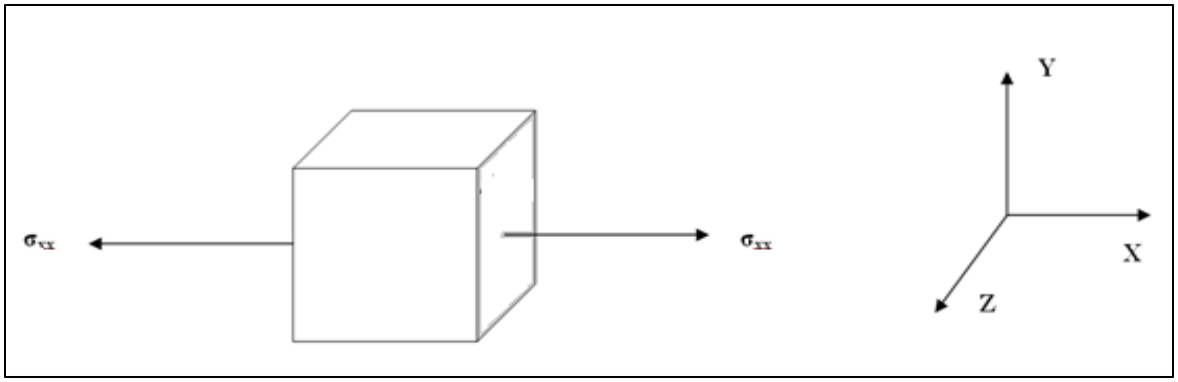

Figure 41: Stress Cube of point A

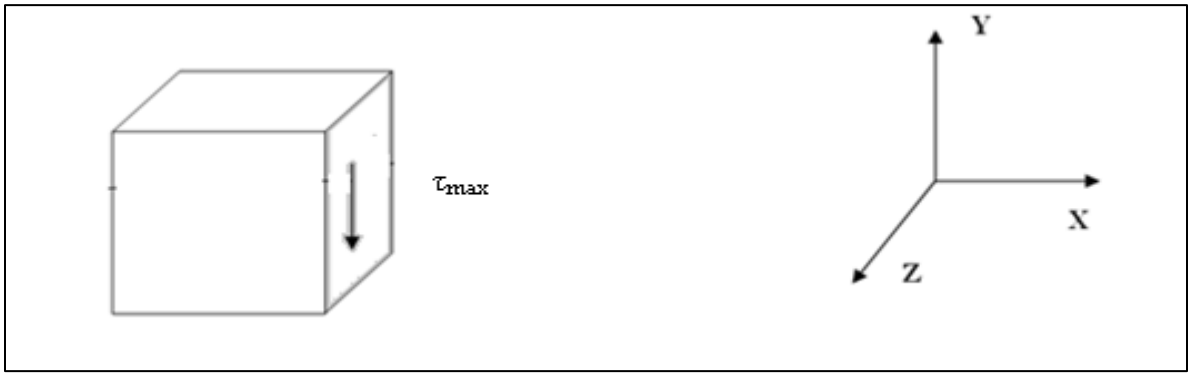

Figure 42: Stress Cube at point B

At the critical cross-section, there are stress concentrations due to geometry. The geometry closely resembles that of a semi-circular notch. From the *Peterson's Stress Concentration Factors* by Walter Pikey, the stress concentration factor was found to be 1.029. The maximum bending moment at the critical cross-section is 7.1 MPa and the calculated von Mises stresses at points A and B are 7.1 MPa and 12.3 MPa. The safety factors found were against the yield strength of A2 tool steel (=359 MPa) and these values for 50.6 and 29.2 for cross-sections A and B. These safety factor values are for the rocker against yielding as they were compared against the yield strength of A2 Tool steel.

The fatigue failure analysis was also performed for the rocker. The ultimate tensile strength of A2 Steel is 723.95 MPa. The calculated endurance strength was then divided by 2 as the tensile strength is less than 1400 MPa. There were several correction factors applied to the endurance strength in order to construct a Strength-Life diagram. The correction factors are as follows (calculations can be seen in

Appendix A – MathCad worksheets for kinematic analysis of the linkages and stress analysis of the):

- C_{LOAD} = 1 (Bending)
- C_{SIZE} = 1.31
- $C_{SURFACE}$ = 0.788
- $C_{TEMPERATURE}$ = 1
- $C_{RELIABILITY}$ = 0.659 (For 99% reliability)
- $C_{IGNORANCE}$ = 0.7 (For any miscalculations)

The corrected endurance limit for the rocker was then found to be 172.3 MPa at 10^6 cycles. **Figure 43** shows the strength-life diagram for the rocker.

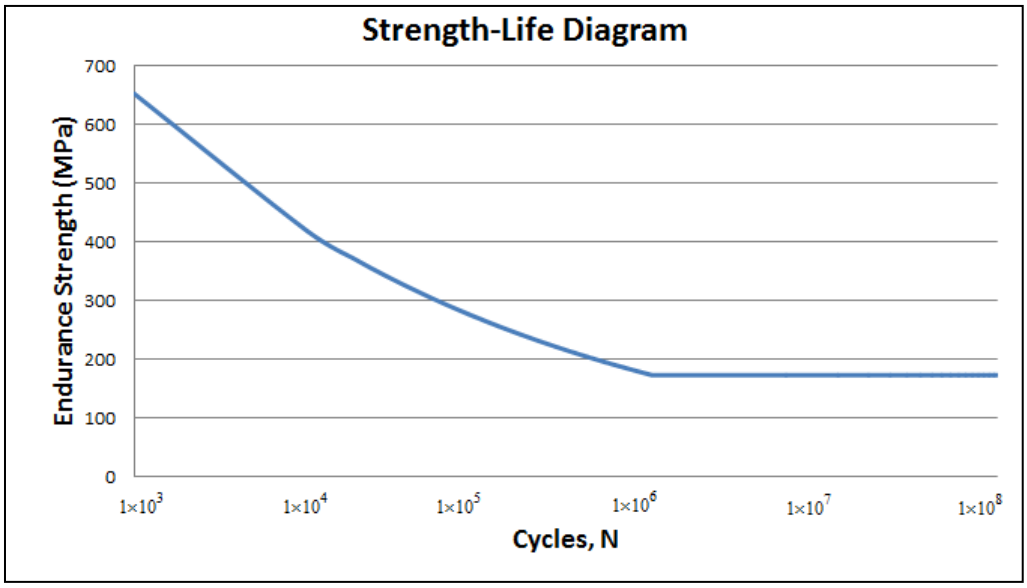

Figure 43: Strength - Life Diagram for the rocker

This has been plotted on a log scale on the horizontal axis. After 10^6 cycles, the rocker will have an endurance strength of 172.3 MPa and its strength decreases from a maximum of 652 MPa at 10^3 cycles.

According to the 0.25 seconds per cycle, the mechanism will run 345600 cycles per day. Therefore, the linkage will reach a million cycles in roughly three days. However, the rocker has the maximum stress of 12.3 MPa and the infinite life endurance strength is 172.3 MPa. The safety factor for infinite life is 14.

The mean stress taken into account was zero because there was no information provided by the sponsor about any impact forces on the end-of-arm-tooling. The mean stress is also zero because the crank undergoes a symmetric rotation about its central axis. Although a safety factor of 29 against yielding is high, it allows for plausible impact forces on the linkage on any machinery. The current geometric design for the rocker does not need any change based on this assumption.

Discussion

The original design uses a sliding and rotating, 2 DOF joint connecting the crank and the output slider. This has the advantage of reducing the number of links. The output is centered horizontally over the central axis of the linkage between the servo pivot and the crank pivot. This means the average of error will be reduced. The second design replaces this joint with a small connecting rod. The rocker has the advantage of reduced wear, and should it wear out, it is easier and cheaper to replace than a larger link. The output motion is now shifted farther from the servo motor and crank, which on its own is neither a benefit nor deficit. The con-rod now oscillates evenly above and below the horizontal output axis, once again reducing the average error by summing positive and negative error values.

Both designs of the linkage have a pseudo-dwell designed into the servo motor motion. This means that the motor does not stop turning as it would in a normal dwell; however, the output point on the slider moves only a negligible distance (less than 0.004 mm over 0.02 seconds). Pseudo-dwells have several advantages. First, like a dwell, they allow the assembly line to do work on a product still attached to the movable linkage. Unlike a typical dwell (with regard to servo-motors), pseudo-dwells do not require the motor or linkage to completely stop. As a result, accelerations are reduced, producing less force on the system.

To achieve a shorter stroke, the servo motor is simply run over a shorter range of input angles. To achieve a larger stroke than 56mm, the linkage would have to be physically altered. The links could be scaled up, which would require more material and space. Alternatively a small portion of the linkages could be increased: the con-rod from the servo to the crank or the length of the crank link below its ground pivot. These options would reduce the total space

increase. Alternatively, the servo and crank pivots could be moved closer together; however, this option would significantly increase accelerations.

The crank pivot can be moved in a straight line closer to the servo pivot to create a larger stroke. Conversely, moving directly away from the servo pivot would produce a shorter stroke. The crank pivot could also be moved perpendicular to this direction in order to achieve uneven output and return strokes. This would produce a similar result to adjusting the length of the output slider link, but without the same structural concerns. It could also be used to create several preset positions, which would allow a dramatically altered stroke with a small, physical adjustment to the linkage.

Several further developments could make the linkage even more flexible and capable. These include moving the ground pivot of the crank and using the full rotation of the servomotor to create a quick return mechanism. The latter possibility requires no change to the current design of the linkage and would allow the motor to run at a constant speed and still create a quick return mechanism, provided maximum stroke is used. Oscillating the servo motor provides some advantages: the capability of less than maximum stroke, the capability of uneven output and return strokes, and reduced accelerations in mm/deg (not necessarily mm/sec however). It was chosen in this report to make the linkage as generic as possible.

Conclusion

The linkage mechanism was successfully designed to meet the requirements provided by the sponsor. The linkage is driven by a servo motor coupled with a low ratio gearbox. The linkage fits within the work envelope in the X (250 mm), Y (250 mm) and Z (1000 mm) directions that were provided. The final design of the linkage meets the stroke length requirement of 56mm .The servo profile can be changed thereby allowing different stroke lengths using the same linkage. The stroke lengths can also be drastically modified by changing the distance between the pivot point of the crank and the pivot point of the rocker. This would require additional modifications to the tooling station; however it would still result in a lower down-time than replacing a cam. The final safety factor was calculated to be of magnitude 29. This is much higher than the required safety factor of 2. However no further modifications were

done to reduce the large safety factor due to a few different reasons; mainly because very little information was provided regarding the works load and any impact forces that would affect it.

The linkage mechanism was designed for the sponsor to incur minimal manufacturing and fabrication costs. Many of the components used in the mechanism were off-the-shelf parts that the sponsor provided. The custom parts were also mainly modifications of the off-the-shelf parts, therefore allowing less time in manufacturing these parts. The servo motor and gearbox were also selected from vendors that the sponsor already uses; again reducing any additional time and expenses in using and finding a new vendor.

Further work can be done in a few areas of the project as mentioned earlier. Overall, these would improve the performance in terms of flexibility of the linkage. This will require additional analysis to provide the sponsor with added adjustability in order to have a versatile linkage.

Bibliography

Mechanism. (2007). Retrieved October 7, 2010, from Answers.com: http://www.answers.com/topic/mechanism

Chuenchom, T., & Khota, S. (1992). Generalized Synthesis of Adjustable Mechanisms. *Mechanical Design and Synthesis, 46*, pp. 253-260.

Gray, D. A., Julian, J. P., & Roberts, J. D. (1999). *Design of a Valve Train Motoring Test Fixture.* Worcester, MA: Worcester Polytechnic Institute.

Hain, K. (1967). *Applied kinematics.* New York: McGraw-Hill Book Company.

Hong, B., & Erdman, A. (2005, May). A Method for Adjustable Planar. *Transactions of the ASME*, pp. 456-463.

Jones, F. D. (1935). *Ingenious Mechanisms for Designers and Inventors Volume I.* New York: The Industrial Press.

Makita, H., Iwasaki, T., & Bamba, T. (1994). Reference Generation for Servo-motors with Cam Motion Curve and Auto-tuning of its Generating Parameter. *The Third International Conference on Automation, Robotics and Computer Vision*, 73-77.

Mechanism. (n.d.). Retrieved October 7, 2010, from Answers.com: http://www.answers.com/topic/mechanism

Naik, D. P., & Amarnath, C. (1989). Synthesis of Adjustable Four Bar Function Generators Through Five Bar Loop Closure Equations. *Mechanism and Machine Theory, 24*(6), pp. 523-526.

Nicholas P. Chironis, N. S. (2007). *Mechanisms and Mechanical Devices Sourcebook.* McGraw-Hill.

Norton, R. L. (2008). *Design of Machinery.* New York NY: McGraw Hill.

Pilkey, W. D. (1997). *Peterson's Stress Concentration Factors.*

Rastegar, J., & Yuan, L. (2001). A Systematic Method for Kinematics Synthesis of High-Speed Mechanisms With Optimally Integrated Smart Materials. *ASME Journal of Mechanical Design, 124*(1), 14-20.

Sclater, N., & Chironis, N. P. (2001). *Mechanisms and Mechanical Devices Sourcebook.* New York: McGraw-Hill Professional.

Yan, H.-S., & Yan, G.-J. (2009). Integrated control and mechanism design for the variable. *Mechatronics, 19*, pp. 274-285.

Zhou, H. (2009). Synthesis of adjustable function generation linkages. *Mechanism and Machine Theory, 44*, pp. 983-990.

Zhou, H., & Ting, K.-L. (2002). Adjustable slider–crank linkages for multiple path generation. *Mechanism and Machine Theory*(37), pp. 499-509.

Appendix A – MathCad worksheets for kinematic analysis of the linkages and stress analysis of the rocker

Kinematic Analysis of Design A for different link length ratios:

Variables:

Distance between the two fixed pivots of the crank and the rocker:

$l_2 := 15mm$

Length of the crank as a ratio of l_2:

$l_1 := 1.1 \cdot l_2, 1.2 \cdot l_2 .. 2.0 l_2$

Distance between the fixed pivot of the rocker and the slider axis:

$h := 25mm$

Increments of input crank angle:

$\theta := 0deg, 1deg .. 360deg$

Equation for the position of the slider with respect to crank angle and l_1:

$$x(\theta, l_1) := -h \cdot \frac{l_2 \cdot \cos(\theta)}{l_1 + l_2 \cdot \sin(\theta)}$$

Derivate of position with respect to crank angle:

$$v(\theta, l_1) := \frac{d}{d\theta} x(\theta, l_1)$$

Second derivative of position with respect to crank angle:

$$a(\theta, l_1) := \frac{d}{d\theta} v(\theta, l_1)$$

Third derivate of position with respect to crank angle:

$$j(\theta, l_1) := \frac{d}{d\theta} a(\theta, l_1)$$

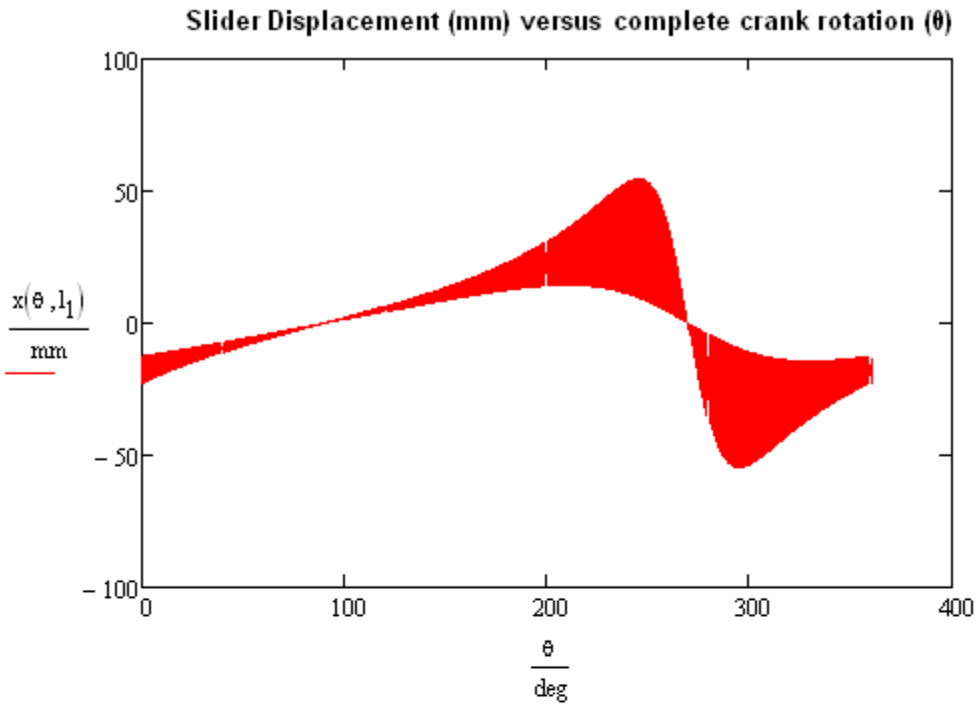
Slider Displacement (mm) versus complete crank rotation (θ)
100
50
0
– 50
– 100
0
100
200
300
400
x(θ, l1)
mm
θ
deg

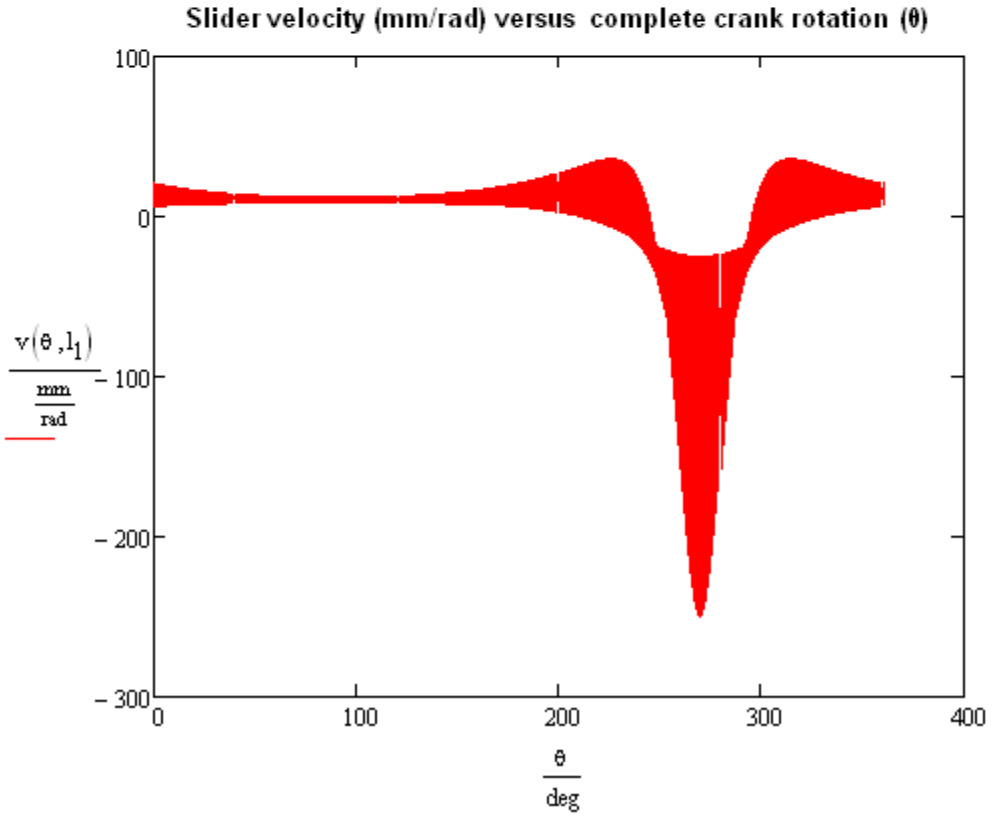
Slider velocity (mm/rad) versus complete crank rotation (θ)
100
0
– 100
– 200
– 300
0
100
200
300
400
v(θ, l1)
mm
rad
θ
deg

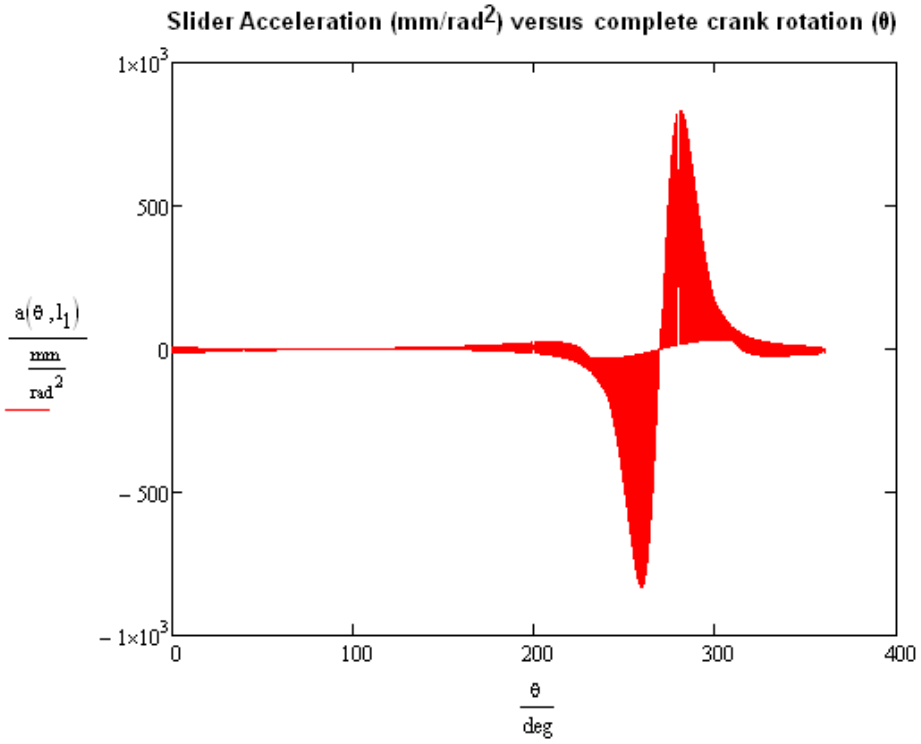

Tabular values exported to Microsoft Excel:

$x(\theta,l_1)$ =	· mm
-22.727	
-22.369	
-22.015	
-21.665	
-21.32	
-20.979	
-20.641	
-20.308	
-19.978	
-19.653	
-19.33	
-19.012	
-18.697	
-18.385	
-18.077	
…	

$v(\theta,l_1)$ =	· mm/rad
20.661	
20.405	
20.155	
19.911	
19.672	
19.439	
19.212	
18.99	
18.773	
18.562	
18.355	
18.154	
17.957	
17.765	
17.578	
…	

$a(\theta,l_1)$ =	· mm/rad2
-14.838	
-14.496	
-14.159	
-13.829	
-13.505	
-13.187	
-12.875	
-12.569	
-12.27	
-11.977	
-11.69	
-11.409	
-11.134	
-10.865	
-10.602	
…	

Kinematic Analysis of the finalized linkage design

This version has an additional con-rod between the slotted rocker and the output slider.

Definitions

d: Length from slotted rocker pivot to horizontal axis of the output slider — $d := 80mm$

h: Length along the slotted rocker from ground pivot to the pin joint with the added con-rod (link 4) — $h := 77.39mm$

l_1: Length from crank ground pivot to slotted rocker ground pivot — $l_1 := 90mm$

l_2: Length of crank — $l_2 := 32mm$

l_4: Length of added con-rod — $l_4 := 32mm$

Equations

This is the equation for the position of the slider with respect to the inputted crank angle, while including the added con-rod. Derived by hand from the geometry of the linkage.

$$X_{slider}(\theta) := \sqrt{l_4^2 - \left(h - d\cdot\cos\left(\operatorname{atan}\left(\frac{l_2\cdot\sin(\theta)}{l_1 + l_2\cdot\cos(\theta)}\right)\right)\right)^2} + d\cdot\sin\left(\operatorname{atan}\left(\frac{l_2\cdot\sin(\theta)}{l_1 + l_2\cdot\cos(\theta)}\right)\right)$$

$v(\theta) := \frac{d}{d\theta}X_{slider}(\theta)$ Velocity of the slider with respect to the crank angle.

$a(\theta) := \frac{d^2}{d\theta^2}X_{slider}(\theta)$ Acceleration of the slider with respect to the crank angle.

$j(\theta) := \frac{d^3}{d\theta^3}X_{slider}(\theta)$ Jerk of the slider with respect to the crank angle.

S, V, A, J Graphs

Position, velocity, acceleration, and jerk shown verse crank angle in degrees

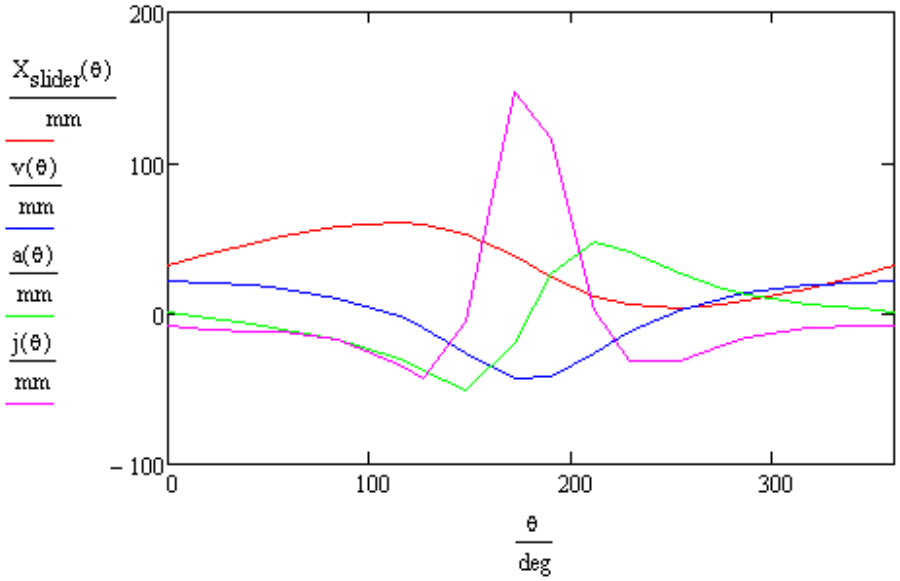

Slider Position

Position (in millimeters) verse Crank Angle (in degrees)

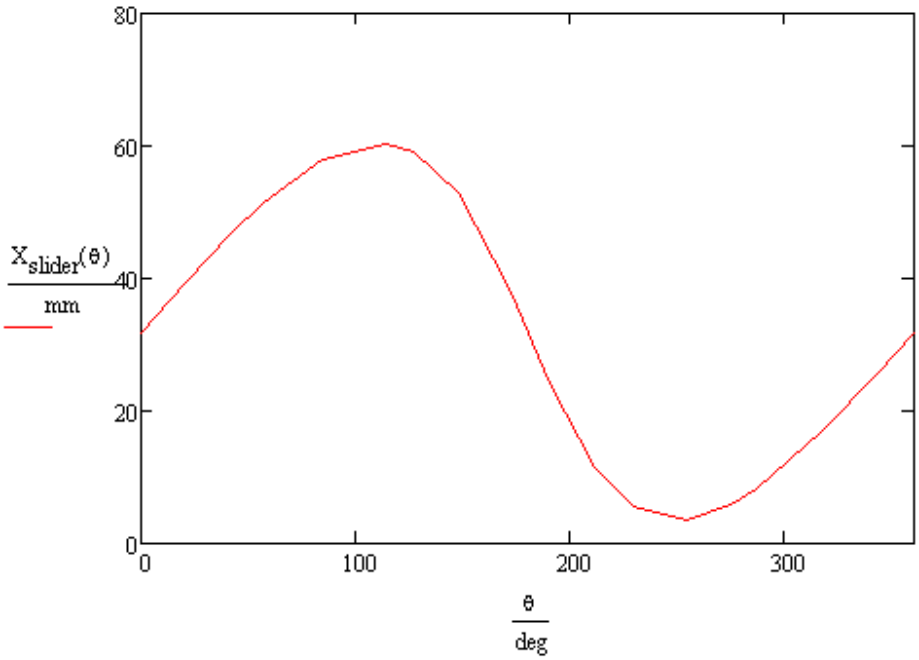

Slider Velocity

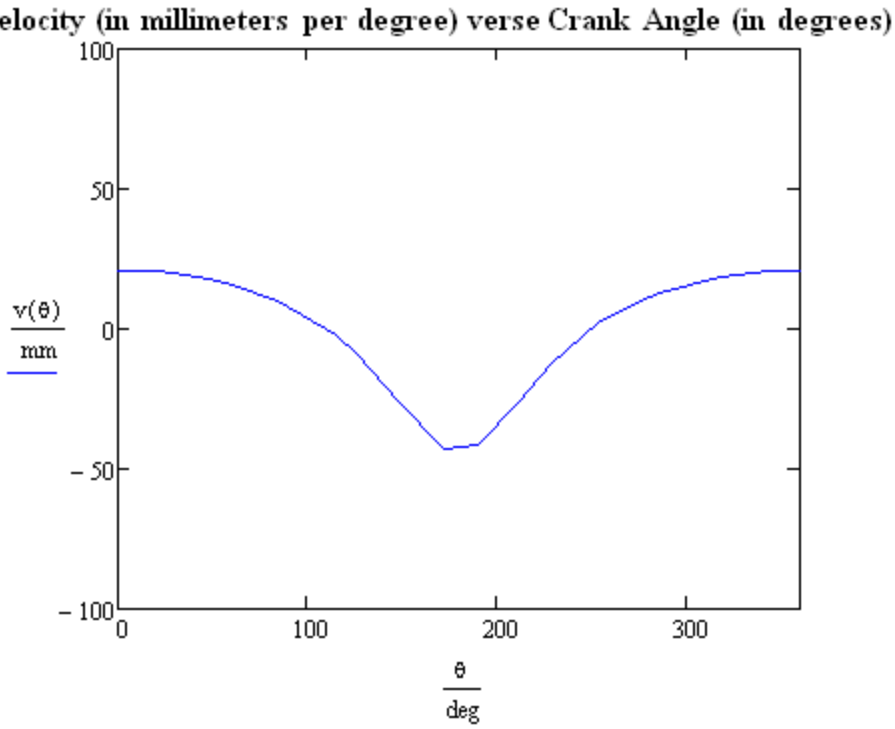

Slider Acceleration

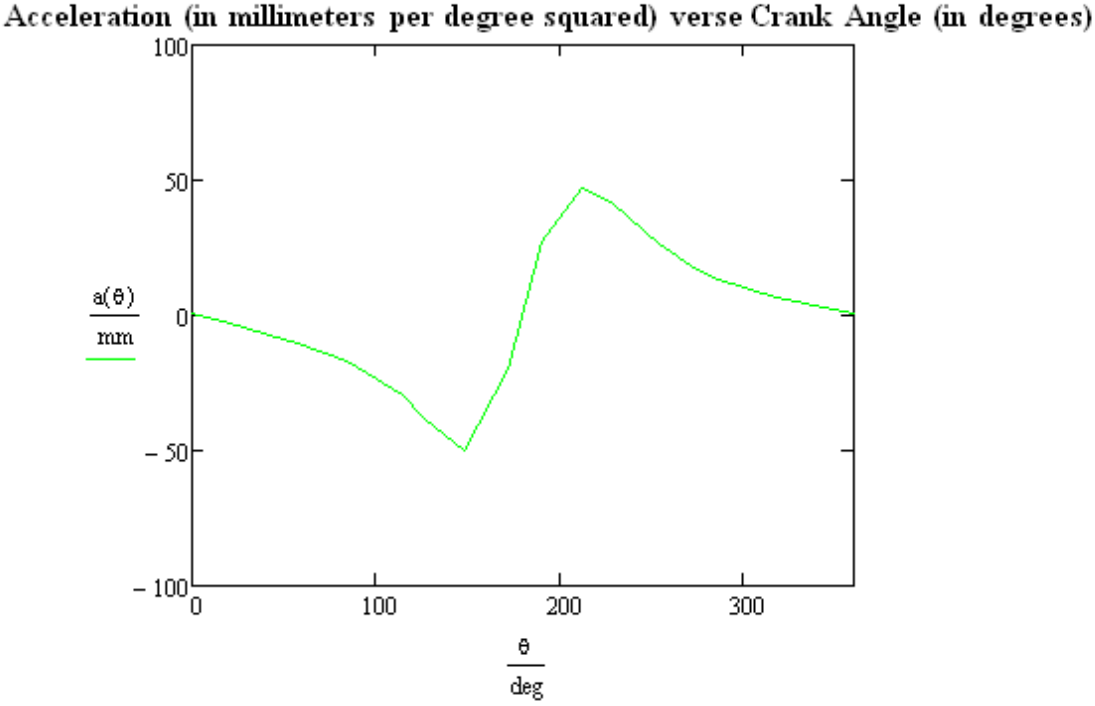

Slider Jerk

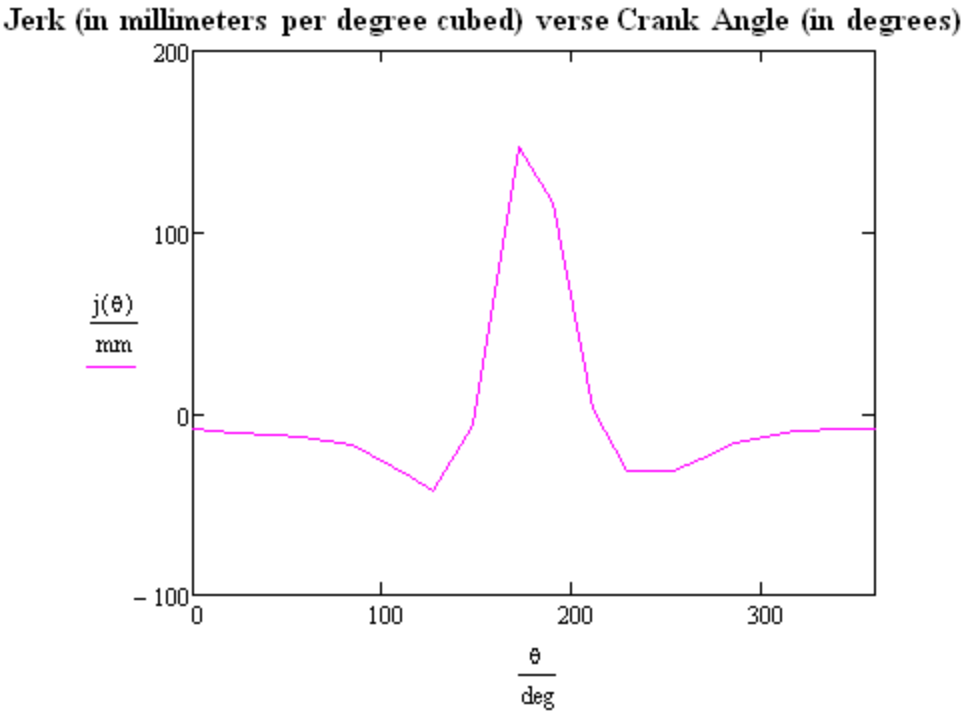
Jerk (in millimeters per degree cubed) verse Crank Angle (in degrees)
200
100
0
– 100
j(θ)
mm
0
100
200
300
θ
deg

Inverse Kinematics of the final design

The linkage was broken into two portions: one above and one below the central ground pivot of the rocker. The two were solved simultaneously to get an output crank angle with respect to the input motion of the slider.

Inverse Kinematic Analysis of the bottom slider-crank

Definitions

Independent Input variable (x), left as a constant here for simplicity. $x := 32$

Input position: Length of R1 $c := x$

Length of R2 $a := 32$

Length of R3 $b := 80$

Length of R4 $d := 77.39$

Angle of R1 $\phi_1 := 0$

Angle of R2 ϕ_2

Angle of R3 ϕ_3

Angle of R4 $\phi_4 := 90$

Closed Loop Vector Equations

$$R_2 + R_3 - R_4 + R_1 = 0$$

Real solution, along X-axis of linkage

$$a\cdot\cos(\phi_2) + b\cdot\cos(\phi_3) - c\cdot\cos(\phi_4) + d\cdot\cos(\phi_1) = 0$$

$$a\cdot\cos(\phi_2) + b\cdot\cos(\phi_3) + d = 0$$

$$b\cdot\cos(\phi_3) = -a\cdot\cos(\phi_2) - d$$

Imaginary solution, along Y-axis of linkage, *j* was dropped.

$$a\cdot j\cdot\sin(\phi_2) + b\cdot j\cdot\sin(\phi_3) - c\cdot j\cdot\sin(\phi_4) + d\cdot j\cdot\sin(\phi_1) = 0$$

$$a\cdot\sin(\phi_2) + b\cdot\sin(\phi_3) - c = 0$$

$$b\cdot\sin(\phi_3) = c - a\cdot\sin(\phi_2)$$

Square both equations and add them

$$b^2\left(\cos(\phi_3)^2 + \sin(\theta_3)^2\right) = \left(-a\cdot\cos(\phi_2) - d\right)^2 + \left(c - a\cdot\sin(\phi_2)\right)^2$$

Simplifying

$$\frac{a^2 - b^2 + c^2 + d^2}{2a} = c\cdot\sin(\phi_2) - d\cdot\cos(\phi_2)$$

Substituting

$$\sin(\phi_6) = \frac{2\cdot\tan\left(\frac{\phi_2}{2}\right)}{1+\tan^2\left(\frac{\phi_2}{2}\right)}$$

$$\cos(\phi_6) = \frac{1-\tan^2\left(\frac{\phi_2}{2}\right)}{1+\tan^2\left(\frac{\phi_2}{2}\right)}$$

$$K_1 := \frac{a^2 - b^2 + c^2 + d^2}{2a}$$

Gives

$$c\cdot\frac{2\cdot\tan\left(\frac{\phi_2}{2}\right)}{1+\tan^2\left(\frac{\phi_2}{2}\right)} - d\cdot\frac{1-\tan^2\left(\frac{\phi_2}{2}\right)}{1+\tan^2\left(\frac{\phi_2}{2}\right)} - K_1 = 0$$

Simplifying

$$(d - K_1)\cdot\tan^2\left(\frac{\phi_2}{2}\right) + 2\cdot c\cdot\tan\left(\frac{\phi_2}{2}\right) + (-d - K_1) = 0$$

Substituting

$$A := d - K_1$$

$$B := 2\cdot c$$

$$C := -d - K_1$$

Gives

$$A\cdot\tan^2\left(\frac{\phi_2}{2}\right) + B\cdot\tan\left(\frac{\phi_2}{2}\right) + C = 0$$

Which can be solved with the quadratic equation

$$\tan\left(\frac{\phi_2}{2}\right) = \frac{-B + \sqrt{B^2 - 4A\cdot C}}{2A}$$

$$\phi_{2.1} := 2\cdot\operatorname{atan}\left(\frac{-B + \sqrt{B^2 - 4A\cdot C}}{2A}\right) = 85.322\ \text{deg}$$

$$\phi_{2.2} := 2\cdot\operatorname{atan}\left(\frac{-B - \sqrt{B^2 - 4A\cdot C}}{2A}\right) = -130.251\ \text{deg}$$

Choosing the positive angle and restating as definitions for MathCad $\phi_2 := \phi_{2.1}$

$$\phi_3(\phi_2) := \operatorname{acos}\left(\frac{c - a\cdot\sin(\phi_2)}{b}\right)$$

This solves the necessary parts of the bottom portion of the linkage. $\phi 3$ will be used in the top portion as well.

$$\phi_3(\phi_2) = 89.924\,\text{deg}$$

Inverse Kinematics of top slider crank section

Definitions:

Length of R5	$g := 90$
Length of R6	$e := 32$
Length of R7	f
Angle of R5	$\phi_5 := 0$
Angle of R6	ϕ_6
Angle of R7	$\phi_7 := \phi_3(\phi_2) + 90\,\text{deg}$

Closed Loop Vector Equations $R_6 - R_7 + R_5 = 0$

Real Solution, or Y-axis of linkage

$$e\cdot\cos(\phi_6) - f\cdot\cos(\phi_7) + g\cdot\cos(\phi_8) = 0$$

$$e\cdot\cos(\phi_6) - f\cdot\cos(\phi_7) + g = 0$$

Imaginary Solution, or X-axis of linkage

$$e\cdot\sin(\phi_6) - f\cdot\sin(\phi_7) + g\cdot\sin(\phi_8) = 0$$

$$e\cdot\sin(\phi_6) - f\cdot\sin(\phi_7) = 0$$

Solve the second for *f*

$$f = \frac{e\cdot\sin(\phi_6)}{\sin(\phi_7)}$$

Insert solution into the first and solve for $\phi 6$

$$e\cdot\cos(\phi_6) - \frac{e\cdot\sin(\phi_6)}{\sin(\phi_7)}\cdot\cos(\phi_7) + g = 0$$

Substituting

$$K_2 := \frac{-e\cdot\cos(\phi_7)}{\sin(\phi_7)} = 2.401 \times 10^4$$

$$\sin(\phi_6) = \frac{2\cdot\tan\left(\frac{\phi_6}{2}\right)}{1+\tan^2\left(\frac{\phi_6}{2}\right)}$$

$$\cos(\phi_6) = \frac{1-\tan^2\left(\frac{\phi_6}{2}\right)}{1+\tan^2\left(\frac{\phi_6}{2}\right)}$$

Gives

$$e\cdot\frac{1-\tan^2\left(\frac{\phi_6}{2}\right)}{1+\tan^2\left(\frac{\phi_6}{2}\right)} - K_2\cdot\frac{2\cdot\tan\left(\frac{\phi_6}{2}\right)}{1+\tan^2\left(\frac{\phi_6}{2}\right)} + g = 0$$

Simplifying

$$-(e+g)\cdot\tan^2\left(\frac{\phi_6}{2}\right) + -2K_2\cdot\tan\left(\frac{\phi_6}{2}\right) + (h-g) = 0$$

Substituting

$$A_2 := -(e+g) = -122$$

$$B_2 := -2\cdot K_2 = -4.803\times 10^4$$

$$C_2 := e - g = -58$$

Gives

$$A_2\cdot\tan^2\left(\frac{\phi_6}{2}\right) + B_2\cdot\tan\left(\frac{\phi_6}{2}\right) + C_2 = 0$$

Which can be solved with the quadratic equation

$$\tan\left(\frac{\phi_6}{2}\right) = \frac{-B.2 + \sqrt{B_2^{\,2} - 4A_2\cdot C_2}}{2A_2}$$

$$\phi_{6.1} := 2\cdot\operatorname{atan}\left(\frac{-B_2 + \sqrt{B_2^{\,2} - 4A_2\cdot C_2}}{2A_2}\right) = -179.709\ \text{deg}$$

$$\phi_{6.2} := 2\cdot\operatorname{atan}\left(\frac{-B_2 - \sqrt{B_2^{\,2} - 4A_2\cdot C_2}}{2A_2}\right) = -0.138\ \text{deg}$$

$$\theta_2 := 180\,\text{deg} + \phi_{6.1} = 0.291\ \text{deg}$$

Stress Analysis of the rocker

Free Body Diagram of the rocker

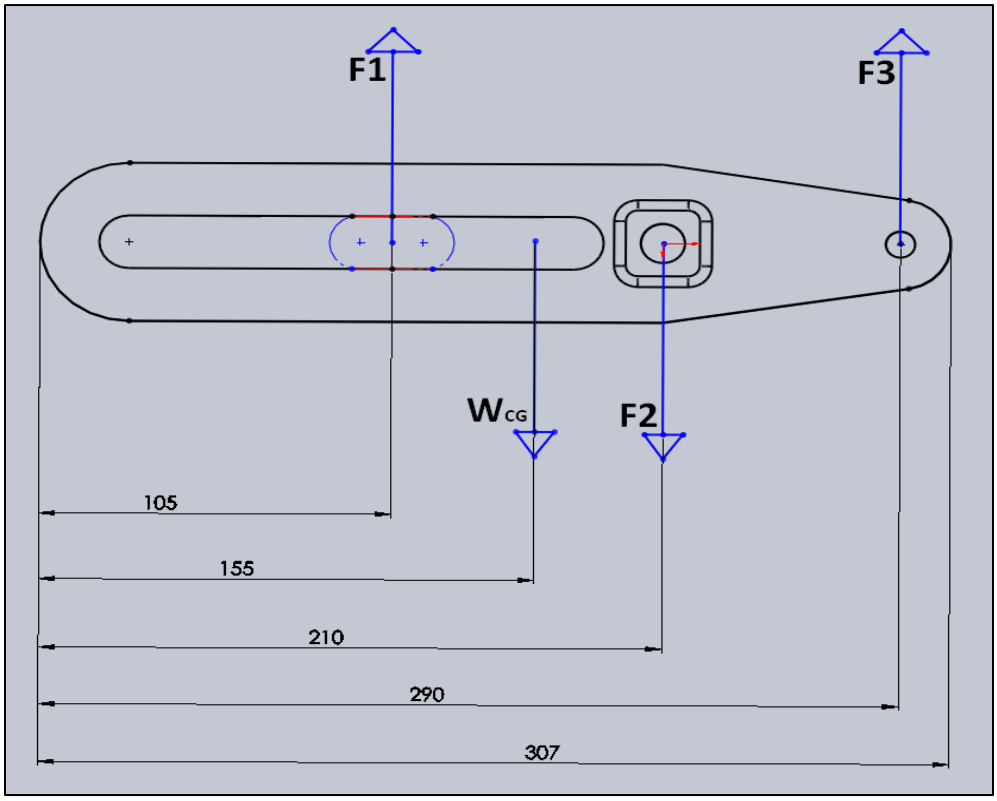

The free body diagram of the rocker above shows the loading on the rocker along one dimension. The following analysis uses the above forces and dimensions to derive singularity functions which serves as the basis for further stress analysis.

Singularity Functions for the rocker:

Variables:

$a := 0.105m$ $b := 0.211m$ $f := 0.290m$ $CG := 0.155m$ $k := 0.307m$

$F_1 := 15N$ $F_2 := 22N$ $F_3 := 11N$ $W_{cg} := 7.759N$

Steel Elastic Modulus: $E := 190000000000 \frac{N}{m^2}$ Moment of inertia $I := 3.337 \cdot 10^{-9} kg \cdot m^2$

Range of x $x := 0 \cdot m, 0.005 \cdot k .. k$

Step Function $S(x,z) := if(x \geq z, 1, 0)$

Shear Equation:

$V(x) := F_1 \cdot S(x,a) - F_2 \cdot S(x,b) + F_3 \cdot S(x,f) - W_{cg} \cdot S(x,CG)$

Moment Equation:

$M(x) := F_1 \cdot S(x,a) \cdot (x - a) - F_2 \cdot S(x,b)(x - b) + F_3 \cdot S(x,f)(x - f) - W_{cg} \cdot S(x,CG) \cdot (x - CG)$

Slope Equation:

$$\theta(x) := \frac{1}{E \cdot I} \cdot \left[\frac{F_1}{2} \cdot S(x,a) \cdot (x - a)^2 + \frac{-F_2}{2} \cdot S(x,b) (x - b)^2 + \frac{F_3}{2} \cdot S(x,f) (x - f)^2 - \frac{W_{cg}}{2} \cdot S(x,CG) \cdot (x - CG)^2 \right]$$

Deflection Equation:

$$y(x) := \frac{1}{E \cdot I} \cdot \left[\frac{F_1}{6} \cdot S(x,a) \cdot (x - a)^3 + \frac{-F_2}{6} \cdot S(x,b) (x - b)^3 + \frac{F_3}{6} \cdot S(x,f) (x - f)^3 - \frac{W_{cg}}{6} \cdot S(x,CG) \cdot (x - CG)^3 \right]$$

Solving for C3 and C4 in the deflection and slope equations:

at x=a, the deflection will be zero $x := b$

guess

$C_3 := 0 m^3 \cdot kg \cdot s$ $C_4 := 0$

Given

$$0 = \frac{1}{E \cdot I} \left[\begin{array}{l} \frac{F_1}{2} \cdot S(x,a) \cdot (x - a)^2 + \frac{-F_2}{2} \cdot S(x,b) (x - b)^2 + \frac{F_3}{2} \cdot S(x,f) (x - f)^2 - \frac{W_{cg}}{2} \cdot S(x,CG) \cdot (x - CG)^2 \ldots \\ + C_3 \end{array} \right]$$

$$Find(C_3) = -0.072 \frac{m^3 \cdot kg}{s^2}$$

$$C_3 := -0.112 \frac{m^3 \cdot kg}{s^2}$$

Given

$$0 = \frac{1}{E \cdot I} \left[\begin{array}{l} \frac{F_1}{6} \cdot S(x,a) \cdot (x - a)^3 + \frac{-F_2}{6} \cdot S(x,b) (x - b)^3 + \frac{F_3}{6} \cdot S(x,f) (x - f)^3 - \frac{W_{cg}}{6} \cdot S(x,CG) \cdot (x - CG)^3 \ldots \\ + C_3 \cdot x + C_4 \end{array} \right]$$

$$\text{Find}(C_4) = 0.021\ \frac{m^4 \cdot kg}{s^2}$$

$$C_4 := 0.018\ \frac{m^4 \cdot kg}{s^2}$$

$$\theta(x) := \frac{1}{E \cdot I}\left[\frac{F_1}{2}\cdot S(x,a)\cdot(x-a)^2 + \frac{-F_2}{2}\cdot S(x,b)\,(x-b)^2 + \frac{F_3}{2}\cdot S(x,f)\,(x-f)^2 \ldots + \frac{-W_{cg}}{2}\cdot S(x,CG)\cdot(x-CG)^2 + C_3\right]$$

$$y(x) := \frac{1}{E \cdot I}\left[\frac{F_1}{6}\cdot S(x,a)\cdot(x-a)^3 + \frac{-F_2}{6}\cdot S(x,b)\,(x-b)^3 + \frac{F_3}{6}\cdot S(x,f)\,(x-f)^3 \ldots + \frac{-W_{cg}}{6}\cdot S(x,CG)\cdot(x-CG)^3 + C_3\cdot x + C_4\right]$$

Defining x as a range from 0 to the end of the rocker: $x := 0\cdot m, 0.005\cdot k\,..\,k$

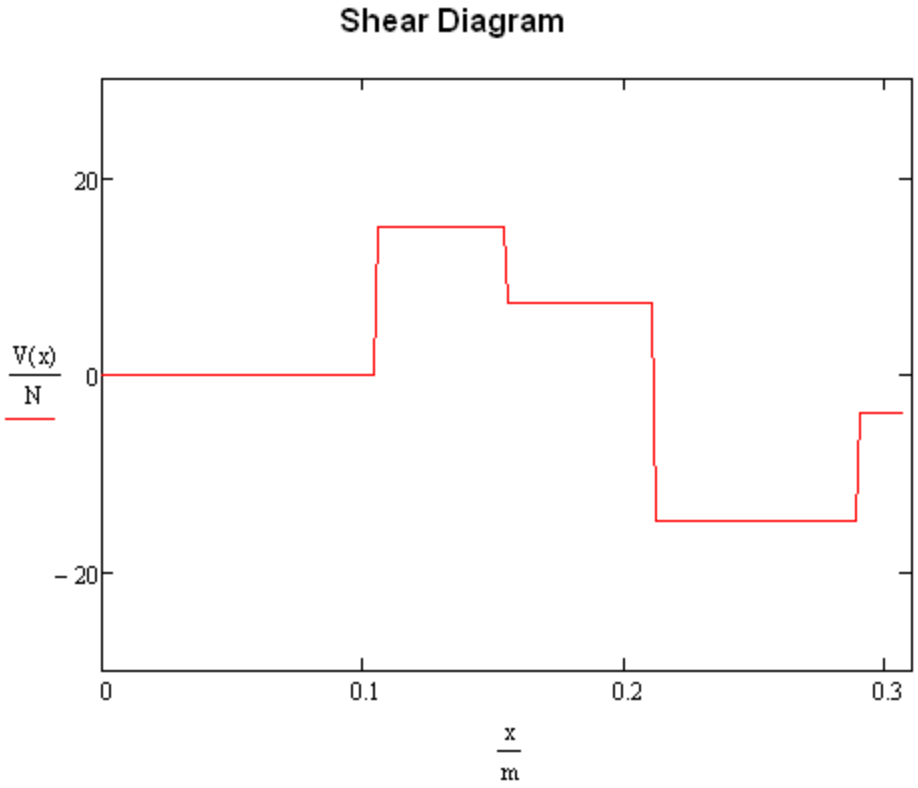

$$V_{max} := |V(0.11m)| = 15\,N$$

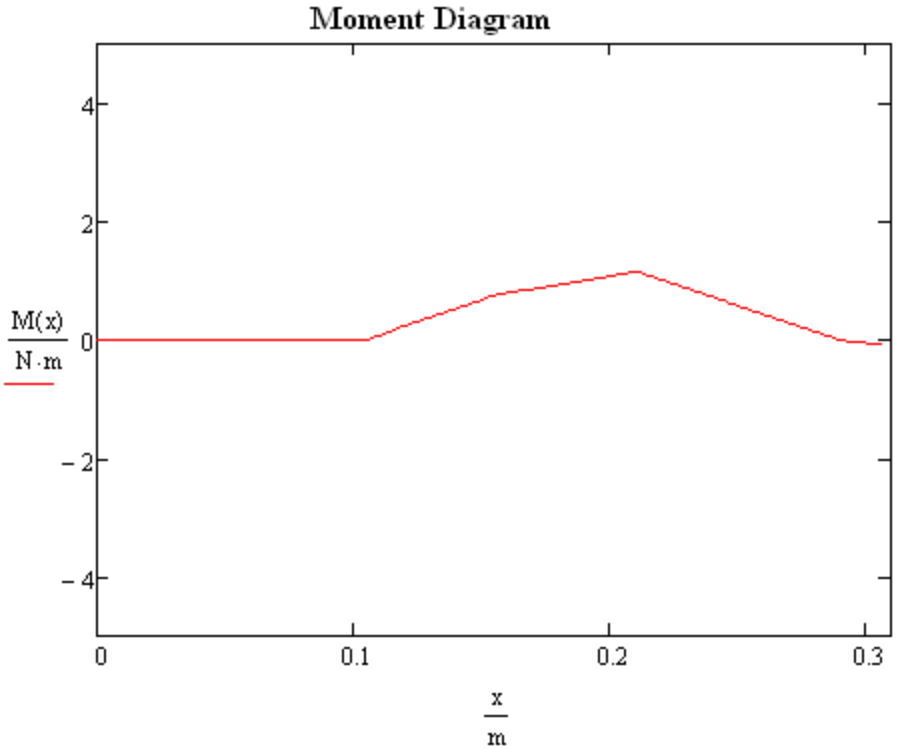

$M_{max} := 1.15N \cdot m$

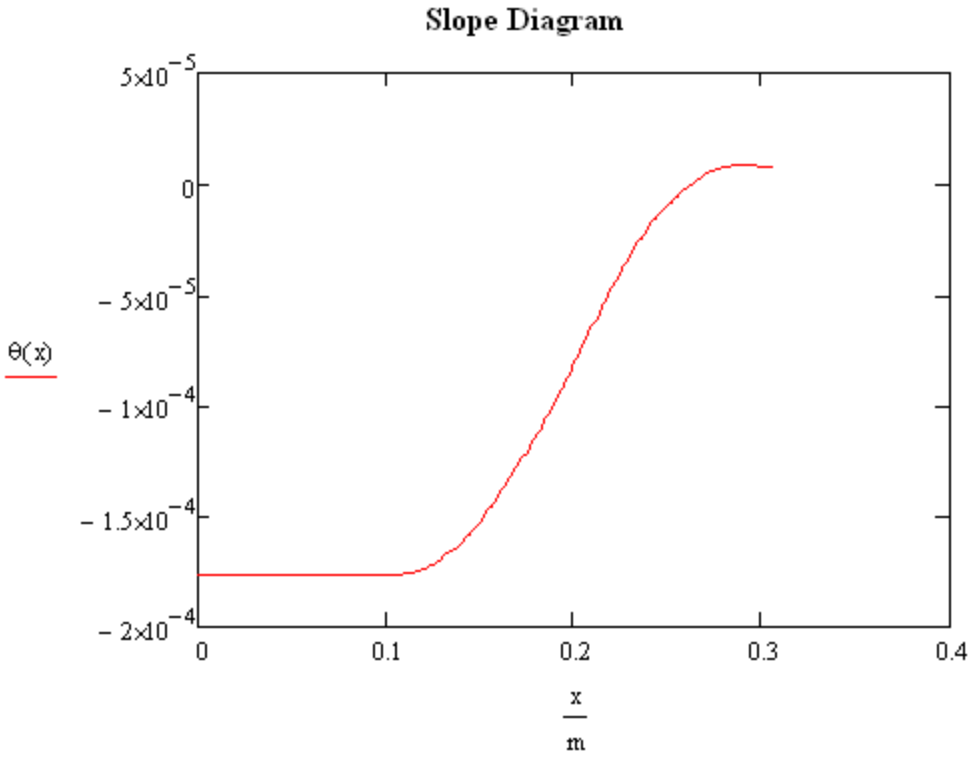

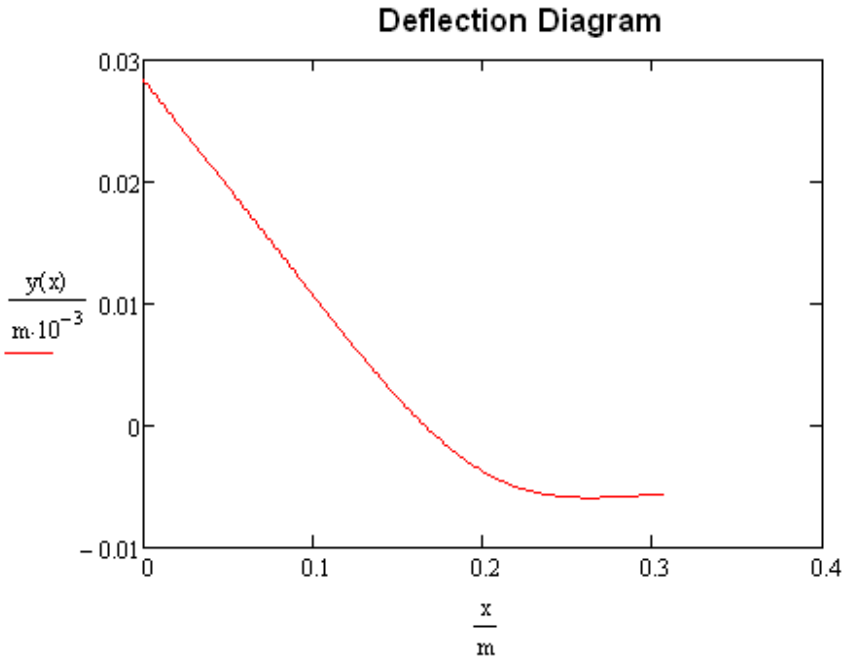

The critical cross-section is the cross section that experiences the maximum amount of bending amount and shear force. According to the above singularity functions, this cross-section is at the end of the rocker i.e. this cross-section has the maximum amount of bending moment.

Further stress analysis will be conducted on this cross-section, which will include the stress concentration factors caused by the pin hole on the shaft, and the fatigue life cycle analysis of the rocker.

Bending and torsional stress concentration factors:

For the shape in consideration:

$H := 0.034m$ $d := 0.029m$ $t := 5mm$ $r := 5mm$

Bending

$\frac{H}{d} = 1.172$ $\frac{t}{r} = 1$ From Peterson's Stress Concentration Factors by Walter Pikey Notches and Grooves page 110

$D_b := \frac{t}{H} = 0.147$

For a semicircular notch:

$K_{tn} := 3.065 - 6.643 \cdot D_b - 6.643 \cdot D_b + 0.205 \cdot D_b^{\,2} - 4.004 \cdot D_b^{\,2} = 1.029$

For the cross-section, the geometric properties used are as follows:

$Area := 53.61mm \cdot 20mm = 1.072 \times 10^{-3}\, m^2$ Rectangular area cross-section right under the hole of 10 mm diameter

$c := \frac{32.5mm}{2} = 16.25 \cdot mm$

$I_{cross} := \frac{32.5mm \cdot (10mm)^3}{12} = 2.708 \times 10^{-9}\, m^4$

$\sigma_{bend} := K_{tn} \cdot \frac{M_{max} \cdot c}{I_{cross}} = 7.1 \times 10^6\, Pa$

Principal Stresses at point A of the cross-section:

$\sigma_{xA} := \sigma_{bend} = 7.1 \times 10^6\, Pa$

$\sigma_{zA} := 0$

$\tau_{xzA} := 0$

$\sigma_{1A} := \frac{\sigma_{xA} + \sigma_{zA}}{2} + \sqrt{\left(\frac{\sigma_{xA} + \sigma_{zA}}{2}\right)^2 + \tau_{xzA}^2} = 7.1 \times 10^6\, Pa$

$\sigma_{2A} := 0 \cdot MPa$

$\sigma_{3A} := \frac{\sigma_{xA} + \sigma_{zA}}{2} - \sqrt{\left(\frac{\sigma_{xA} - \sigma_{zA}}{2}\right)^2 + \tau_{xzA}^2} = 0 \cdot MPa$

$\tau_{13A} := \frac{\sigma_{1A} - \sigma_{3A}}{2} = 3.55 \cdot MPa$

von Mises stresses at A:

$\sigma'_A := \sqrt{\sigma_{1A}^2 - \sigma_{1A} \cdot \sigma_{3A} + \sigma_{3A}^2}$ $\sigma'_A = 7.1 \cdot MPa$

Principal Stress at point B

$\sigma_{xB} := 0 \cdot MPa$ $\sigma_{yB} := 0 \cdot MPa$

$\tau_{max} := \sigma_{bend}$

$\sigma_{1B} := \frac{\sigma_{xB} + \sigma_{yB}}{2} + \tau_{max} = 7.1 \cdot MPa$

$\sigma_{2B} := 0 \cdot MPa$

$\sigma_{3B} := \frac{\sigma_{xB} + \sigma_{yB}}{2} - \tau_{max} = -7.1 \cdot MPa$

$\tau_{13B} := \frac{\sigma_{1B} - \sigma_{3B}}{2} = 7.1 \cdot MPa$

*von Mises Stresses at point B

$\sigma'_B := \sqrt{\sigma_{1B}^2 - \sigma_{1B} \cdot \sigma_{3B} + \sigma_{3B}^2}$ $\sigma'_B = 12.3 \cdot MPa$

Safety Factors

$S_y := 359 \cdot 10^6 Pa$ Yield Strength of A2 Tool steel annealed

$N_A := \frac{S_y}{\sigma'_A} = 50.562$

$N_B := \frac{S_y}{\sigma'_B} = 29.192$

Fatigue Failure Analysis

$S_{ut} := 105000psi = 723.95 \cdot MPa$ for annealed A2 Steel

$S_{e'} := 0.5 S_{ut} = 361.975 \cdot MPa$ For steels with $S_{ut} < 1400MPa$

Calculating the correction factors, C's for size, surface finish, temperature, reliability, ignorance.

$C_{load} := 1.0$ *Since there is bending loading*

$A_{95} := 0.05 \cdot 32.5mm \cdot 10mm = 1.625 \times 10^{-5} m^2$

$d_{equiv} := \sqrt{\frac{A_{95}}{0.0766}}$ $d_{equiv} := 0.573in$

$C_{size} := 0.869 \cdot \left(\frac{d_{equiv}}{m} \right)^{-0.097}$ *Since the equivalent diameter is between 0.3 in and 10 in*

$C_{size} = 1.31$ Page 327 of Machine Design by Norton

$A_{machined} := 4.51$ $b_{machined} := -0.265$

$C_{surf} := A_{machined} \cdot \left(\frac{S_{ut}}{MPa} \right)^{b_{machined}} = 0.788$ *For a post-machined shaft*

From Table 6-3 Machine Design by Norton

$C_{temp} := 1$ *Since temperature never exceeds 450 C*

$C_{reli} := 0.659$ *For a reliability of R=99.999* From Table 6-4 Machine Design by Norton

$C_{ign} := 0.7$ *Based on our inaccuracy and misjudgment as first attempt of design*

Hence, corrected endurance limit:

$S_e := C_{load} \cdot C_{size} \cdot C_{surf} \cdot C_{temp} \cdot C_{reli} \cdot C_{ign} \cdot S_{e'} = 172.264 \cdot MPa$ *at $1x10^6$ cycles*

Equation of the SN line => $S_f = aN^b$ From eq 6-10 of Machine Design by Norton

Table 6-5 of Machine Design by Norton: z= -3 at N = 10^6 cycles

$z := -3$ $N_2 := 1 \cdot 10^6$

$S_m := 0.9 \cdot S_{ut} = 651.555 \cdot MPa$ *at 10^3 cycles* For bending loading

$b := \frac{1}{z} \cdot \log\left(\frac{S_m}{S_e} \right) = -0.193$ $a := \frac{S_m}{(10^3)^b} = 2.464 \times 10^3 \cdot MPa$ Equation => $S_f = 147(N)^{-0.172}$

Plotting S-N Diagram using a return function:

$$S_f(N) := \begin{cases} \text{return } a \cdot N^b & \text{if } N < 10^6 \\ S_e & \text{otherwise} \end{cases}$$

where $N := 10^3, 10^4 .. 10^8$

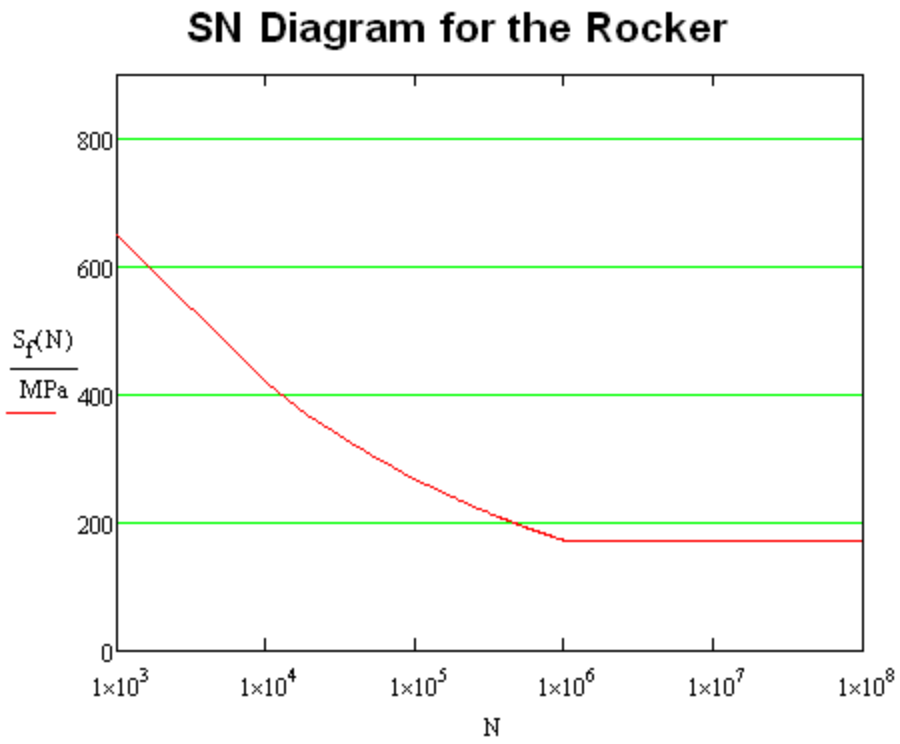
SN Diagram for the Rocker
800
600
400
200
0
$S_f(N)$
MPa
1×10^3
1×10^4
1×10^5
1×10^6
1×10^7
1×10^8
N

Appendix B – Custom Parts Drawings

The following section shows dimensioned drawings of the parts that need to be machined.

These part drawings (in order) are as follows:

1. Crank
2. The rocker
3. Slider block inside the rocker
4. Rail mount on the THK rail

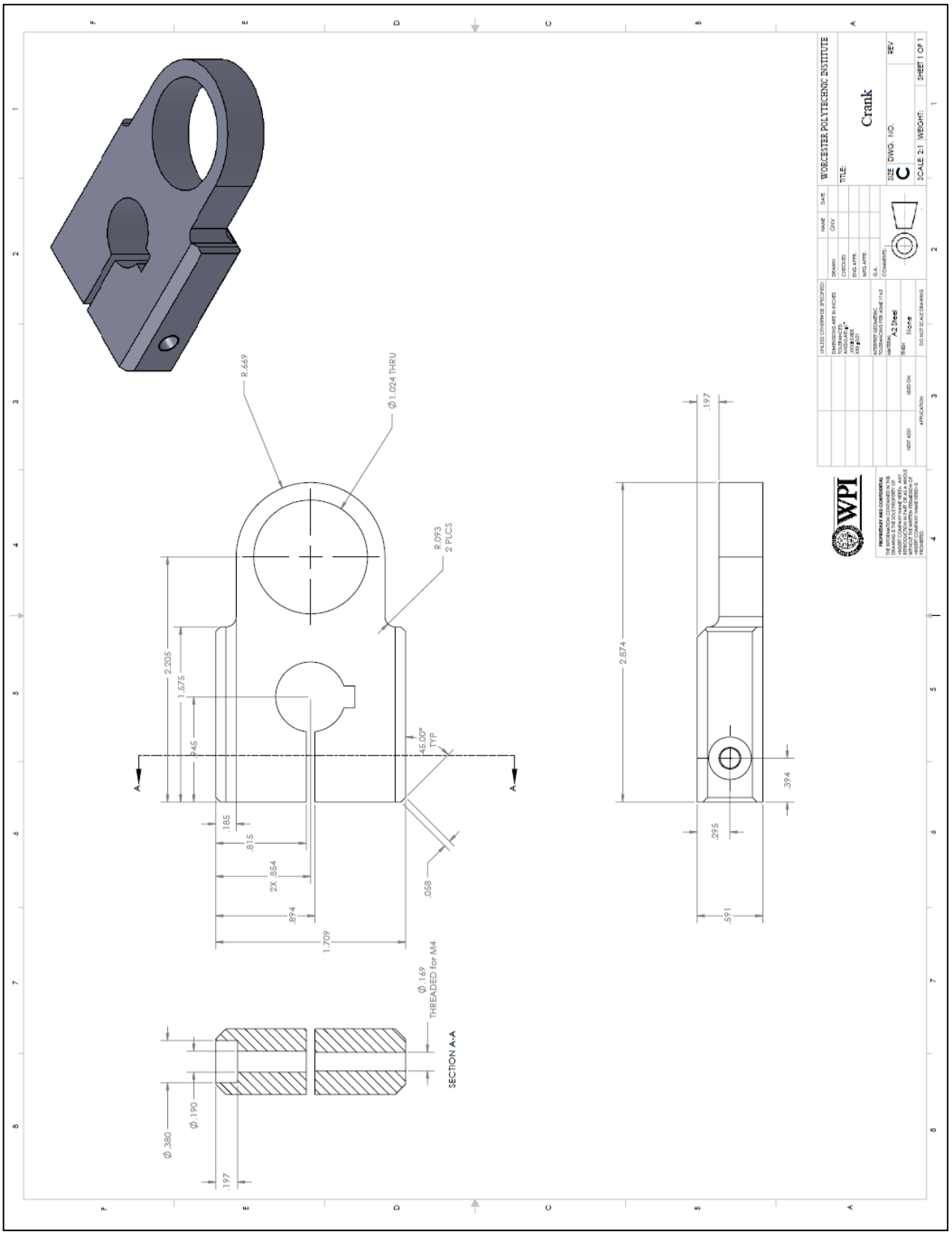
R.669
Ø 1.024 THRU
R.093
2 PLCS
2.205
1.575
.945
45.00°
TYP
.185
.815
2X .854
.894
1.709
.058
Ø .169
THREADED for M4
SECTION A-A
Ø .380
Ø .190
.197
2.874
.197
.295
.591
.394
WORCESTER POLYTECHNIC INSTITUTE
Crank
SIZE
C
DWG. NO.
REV
SCALE: 2:1
WEIGHT:
SHEET 1 OF 1
WPI

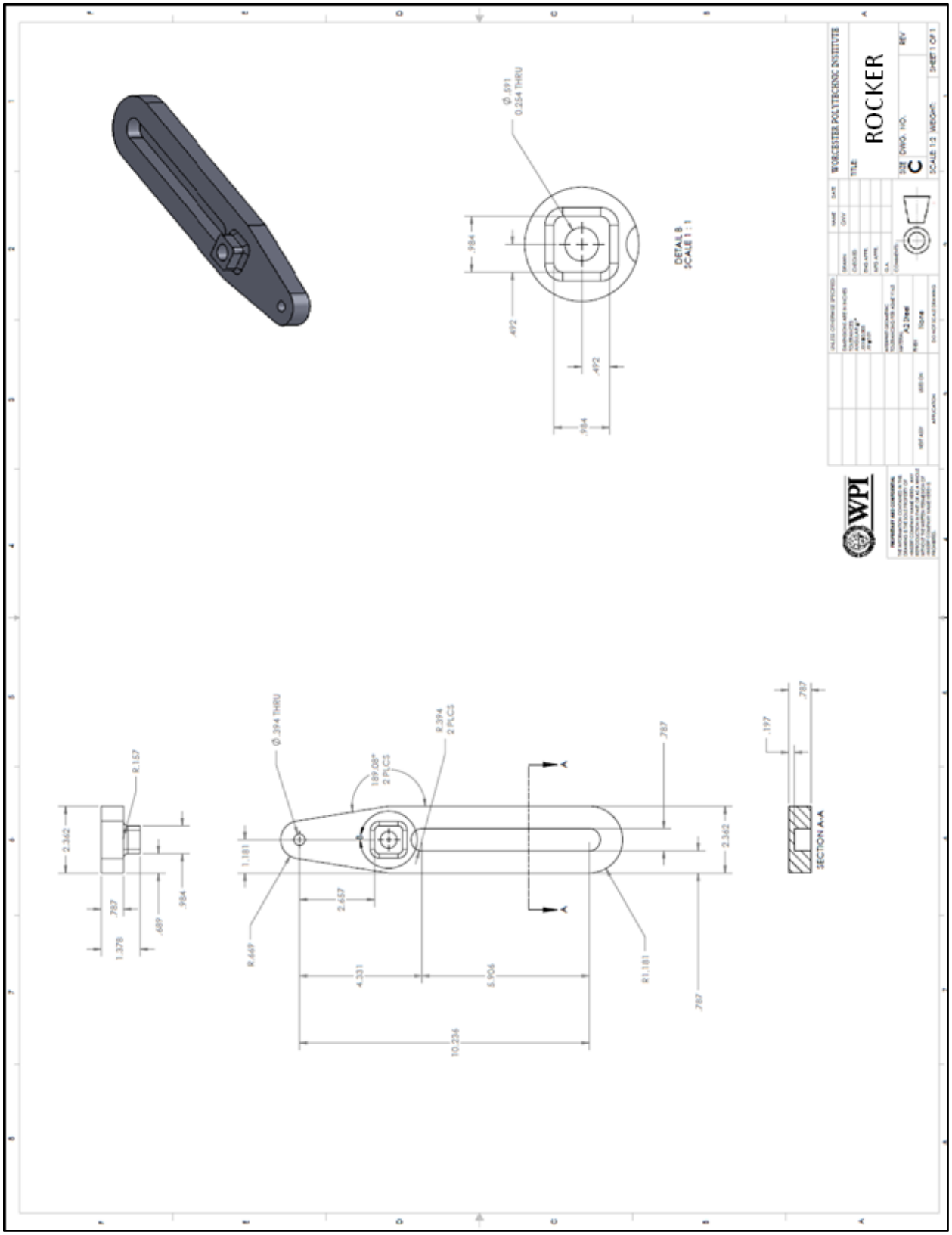
ROCKER
WORCESTER POLYTECHNIC INSTITUTE
DETAIL B
SCALE 1 : 1
SECTION A-A

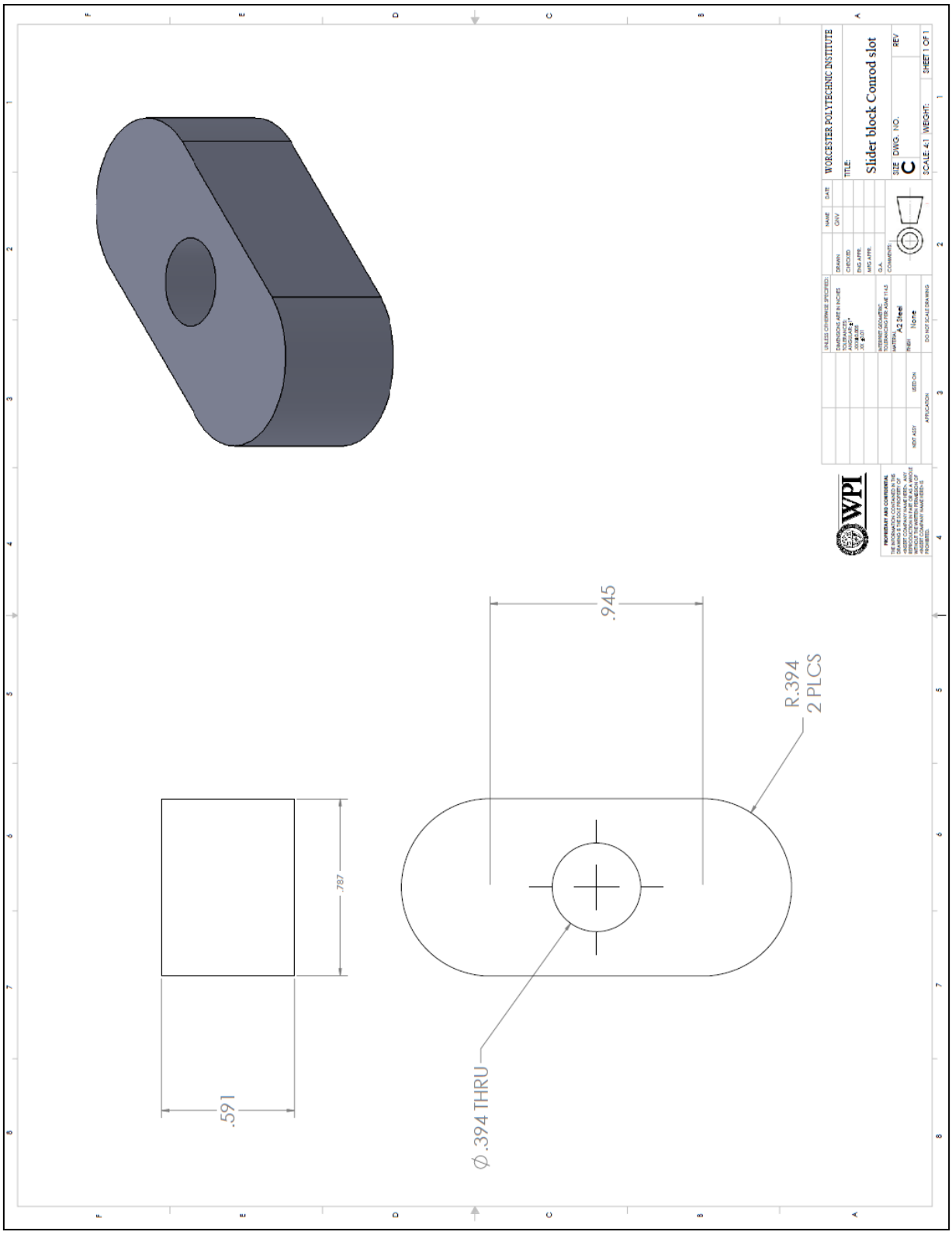
.591
.787
Ø .394 THRU
.945
R.394
2 PLCS
WORCESTER POLYTECHNIC INSTITUTE
TITLE:
Slider block Conrod slot
SIZE
C
DWG. NO.
REV
SCALE: 4:1
WEIGHT:
SHEET 1 OF 1
WPI
A2 Steel
None
DO NOT SCALE DRAWING

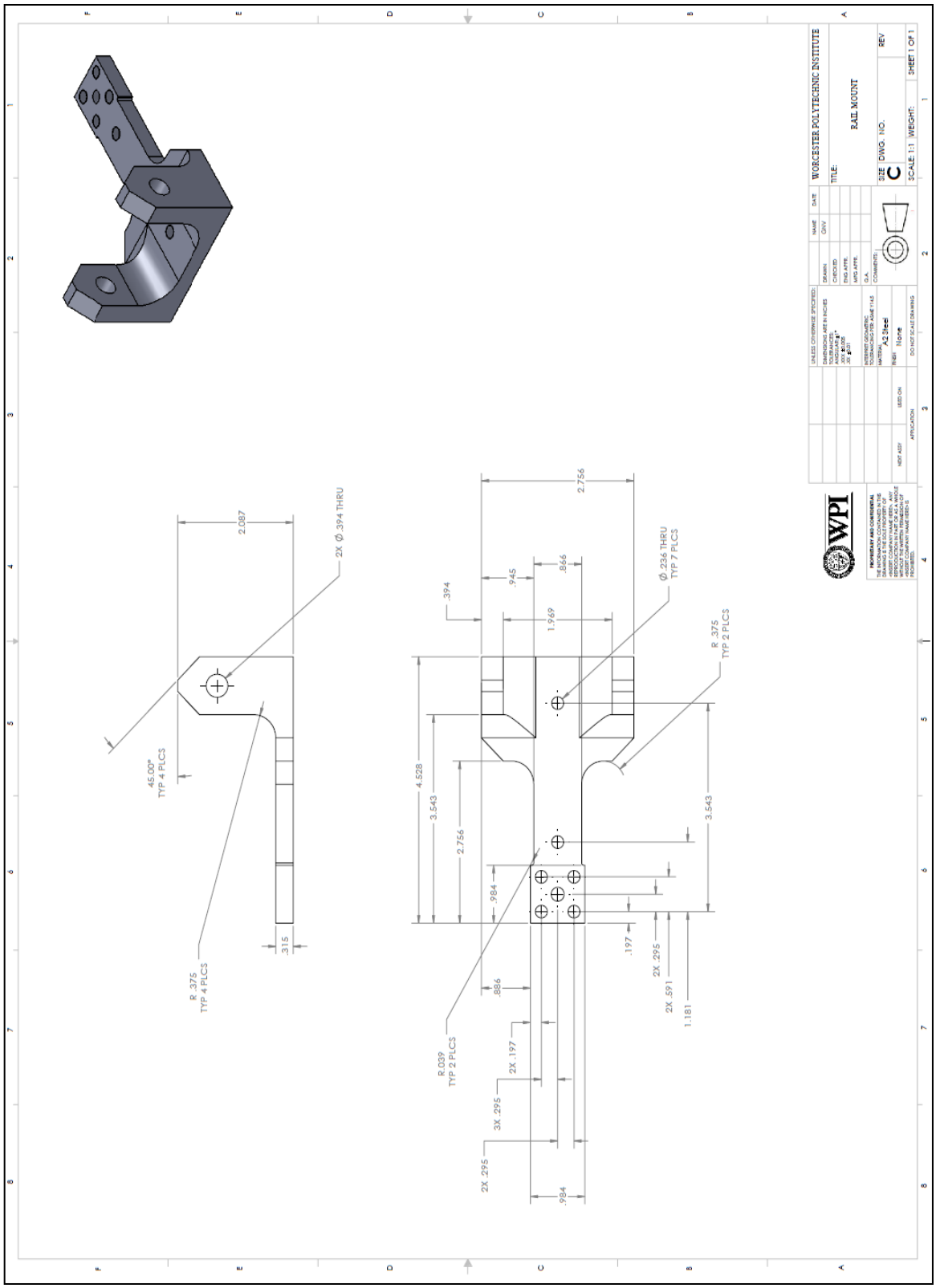
WORCESTER POLYTECHNIC INSTITUTE
RAIL MOUNT
SIZE C
DWG. NO.
REV
SCALE: 1:1 WEIGHT:
SHEET 1 OF 1
2X Ø .394 THRU
2.087
45.00°
TYP 4 PLCS
R .375
TYP 4 PLCS
.315
2.756
.394
.945
.866
1.969
Ø .236 THRU
TYP 7 PLCS
R .375
TYP 2 PLCS
4.528
3.543
2.756
.984
3.543
.197
2X .295
2X .591
1.181
.886
R.039
TYP 2 PLCS
2X .197
3X .295
2X .295
.984

Appendix C – Motor and Gearbox Specifications

The following section has the following information:

1. Specification sheet of the Siemens 1FK7 series servo motor (selected motor marked in red)
2. Specification sheet of the Wittenstein SK060 series right-angle gearbox (selected gearbox marked in red)
3. Dimension drawing of the Wittenstein SK060 series right-angle gearbox

Rated speed	Shaft height SH	Rated power	Stall torque	Rated torque [1]	Rated current	1FK7 Synchronous Motor Compact Natural cooling	Pole pair number	Rotor moment of inertia (without brake)	Weight (without brake)
n_N	h	P_N with ΔT=100 K	M_0 with ΔT=100 K	M_N with ΔT=100 K	I_N with ΔT=100 K	Order No. Core type		J	m
RPM	mm	kW	Nm	Nm	A			10^{-4} kgm^2	kg
2000	100	7.75	48	37	16	1FK7105-5AC7 1 - 1 ■■■	4	156	39.1
3000		0.82	3	2.6	1.95	1FK7042-5AF7 **1 - 1** ■■■	4	3.01	4.9
	63	1.48	6	4.7	3.7	1FK7060-5AF7 1 - 1 ■■■	4	7.95	7
		2.29	11	7.3	5.6	1FK7063-5AF7 1 - 1 ■■■	4	15.1	11.5
	80	2.14	8	6.8	4.4	1FK7080-5AF7 1 - 1 ■■■	4	15	10
		3.3	16	10.5	7.4	1FK7083-5AF7 1 - 1 ■■■	4	27.3	14
	100	3.77	18	12	8	1FK7100-5AF7 1 - 1 ■■■	4	55.3	19
		4.87	27	15.5	11.8	1FK7101-5AF7 1 - 1 ■■■	4	79.9	21
		5.37 [4]	36	20.5 [4]	16.5 [4]	1FK7103-5AF7 1 - 1 ■■■	4	105	29
		8.17	48	26	18	1FK7105-5AF7 1 - 1 ■■■	4	156	39.1
4500	63	1.74	6	3.7	4.1	1FK7060-5AH7 **1 - 1** ■■■	4	7.95	7
		2.09 [5]	11	5 [5]	6.1 [5]	1FK7063-5AH7 1 - 1 ■■■	4	15.1	11.5
	80	2.39 [5]	8	5.7 [5]	5.6 [5]	1FK7080-5AH7 1 - 1 ■■■	4	15	10
		3.04 [6]	16	8.3 [6]	9 [6]	1FK7083-5AH7 1 - 1 ■■■	4	27.3	14
6000	28	0.4	0.85	0.6	1.4	1FK7022-5AK7 1 - 1 ■■■	3	0.28	1.8
	36	0.5	1.1	0.8	1.3	1FK7032-5AK7 1 - 1 ■■■	3	0.61	2.7
		0.63	1.6	1	1.3	1FK7034-5AK7 1 - 1 ■■■	3	0.9	3.7
	48	0.69	1.6	1.1	1.7	1FK7040-5AK7 1 - 1 ■■■	4	1.69	3.5
		1.02 [7]	3	2 [7]	3.1 [7]	1FK7042-5AK7 1 - 1 ■■■	4	3.01	4.9

• Encoder systems:	Incremental encoder sin/cos 1 Vpp 2048 pulses/revolution Absolute value encoder EnDat 2048 pulses/revolution [1) 2)] Absolute value encoder EnDat 512 pulses/revolution [1) 3)] Simple absolute encoder EnDat 32 pulses/rev [1) 2)] Multi-pole resolver [10)] 2-pole resolver	A E H G S T
• Shaft end: With key and keyway With key and keyway Plain shaft Plain shaft	• Radial eccentricity tolerance: N N N N	• Holding brake: without with without with
• Degree of protection:	IP64 IP65 and additional IP67 drive end flange IP64, anthracite paint finish IP65 and additional drive end flange IP67, anthracite paint finish IP65 and additional drive end flange IP67, anthracite paint finish and metal rating plate on motor	0 2 3 5 8

SK+ 060 1/2-stage

				1-stage					2-stage									
Ratio [a]			*i*	**3**	**4**	**5**	**7**	**10**	**12**	**16**	**20**	**25**	**28**	**35**	**40**	**50**	**70**	**100**
Max. acceleration torque (max. 1000 cycles per hour)			T_{2B} Nm	30	30	30	25	20	30	30	30	30	30	30	30	30	25	20
			T_{2B} in.lb	266	266	266	221	177	266	266	266	266	266	266	266	266	221	177
Nominal output torque (with n_{1N})			T_{2N} Nm	22	22	22	20	15	22	22	22	22	22	22	22	22	20	15
			T_{2N} in.lb	195	195	195	177	133	195	195	195	195	195	195	195	195	177	133
Emergency stop torque (permitted 1000 times during the service life of the gearhead)			T_{2Not} Nm	40	50	50	45	40	50	50	50	50	50	50	50	50	45	40
			T_{2Not} in.lb	354	443	443	398	354	443	443	443	443	443	443	443	443	398	354
Nominal input speed (with T_{2N} and 20°C ambient temperature) [b], [c]			n_{1N} rpm	2500	2700	3000	3000	3000	4400	4400	4400	4400	4400	4400	4400	4800	5500	5500
Max. continuous speed (with 20% T_{2N} and 20°C ambient temperature)			n_{1Ncym} rpm	3000	3500	4000	3500	3500	5000	5000	5000	5000	5000	5000	5000	5000	5500	5500
Max. input speed			n_{1Max} rpm	6000	6000	6000	6000	6000	6000	6000	6000	6000	6000	6000	6000	6000	6000	6000
Mean no load running torque (with n_1 = 3000 rpm and 20°C gearhead temperature) [d]			T_{012} Nm	1.2	1.1	1.0	1.2	1.1	0.2	0.2	0.2	0.2	0.2	0.2	0.1	0.1	0.1	0.1
			T_{012} in.lb	10.6	9.7	8.9	10.6	9.7	1.8	1.8	1.8	1.8	1.8	1.8	0.9	0.9	0.9	0.9
Max. torsional backlash			j_t arcmin	≤ 5														
Torsional rigidity			C_{t21} Nm/arcmin	2.0	2.1	2.2	2.0	1.8	2.1	2.1	2.1	2.1	2.1	2.1	2.1	2.2	2.0	1.8
			C_{t21} in.lb/arcmin	18	19	19	18	16	19	19	19	19	19	19	19	19	18	16
Max. axial force [e]			F_{2AMax} N	2400														
			F_{2AMax} lb_f	540														
Max. radial force [e]			F_{2RMax} N	2700														
			F_{2RMax} lb_f	608														
Max. tilting moment			M_{2KMax} Nm	251														
			M_{2KMax} in.lb	2220														
Efficiency at full load			η %	96					94									
Service life (For calculation, see the Chapter "Information")			L_h h	> 20000														
Weight incl. standard adapter plate			*m* kg	2.9					3.2									
			m lb_m	6.4					7.1									
Operating noise (with n_1 = 3000 rpm no load)			L_{PA} dB(A)	≤ 64														
Max. permitted housing temperature			°C	+90														
			F	194														
Ambient temperature			°C	0 to +40														
			F	32 to 104														
Lubrication				Lubricated for life														
Paint				Blue RAL 5002														
Direction of rotation				Motor and gearhead opposite directions														
Protection class				IP 65														
Moment of inertia (relates to the drive) Clamping hub diameter [mm]	B	11	J_t kgcm²	–	–	–	–	–	0.09	0.09	0.07	0.07	0.06	0.06	0.06	0.06	0.06	0.06
			J_t 10^{-4} in.lb.s²						0.08	0.08	0.07	0.06	0.06	0.06	0.05	0.05	0.05	0.05
	C	14	J_t kgcm²	0.52	0.44	0.40	0.36	0.34	0.20	0.20	0.19	0.19	0.18	0.18	0.17	0.17	0.17	0.17
			J_t 10^{-4} in.lb.s²	0.46	0.39	0.35	0.32	0.30	0.18	0.18	0.17	0.16	0.16	0.16	0.15	0.15	0.15	0.15
	E	19	J_t kgcm²	0.87	0.79	0.75	0.71	0.70	–	–	–	–	–	–	–	–	–	–
			J_t 10^{-4} in.lb.s²	0.77	0.70	0.66	0.63	0.62										

[a] Other ratios available on request
[b] Higher speeds are possible if the nominal torque is reduced
[c] For higher ambient temperatures, please reduce input speed
[d] Idling torques decrease during operation
[e] Refers to center of the output shaft or flange

Please contact us for information on the best configuration for S1 conditions of use (continuous operation).

Ansicht von rechts / view from right

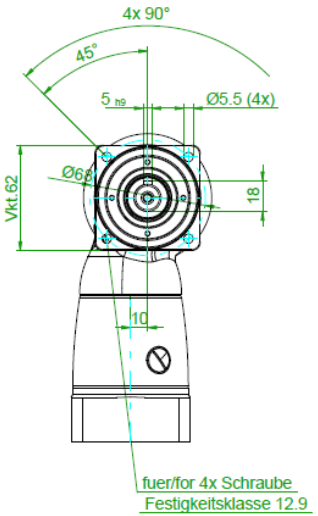

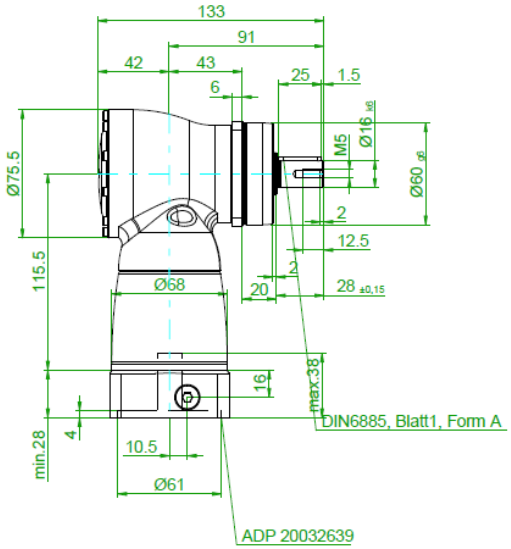

Ansicht von unten / view from bottom

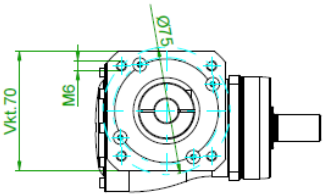

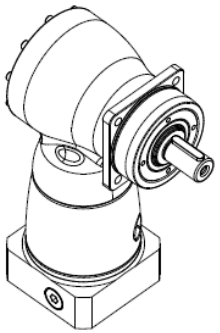

1) Motorwellenpassung pruefen
Check motor shaft fit.

ACHTUNG: Motoranbau gemaess Betriebsanleitung
Attention: motor mounting according to operation manual

Nicht tolerierte Masse ±1mm / Not tolerated measures ±1mm

gez/draft	Automatisch erstellt / automatical created	Massstab Scale	WITTENSTEIN alpha GmbH Igersheim - Germany
Datum/date	27.04.2011	auto	
Eigentumsvorbehalt nach DIN 34 beachten !	Observe copyright note according to DIN 34 !		
Benenn. Desor.	SK+060S-MF1-10-1C1		
Kommentar Note	Motor: /		
DIN A3	Ursp./Ref-Drwg: 2.5 /cymex 3.2.5	Blatt/Sheet: 1	

Technische Aenderungen vorbehalten / Technical modifications reserved